CANADIAN THESES

THÈSES CANADIENNES

NOTICE

The quality of this microfiche is heavily dependent upon the quality of the original thesis submitted for microfilming. Every effort has been made to ensure the highest quality of reproduction possible.

If pages are missing, contact the university which granted the degree

Some pages may have indistinct print especially if the original pages were typed with a poor typewriter ribbon or if the university sent us an inferior photocopy.

Previously copyrighted materials (journal articles, published tests, etc.) are not filmed.

Reproduction in full or in part of this film is governed by the Canadian Copyright Act, R.S.C. 1970, c. C-30.

AVIS

La qualité de cette microfiche dépend grandement de la qualité de la thèse soumise au microfilmage. Nous avons tout fait pour assurer une qualité supérieure de reproduction

S'il manque des pages, veuillez communiquer avec l'université qui a conféré le grade.

La qualité d'impression de certaines pages peut laisser à désirer, surtout si les pages originales ont été dactylographiées à l'aide d'un ruban usé ou si l'université nous a fait parvenir une photocopie de qualité inférieure

Les documents qui font déjà l'objet d'un droit d'auteur (articles de revue, examens publiés, etc.) ne sont pas microfilmés.

La reproduction, même partielle, de ce microfilm est soumise à la Loi canadienne sur le droit d'auteur, SRC 1970, c. C-30.

THIS DISSERTATION HAS BEEN MICROFILMED EXACTLY AS RECEIVED

LA THÈSE A ÉTÉ MICROFILMÉE TELLE QUE NOUS L'AVONS REÇUE

Preloaded Frame Structures

Safwat A. H. Ibrahim

A Thesis

in

The Department

of

Civil Engineering

Presented in Partial Fulfillment of the Requirements
for the degree of Master of Engineering at
Concordia University
Montréal, Québec, Canada

March 1987

ISBN 0-315-35555-7

ABSTRACT

Preloaded Frame Structures

Safwat A. H. Ibrahim

The intent of this analytical research work is to study a new concept which is the preloading method. The preloading method is presented as a means of constructing new cable supported systems by using external cable.

Analysis for this method and comparison with the prestressing method are presented. A numerical design example is also included.

The results obtained present the preloaded structure as a system where moments are distributed similarly as in continuous beam. Also, the results indicate the preloading technique requires less pretensioning than in case of prestressing technique, it does not require complicated bearings and it develops a structure which is better adjusted to differential settlements.

ACKNOWLEDGEMENTS

The author wishes to express his gratitude to Dr. Z. A. Zielinski and Dr. M. S. Troitsky for their invaluable advice and guidance throughout the research and preparation of this thesis.

To my parents

CONTENTS

ABSTRACT iii

ACKNOWLEDGEMENT iv

LIST OF FIGURES viii

LIST OF NOTATIONS xiii

INTRODUCTION 1

CHAPTER 1 7

BEAM SUPPORTED BY HANGING CABLES 8

1.1 The mechanism of the structure 8

1.2 The value of the tension force F 12

CHAPTER 2 16

THE PRELOADING TECHNIQUE 17

2.1 The basic concept of preloading 17

2.2 The preloading technique versus the prestressing technique 22

CHAPTER 3 33

DESIGN OF SECTIONS 34

3.1 Behavior of the structure under initial and final stresses 34

3.2 Analysis for the horizontal member 34

3.3 The increment in the pretensioning force Fi 41

3.4 Loss of preload 44

Example 48

CHAPTER 4 59

UNIFORMLY DISTRIBUTED LOADS 60

4.1 Cable response to a point load 60

4.2 Cable response to several point loads 62

4.3 Cable response to a uniformly distributed load 64

4.4 Cables supporting several stops (saddles) 66

4.5 Cable placed with exact parabolic profile 79

CHAPTER 5 89

BUCKLING, BEARING AND DIFFERENTIAL SETTLEMENT 90

5.1 Buckling due to preloading 90

5.2 The bearing system 91

5.3 Differential settlements 95

5.4 Multi-bay preloaded frame 100

5.5 The advantages of the preloading technique 101

CONCLUSION 105

APPENDIX A 106

APPENDIX B 108

REFERENCES 116

LIST OF FIGURES

Figure 1	The bearing tower of Jacques Cartier bridge at Montreal, Canada, strengthened with exterior cables.
Figure 2	Cable supported roof of the North Carolina state Fair Arena at Raleigh, U. S. A.
Figure 3	Diagram showing the action of the main balancing forces in the North Carolina Arena
Figure 4	Roof with cables suspended radially between an inner tension ring and outer compression ring
Figure 1. 1	Beam supported by hanging cable (no service load)
Figure 1. 2	Cable supporting a superstructure
Figure 1. 3	Mechanism of the system
Figure 1. 4	The forces acting on the right side column
Figure 2. 1	The cable under initial pretensioning force F_i before the application of the service load
Figure 2. 2	The forces acting on the right side column
Figure 2. 3	Stresses in case of rectangular beam
Figure 2. 4	The cable under pretensioning force (F-ΔF) before applying the service load
Figure 2. 5	The forces acting on the right side column
Figure 2. 6	The B. M. D. before the application of the service load
Figure 2. 7	Preloaded frame subjected to concentrated load

Figure 2.8 The B.M.D. after the application of the service load Q

Figure 2.9 The N.F.D.

Figure 2.10 The S.F.D.

Figure 2.11 Prestressed frame

Figure 2.12 The B.M.D. due to prestressing only

Figure 2.13 The B.M.D. due to Q only

Figure 2.14 The final B.M.D. due to Q + F

Figure 2.15 The final N.F.D.

Figure 2.16 The final S.F.D.

Figure 3.1 The pretensioning force is zero

Figure 3.2 The initial force in the cable is the pretensioning force F_i

Figure 3.3 After the application of the service load, the final force F_{final} will act on the cable

Figure 3.4 Initial B.M.D. on the horizontal member

Figure 3.5 The B.M.D. due to Q on simply supported beam

Figure 3.6 The B.M.D. due to F, Q and V

Figure 3.7 The final bending moment on the horizontal member

Figure 3.8 The interaction diagram

Figure 3.9a The behavior of the horizontal member due to the action of F_i

Figure 3.9b The corresponding elastic line.

Figure 3.10a The behavior of the horizontal member due to the action of the final forces

Figure 3.10b The corresponding elastic line

Figure 3.11a The deflection of the columns

Figure 3.11b The elastic line of the right side column showing the deflection δ at the top of the column

Figure 3.12 Preloaded frame

Figure 3.13 The forces acting on the right side column

Figure 3.14 Analysis for the section

Figure 3.15 The forces acting on the column

Figure 3.16 Analysis for the section

Figure 4.1 Freely hanging cable under its own weight

Figure 4.2 Cable response to a point load

Figure 4.3 Cable response to several point loads

Figure 4.4 Cable response to a distributed load

Figure 4.5 Cables resting on several saddles

Figure 4.6 Cable placed in groove inside the beam

Figure 4.7 The forces acting on the cable due to the initial pretensioning F

Figure 4.8 The value of the reaction R_2 located at midspan

Figure 4.9 The reaction force acting on the cable at midspan

Figure 4.10 The forces acting on the cable due to the initial pretensioning "F"

Figure 4.11 The forces acting on the beam and the columns due to the initial pretensioning force F and

the weight of the cable

Figure 4.12 The forces acting on the column

Figure 4.13 Preloaded frame carrying a uniformly distributed load

Figure 4.14 The forces acting on the column after the application of the service load

Figure 4.15 Preloaded frame under the final forces

Figure 4.16 The cable placed in groove to have the exact required parabolic profile

Figure 4.17 The forces acting on the column before the application of the service load

Figure 4.18 The dashed line shows the imaginary position of the cable, if it is freely hanging at the tops of the columns and not loaded

Figure 4.19 Uniformly distributing load acting on a preloaded frame

Figure 4.20 The forces acting on the column after the application of the service load

Figure 5.1 Flexible integral connection

Figure 5.2 The joint between the horizontal member and the column

Figure 5.3 Using Teflon in the joint

Figure 5.4 Shearing force acting at section A-A

Figure 5.5 Reinforcement of the joint

Figure 5.6 Statically determinate single bay frame

Figure 5.7 Differential settlement acting of prestressed

frame

Figure 5.8 Differential settlement acting on preloaded frame

Figure 5.9 Multi-bay preloaded frame

Figure 5.10 Prestressed beam

Figure 5.11 Prestressed frame

Figure 5.12 Preloaded frame

LIST OF NOTATIONS

A	Cross-section area of a beam
A_{ca}	The cross-section area of the cable
b	Width of the cross-section of a beam
C_d	The cable's deflection due to unit force
E	Modulus of elasticity for steel cable
E_c	Modulus of elasticity for concrete
E_e	Equivalent modulus of elasticity for cable having sag
F	The force acting in the cable
h	The height of the cross-section of a beam
H	The height of the column
I	Moment of inertia for the cross-section of a beam
L, l	Span length
M	Bending moment
mg	The weight of the cable per unit length
P	Horizontal compression force
Q	Concentrated load
r	Uniformly distributed load acting on the cable
R	Point load
S, s	Length of cable
S_p	The horizontal projection of the cable
t	The increment in the horizontal component T owing to point load acting on the cable
T	The horizontal component of the cable tension under its own weight

V	Vertical reaction at the saddle
W	The vertical deflection of the cable
α	Specific weight of the cable
β	The deflection of the cable due to a unit point load
δ	Deflection
Δ	Differential settlement
θ	The angle of cable's inclination with the horizontal
ϕ	The inclination angle of the cable with the horizontal plan at midspan
σ	Tensile stress in the cable

INTRODUCTION

INTRODUCTION

The development of the high-tensile steel cable has enabled the engineers to transmit a large force at a relatively low cost.

Ever-increasing demand for long spans, economy of cable supported structures, is the main reason why designers are searching for new methods and techniques to further the development and use of cables. The intent of this research work is to study the preloading technique as a means of constructing new cable supported systems.

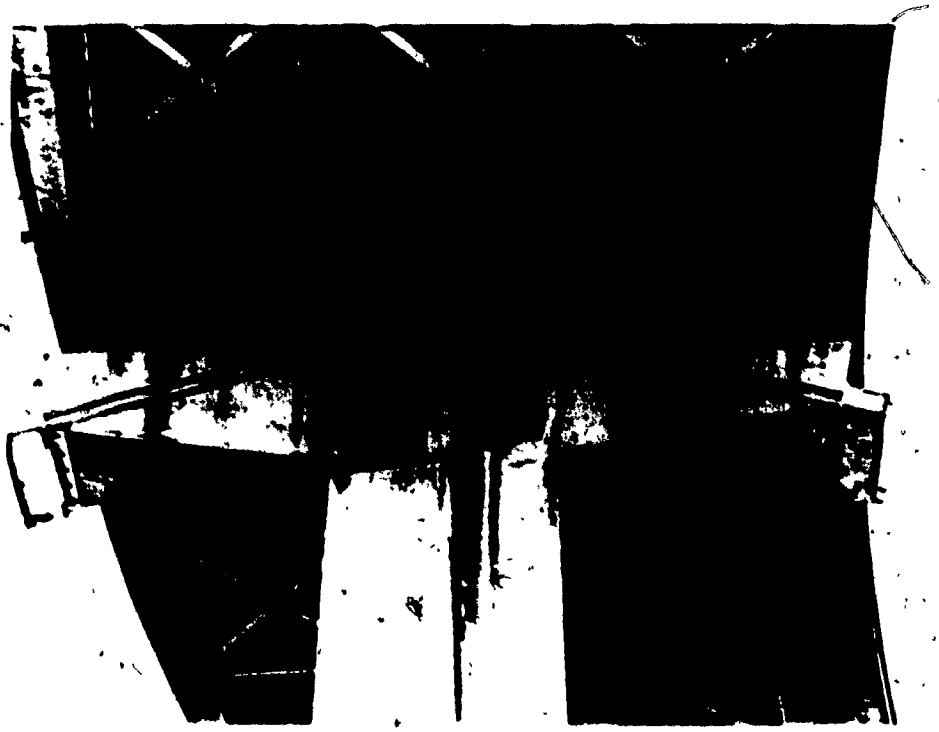

Figure 1 The bearing tower of Jacques Cartier bridge at Montreal, Canada, strengthened with exterior cables

Successful use of the steel cable in suspension and cable-stayed bridges has introduced the use of cables to many other types of structures, such as long span roofs. Furthermore, attempts have been made to use external cables to strengthen or support beams and girders (15), as in the case of the bearing towers of Jacques Cartier bridge in Montreal, Canada, as shown in Fig. 1.

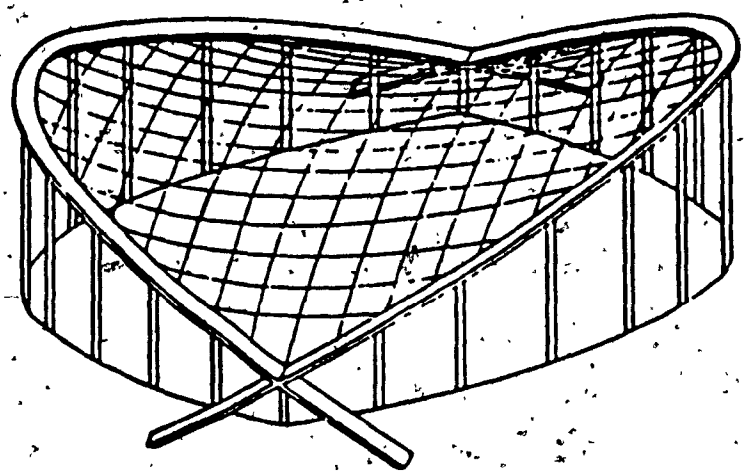

Figure 2 Cable supported roof of the North Carolina State Fair Arena at Raleigh, U.S.A.

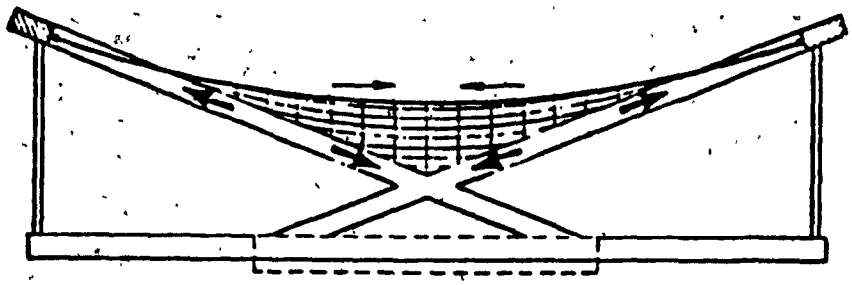

Figure 3 Diagram showing the action of the main balancing forces in the North Carolina Arena

The use of cables for long span roofs has inspired engineers to experiment with new techniques. For instance, the Fair Arena in Raleigh, North Carolina, in the U.S.A., built in 1953, designed by Matier Newicki was one of the first structures covered by a large span cable roof(1). The main structure of this building consists of an orthogonal double curvature cable net supported by two intersecting concrete arches, each inclined at approximately 21° degrees to the horizontal (Fig. 2). The important feature of this concept is that the tensile force from the cables is transmitted to the concrete arches which are subjected to compression. A diagram demonstrating the way in which the tensile forces in the cables are balanced by the compressive forces in the arches is shown in Figure 2 and Figure 3.

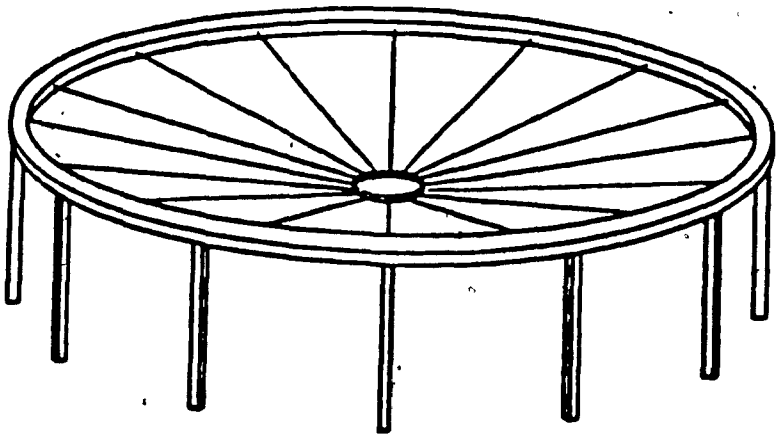

Figure 4 Roof with cables suspended radially between an inner tension ring and outer compression ring

For long span roofs, several methods were tried out to transmit the tensile forces in the cables to a compression

supporting member, such as using a compression ring beam as shown in Figure 4.

High strength cables are effectively used in prestressed concrete structures. The prestressing technique can be used with a wide range of structures from simply supported prestressed beams to more sophisticated structures(2)(9)(12)(17)(20)(21). For example, in the design of conventional prestressed structures, it has long been recognized that considerable savings can be achieved by making the structure prestressed and continuous over supports. In fact, a relatively large number of multi-span prestressed structures are designed with partial or total continuity. However, in view of the fact that these continuous prestressed structures may be more sensitive to differential settlements than simply supported prestressed structures, the continuous prestressed structures should be built on piles, or other deep foundations, unless rock or a hard foundation material is located close to the proposed foundation level. In many instances, the cost of these deep foundations may be substantially greater than the savings achieved by making the prestressed structure continuous(3).

It is necessary to redirect efforts to the development of the use of cables in the superstructure of the bridge systems to solve these problems. The preloading technique described in this research work is presented as an attempt to develop a structure which is better adjusted to

differential settlements. It represents a system where moments are distributed similarly to the continuous beam, requires less pretensioning than in case of conventional prestressing and does not require a complicated bearing to transfer the vertical loads from the superstructure to abutments, since flexible integral joints are used between the superstructure and the abutments. The preloading technique can be seen as a multi-stage prestressing technique(4)(5), where pretensioning procedure is required for the first stage, however the second stage of prestressing is the result of the built-in mechanism of the structure resulting in self prestressing.

The preloading technique can be applied to any single or multi-bay frame structure. The application of this technique to the single bay frame structure is analyzed and described in more detail in this research paper.

CHAPTER 1

CHAPTER 1

BEAM SUPPORTED BY HANGING CABLE

1.1 The Mechanism Of The Structure

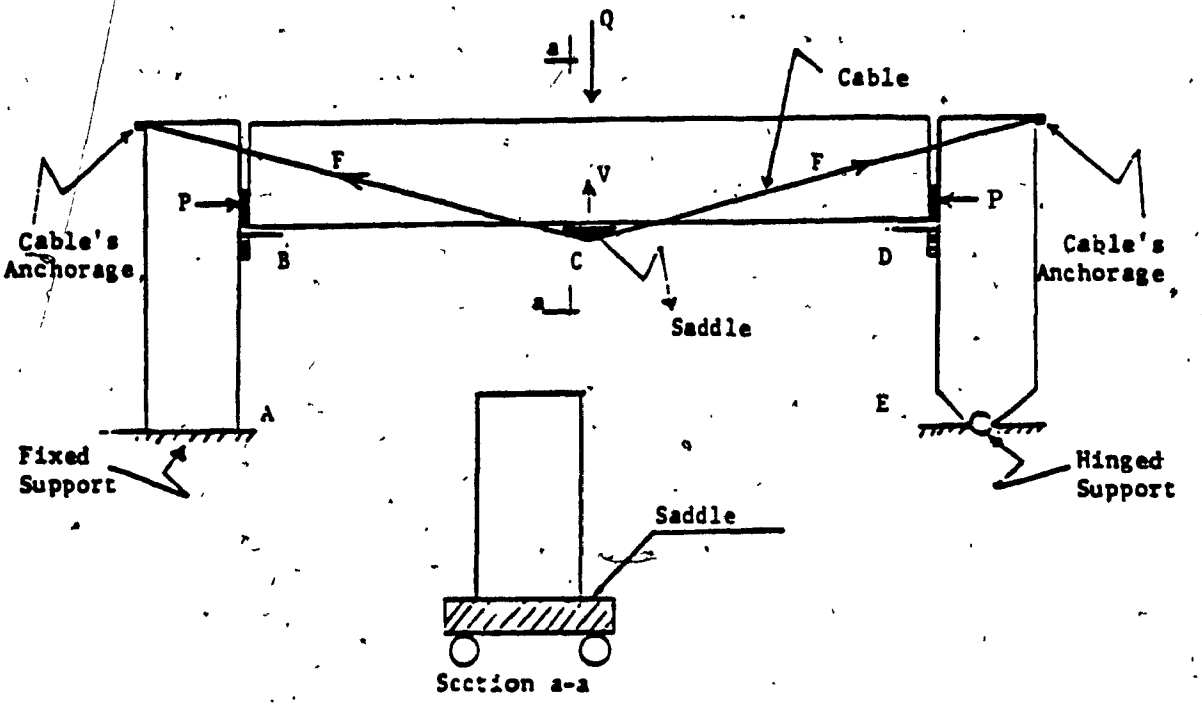

Figure 1-1 Beam supported by hanging cable

Figure 1-1 shows an example of structural mechanism, where the beam is supported by the cables at midspan at point C. The cables are placed outside the beam and support a saddle which supports the beam at the midspan, as shown in the cross-section in Figure 1-1. Both ends of the cables are anchored to the tops of the columns. Both ends of the

beam are attached to the columns by means of hinges (pins) at points B and D. One column is hinged and supported at point E, while the other is fixed at point A.

Before applying the external load Q, assuming the beam is weightless, the force in the cable is zero, and the deflection of the beam at midspan is zero. However, after applying the external load Q, the midspan of the beam will move downward forcing also the saddle to move downward. Sequentially, the cables will elongate, and a force F will develop in the cables due to this elongation.

This force F will create two components acting on the beam; a vertical component V acting at the midspan of the beam through the saddle and a horizontal strut component P acting axially at the ends of the beam through the hinge connection with the columns at points B and D in Figure 1-1. Also the columns will be loaded with bending moment which will be discussed later.

The horizontal component P will produce a compression stress along the beam and a constant negative bending moment due to its eccentricity with the center line of the beam. The vertical component V will act on the beam upward in the transverse direction creating a negative bending moment.

1.2 The Value of the Tension Force F

The value of the tension force F acting in the cables depends upon many different parameters such as: The length

of the beam, the dimensions of the cross-section of the beam, the value of the external load, the angle of the cable's inclination with the horizontal, the cross-section area of the cables and the permissible deflection at midspan.

Using a small cross-section area of the cables will result in a negligible force F. But, using a bigger cross section area of the cables will result in a very significant force F. Obviously, a small force is required to elongate a cable of small diameter, but a larger force is required for a cable of larger diameter.

At big cross-section area of the cables, the resulting force F in the cable will be much smaller than the ultimate capacity of the cables. In such a case, the full capacity of the cables is not utilized. However, as shown in the following chapter the use of the full capacity of the cable is possible.

To determine the value of the force F, the deflection of the beam at midspan should be analyzed.

The external load Q will cause a downward deflection, however, the vertical component V and the horizontal component P will cause an upward deflection at midspan, thus the total deflection δ will be as follows:

$$\delta_q \cdot Q' - \delta_v \cdot V - \delta_p \cdot P = \delta \cdot 1 \qquad (1.1)$$

Where

δ_q = the vertical deflection of the beam at point C due to a unit value of Q

δ_V = the vertical deflection of the beam at point C due to a unit value of V

δ_p = the vertical deflection of the beam at point C due to a unit value of P

At midspan, the deflection at the saddle due to the elongation of the cable will be equal to the deflection of the beam δ. The deflection of the beam is given in equation 1-1, although V and P in this equation are unknown. An equation to calculate the deflection of the cables is therefore necessary.

Podolny & Scalzi (6) and Troitsky (7) used an equation to calculate the deflection of a cable supporting a superstructure of a bridge. This equation is applicable to the cable system shown in Figure 1-2.

The deflection equation of the cable shown in Figure 1-2 is the following:

$$\frac{0.5\ S}{2\ E_e\ A_{ca}\ \sin^2\Theta}\ V = \delta \qquad (1.2)$$

where:

E_e = Equivalent modulus of elasticity introduced by Ernest (8) for a cable with sag

$$E_e = \frac{E}{1 + [\ (\gamma S_p)^2 \ /\ 12\sigma^3\ ]}$$

S = The total length of the cable

A_{ca} = The total cross section area of the cables

Θ = The angle of the cable's inclination with the horizontal

V : The vertical reaction at the saddle

E : Modulus of elasticity for steel cable

σ : Tensile stress in the cable

S_p : The horizontal projection of the cable's length

γ : Specific weight of the cable

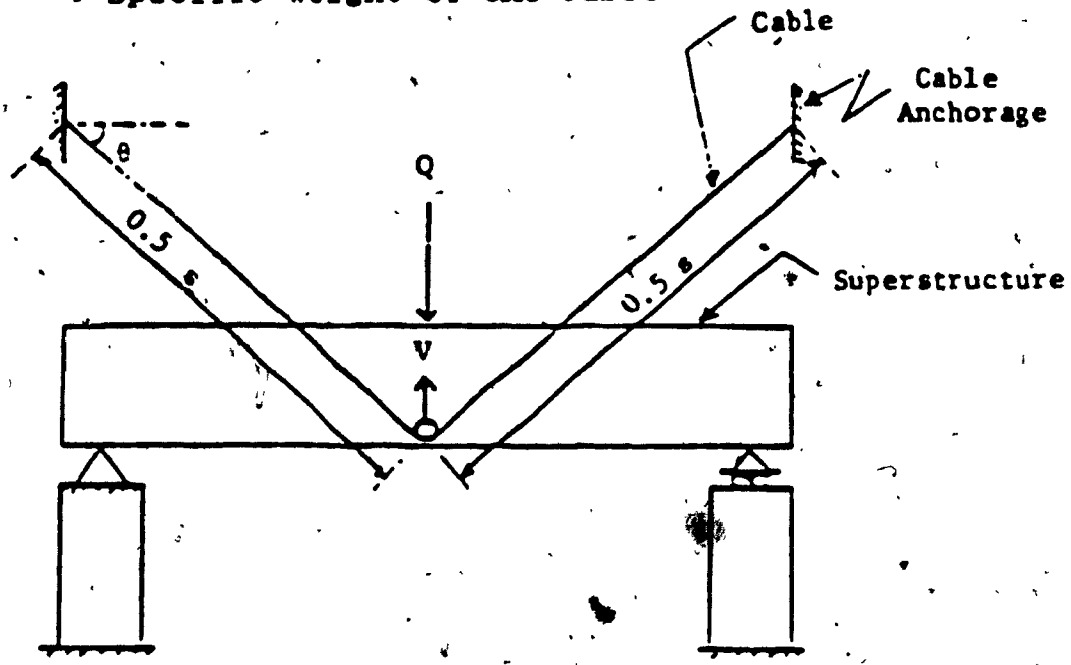

Figure 1-2 Cable supporting a superstructure

The cable system shown in Figure 1-2 is similar to the cable system shown in Figure 1-1, however the cable in Figure 1-1 is supported on the saddle at midspan, while the cable in Figure 1-2 is clamped to the saddle. These two cable systems have the same behavior because the vertical load Q is applied at midspan. Therefore, equation 1.2 is applicable to the system shown in Figure 1-1. In the system shown in Figure 1-1, there is a loss in the force acting in the cable, this loss will be considered in Section 3.4 of

Chapter 3. This loss may cause additional deflection in the cable which can be considered separately.

Assuming:

$$C_d = \frac{0.5\,S}{2\,E_e\,A_{ca}\,\sin^2\Theta} \qquad (1.3)$$

thus,

$$C_d \; V_{\ell}^{2} \; \delta \qquad (1.4)$$

Since at midspan, the deflection of the cable is equal to the deflection of the beam, equation 1.4 is equal to equation 1.1.

$$\delta_q \cdot Q - \delta_v \cdot V - \delta_p \cdot P = C_d \cdot V \qquad (1.5)$$

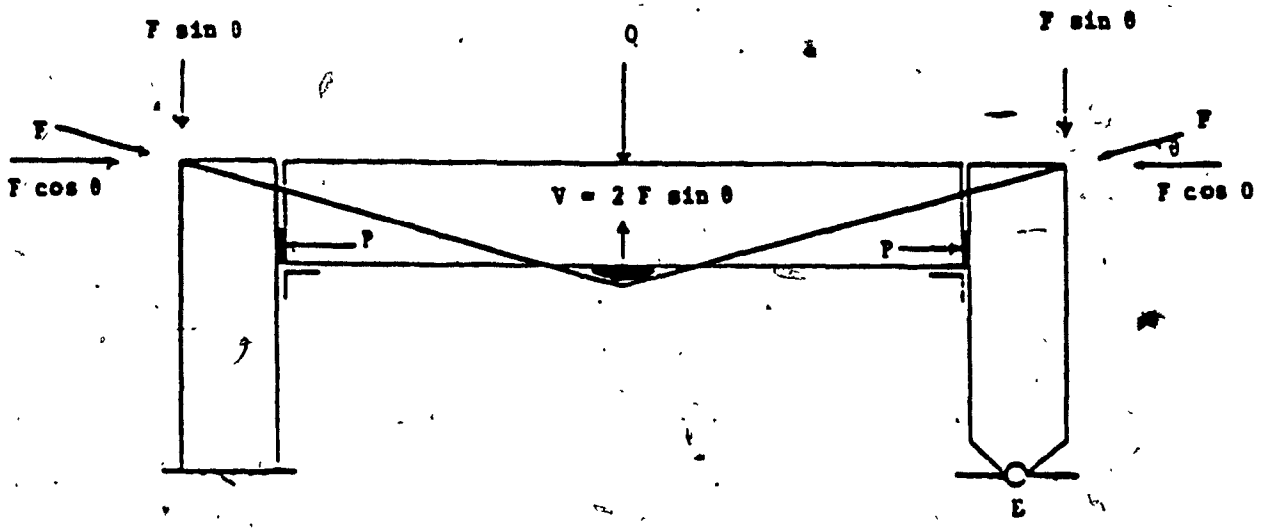

Figure 1-3 Mechanism of the system

$$V = 2\,F\,\sin\Theta \qquad (1.6)$$

To determine the value of the force P, the column on the right side in Figure 1-3 will be analyzed as shown in Figure 1-4.

By taking the moment at the bottom of the column where the center line intersects with the horizontal, the following equations are obtained:

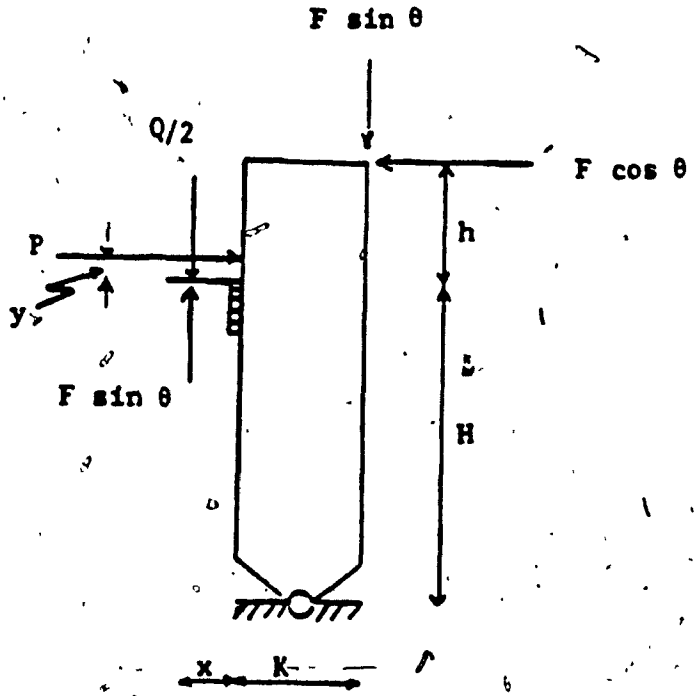

Figure 1-4 The forces acting on the right side column

$$\Sigma M = 0.0$$

$$F\cos\theta\,(h + H) + \frac{Q}{2}\left(X + \frac{k}{2}\right) - P\,(y + H) - F\sin\theta\left(X + \frac{k}{2}\right) - F\sin\theta\,\frac{k}{2} = 0.0$$

$$\text{i.e.}\quad P = F\cos\theta\left(\frac{h + H}{y + H}\right) + \left[\frac{Q}{2}\left(X + \frac{k}{2}\right) / (y + H)\right] - \left[F\sin\theta\,(X + k/2) / (y + H)\right] \qquad (1.7)$$

In equation (1.7), the value of all the terms are given, except for the values of F and P.

By substituting from equations (1.6) and (1.7) into equation (1.5), considering the value of Q is known, the value of F will be the only unknown value in equation (1.5). In solving this equation, the value of F will be determined.

CHAPTER 2

CHAPTER 2

THE PRELOADING TECHNIQUE

2.1 The Basic Concept of Preloading

In order to utilize the allowable capacity of the cable, the cable must be pretensioned by an initial pretensioning force F_i before the service load is applied.

This initial pretensioning force F_i will load the beam by an initial eccentric horizontal compression component P_i acting at the ends of the beam and an initial vertical component V_i acting at the midspan of the beam, at the location of the saddle, as shown in Figure 2-1.

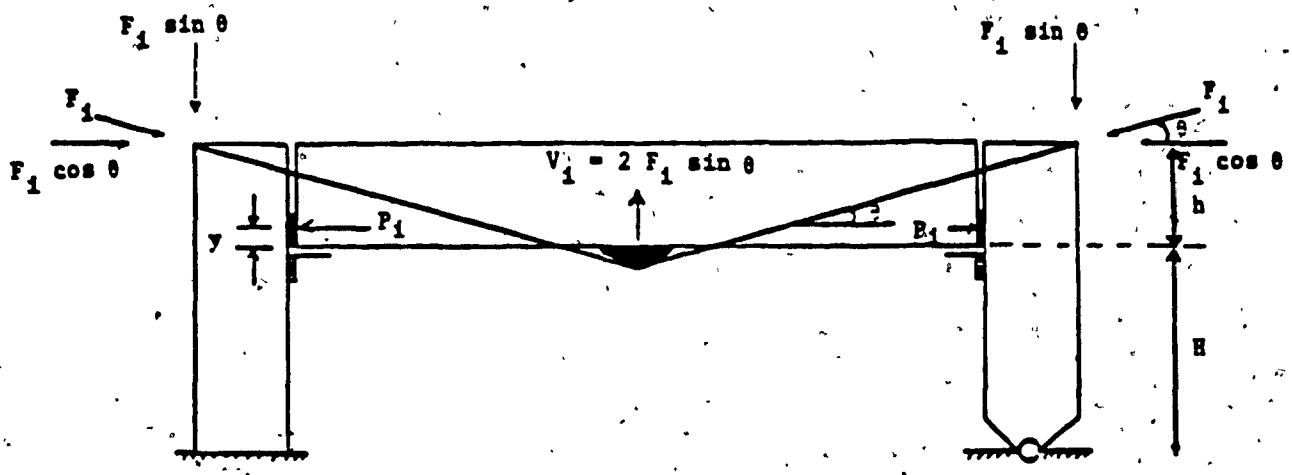

Figure 2-1 The cable under initial pretensioning force F_i before the application of the service load

The horizontal member in Figure 2-1 is initially loaded by the two external forces P_i and V_i, before the application of the service load. Therefore the term preloading has been

chosen as a name for this technique. These forces P_i and V_i create initial stresses at midspan opposing the expected stresses due to the service load.

Since the value of the initial pretensioning force F_i will be known, as will be explained in Chapter 3, the value of V_i can be obtained as shown in Figure 2-1, where,

$$V_i = 2 F_i \sin\theta$$

To determine the value of the initial horizontal compression force P_i, an analysis of the support column should be carried out. The support column at the right side of Figure 2-1 will be analyzed as shown below.

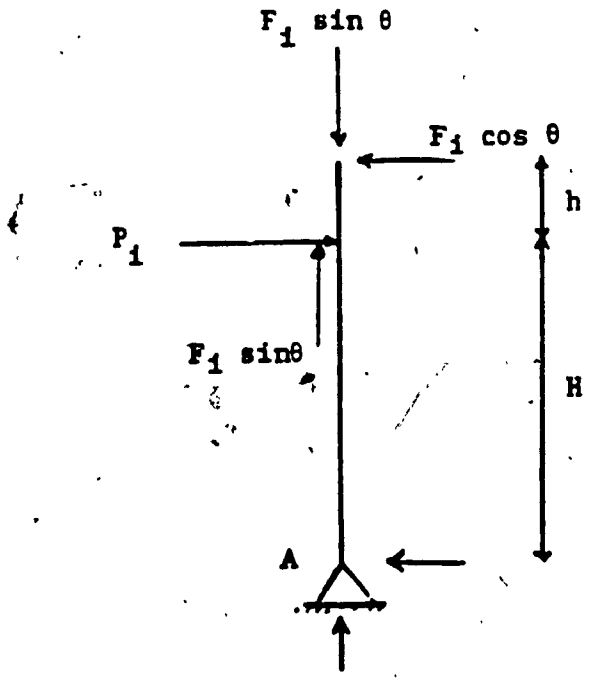

Figure 2-2 The forces acting on the right side column

In Figure 2-2, all the vertical forces that are acting on the column are assumed to be located at the center line

of the column. The initial horizontal compression force P_i is assumed to be acting at the bottom fiber of the beam, which means the distance y shown in Figure 2-1 is assumed to be zero. To determine the value of P_i, the moment at support A should be taken, see Figure 2-2.

$$\Sigma M_A = 0.0$$

$$= F_i \cos\theta\ (h + H) - P_i H$$

$$\text{i.e} \quad P_i = F_i \cos\theta\ [\ (h/H) + 1\ ] \qquad (2.1)$$

Assuming,

$$\text{i.e} \quad h/H = 0.1 \qquad (2.2)$$

By substituting in equation (2.1):

$$P_i = F_i \cos\theta\ (\ 0.1 + 1\ )$$

$$P_i = 1.1\ F_i \cos\theta$$

$$\text{i.e} \quad P_i \approx F_i \cos\theta \qquad (2.3)$$

The assumption in equation (2.2) is a practical assumption, however diffrent values for the ratio h/H may be used. The value of the force P_i in most cases will be slightly greater than the horizontal component of the tension force $F_i \cos\theta$ that is acting at the ends of the cable.

After determining the minimum value of P_i, the stress distribution on the cross-section of the beam at its midspan will be calculated using the elastic theory.

The forces V_i and P_i that are acting on the horizontal member of Figure 2-1 are already determined. The distribution of the stresses on the cross section area at midspan of the beam that are shown in Figure 2-3-c through 2-3-f are

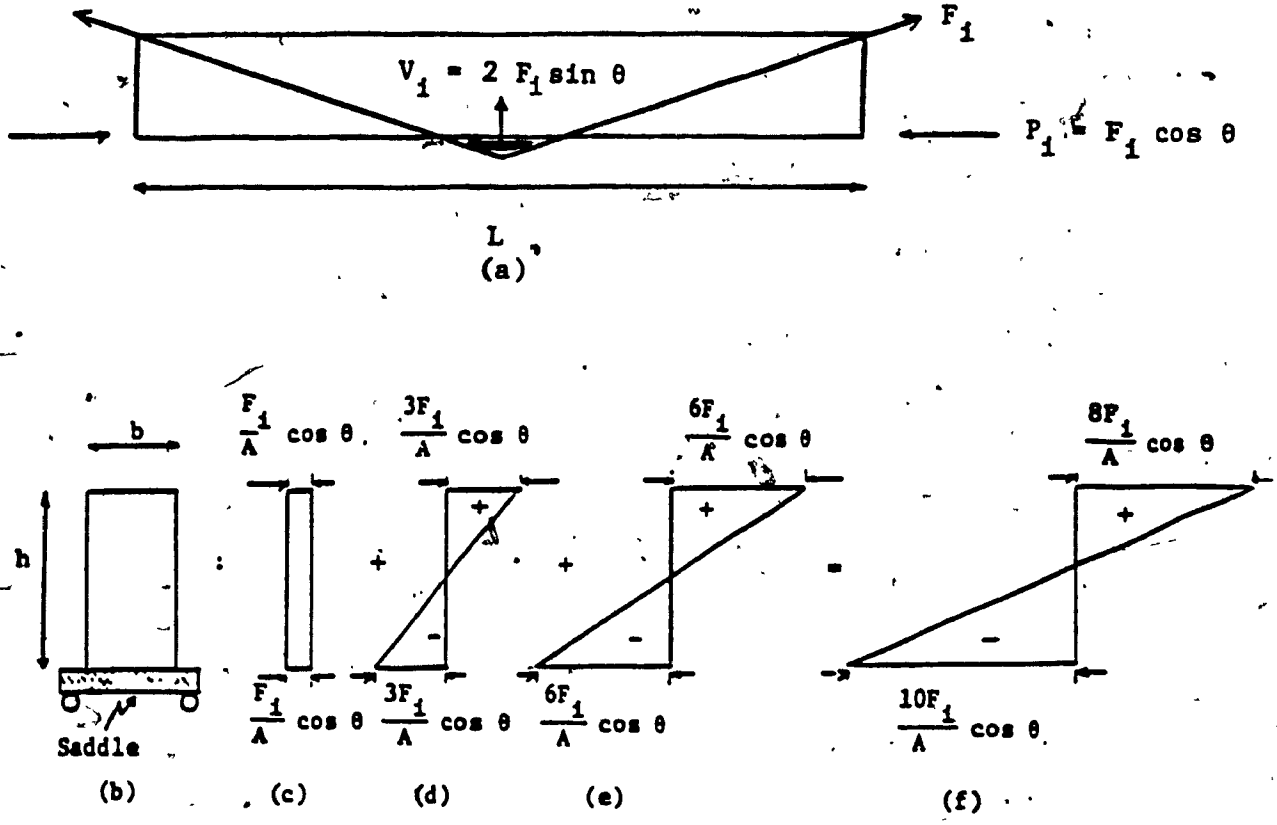

Figure 2-3 Stresses in rectangular beam

a) Preloading member

b) Cross section at midspan shows outside tendons

c) Stress due to the compression force Pi

d) Stress due to the eccentricity of the force Pi

e) Stress due to the vertical force Vi

f) The total stresses on the cross section at midspan

calculated as follows:

In Figure 2-3-c

$\sigma_1 = - P_i/A$

where

A = The cross section area of the beam.

σ_1 = The normal stress

$\sigma_1 = -(F_i/A)\cos\theta$

In Figure 2-3-d

$\sigma_2 = \pm (M_1 y)/I$

where

Mi = the moment due to the eccentricity of P_i

$Mi = (h/2) F \cos\theta$

$y = h/2$

$I = (b h^3) / 12$

b = The width of the beam.

i.e $\sigma_2 = \pm (3F_i/A)\cos\theta$

In Figure 2-3-e

$\sigma_3 = \pm (M_2 y)/I$

where

M2 = the moment at midspan due to V_i

$M2 = (V_i L) / 4$

L = The span length

$M2 = [(F_i L)/2] \sin\theta$

i.e. $\sigma_3 = \pm \frac{3 L F_i}{b h^2} \sin\theta$

Multiply the right term of the above equation by $\frac{\cos\theta}{\cos\theta}$

$\sigma_3 = \pm \frac{3 L F_i}{b h^2} \tan\theta \cos\theta$

where

$\tan\theta = \frac{2h}{L}$

$\sigma_3 = \pm \frac{6 F_i}{A} \cos\theta$

The total stress distribution on the cross section area shown in Figure 2-3-f is calculated as follows:

$$\sigma = - \sigma_1 \pm \sigma_2 \pm \sigma_3$$

The initial stress on the cross section area at midspan of the beam, Figure 2-3-f, will oppose the expected stress due to the application of the service load.

The concept of creating initial stress to oppose the stress resulting from the application of the service load is the basic concept of the prestressing technique. Since the preloading technique, as with the prestressing technique, is based upon this basic concept, it is important to compare these two techniques. In the following section, this comparison will take place.

2.2 The Preloading Technique Versus the Prestressing Technique

In this section, two frames will be compared, one of them will be preloaded, the other will be prestressed. Both these frames will be subjected to the same concentrated load Q.

The two frames have exactly the same dimensions and the cables used by both are of the same length and have the same cross section area. The cable profiles are similar.

In the preloaded frame, there is a significant increment ΔF in the force acting in the cable that will take place after the application of the service load, due to the

mechanism of the structure. However, in the prestressed frame, the increase in the force acting in the cable due to the application of the service load is negligible.

To obtain similar and final forces in the cables of both systems, equal to F , after the applications of the service loads. The cable of the preloaded frame will be jacked to a pretensioning force equal to (F - ΔF). The final force in the cable in this case, after the application of the service load, will be:

$$(F - \Delta F) + \Delta F = F$$

In the prestressed frame, the cable will be pretensioned to a force F. Therefore, the only difference will be with the pretensioning force in the cable of each frame.

The comparison will include the bending moment diagram, the normal force diagram and the shearing force diagram(16) (18).

Case #1 - Preloading

To calculate the initial bending moment due to the pretensioning force (F - ΔF), the column located at the right side in Fig.2-4 must be analyzed (before the application of the service load).

When taking the moment at the location of the hinge at the bottom of the column, Figure 2-5, the following equations are obtained:

$$11\ h\ (F - \Delta F)\cos\Theta = 10.2\ h\ P_1 + 0.5\ h.(F - \Delta F).\sin\Theta + h\ (F - \Delta F)\sin\Theta$$

i.e. $P_i = (F - \Delta F)(1.08 \cos\theta - 0.15 \sin\theta)$

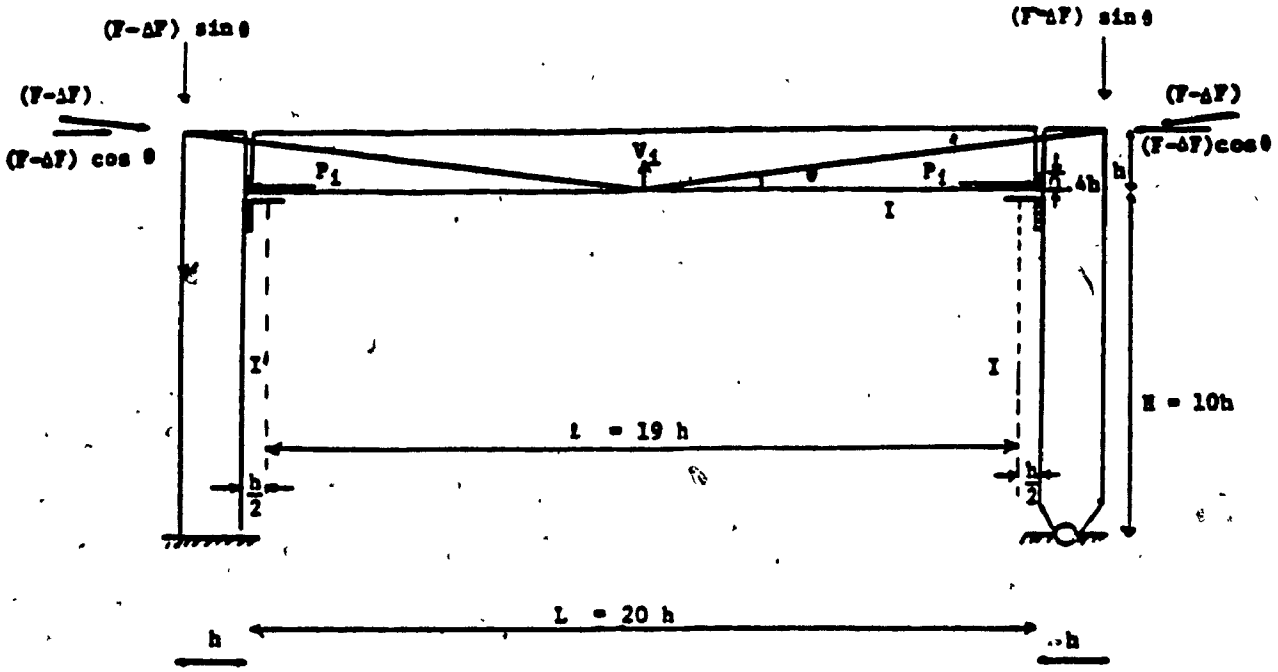

Figure 2.4 The cable under pretensioning force (F-ΔF) before applying the service load

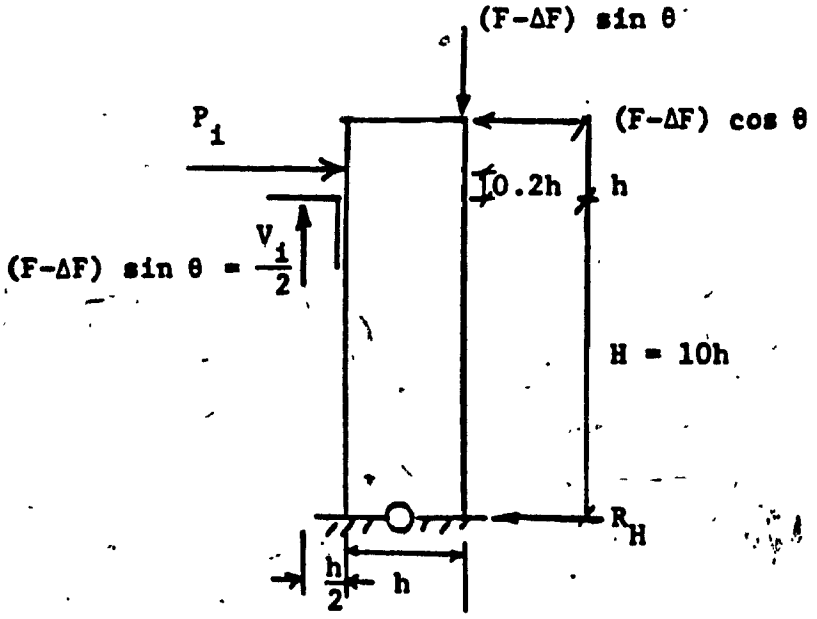

Figure 2-5 The forces acting on the right side column

from Figure 2-4

$\tan\theta = h/11h = 1/11$

$\theta = 5.194$

$\sin\theta = 0.091$

$\cos\theta = 0.996$

$P_i = 1.062\ (F - \Delta F)$

$V_i = 2\ (F - \Delta F)\ \sin\theta$

$V_i = 0.182\ (F - \Delta F)$

By determining the values of P_i and V_i, the initial bending moment diagram can be drawn, as shown in Figure 2.6

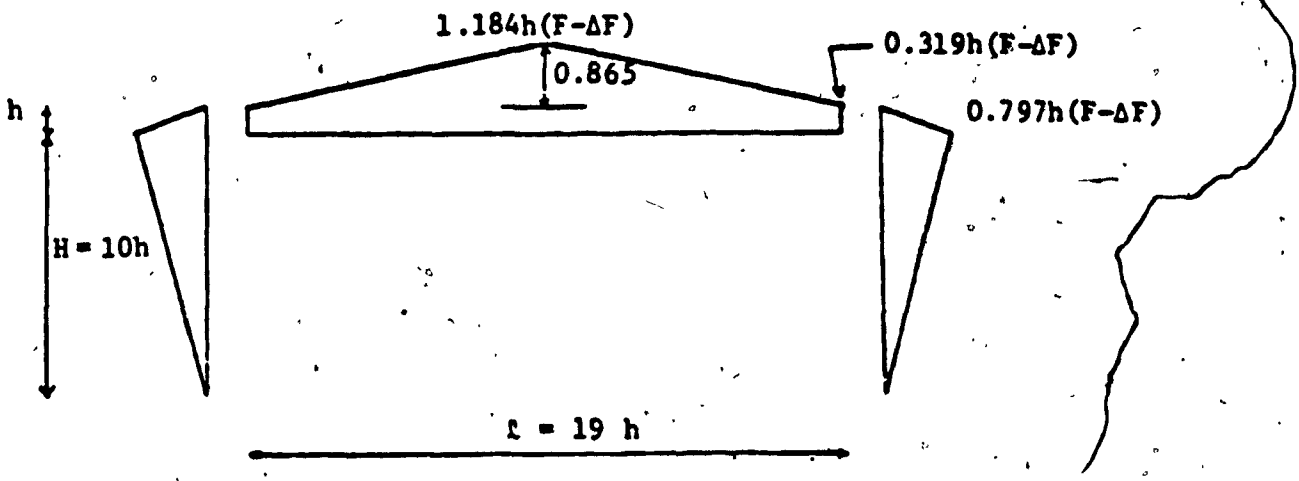

Figure 2.6 The B.M.D. before the application of the service load

Due to the application of the concentrated load Q at midspan, the pretensioning force (F - ΔF) will be increased. Also, by increasing the value of Q, the value of this increment will be greater.

Assuming the preloaded frame is now subjected to a

concentrated load Q, as shown in Figure 2-7, and the value of Q is increasing from zero to F. When the value of Q reaches F, the value of the pretensioning force in the cable (F - ΔF) will increase to become F. The corresponding increase in the bending moment due to the increase of Q is shown in the bending moment diagram, in Figure 2-8.

The bending moment of the columns in Figure 2-8 is calculated with the assumption that all the vertical forces acting on these columns are located at the center line of the columns.

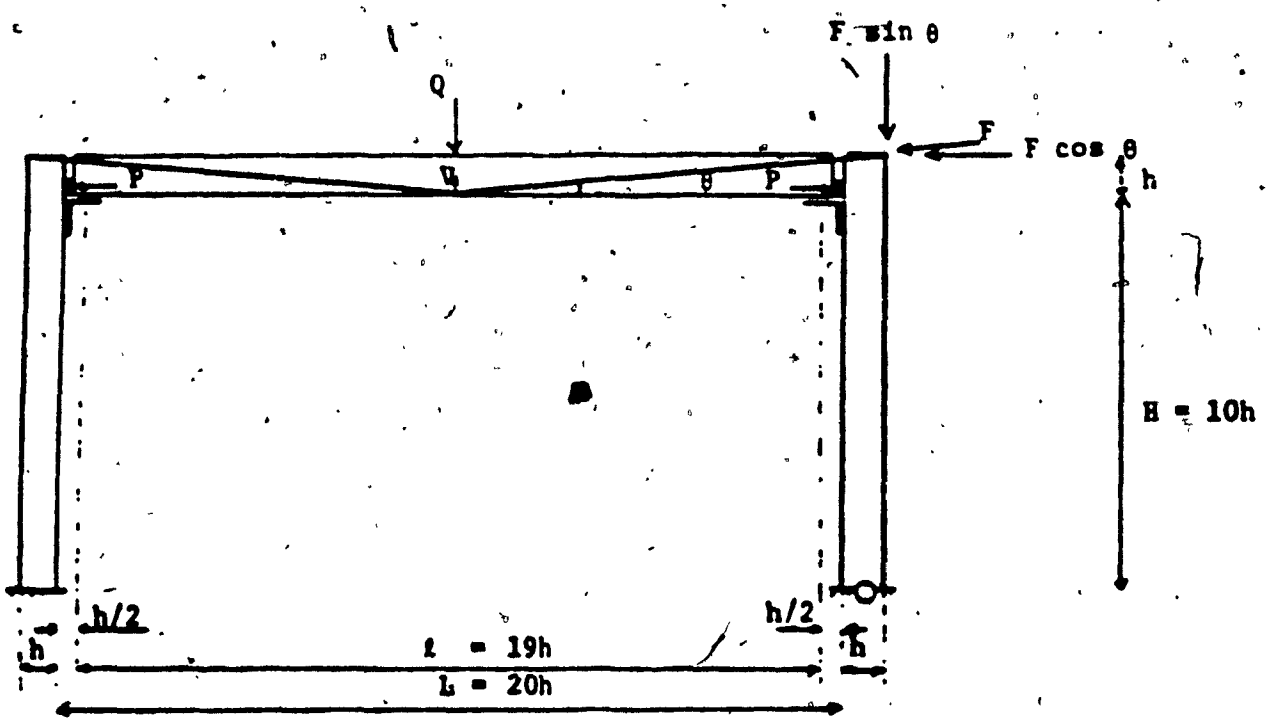

Figure 2-7 Preloaded frame subjected to concentrated load

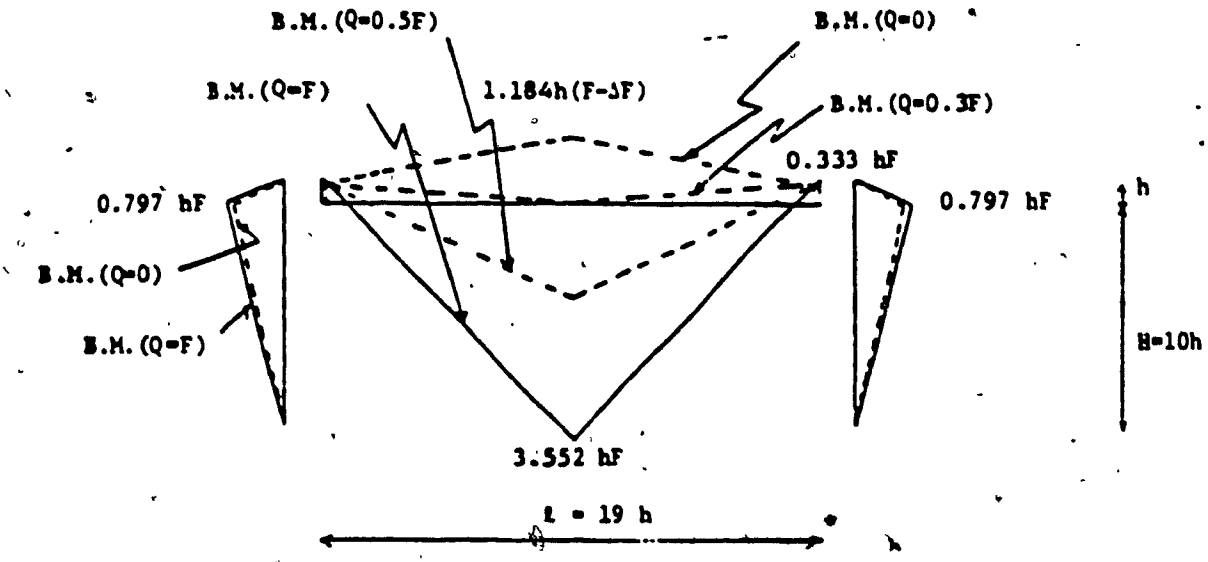

Figure 2-8 The B.M.D. after the application of the service load Q

Note: Q changes from zero to F

Consequently, the bending moment due to the eccentricities of these forces will be zero. A special joint will be used to connect the horizontal member to the columns (Chapter 5, Section 5.2), therefore the vertical forces will be located very close to the center line of each column. Hence, the resulting bending moment due to the eccentricities of these vertical forces can be neglected.

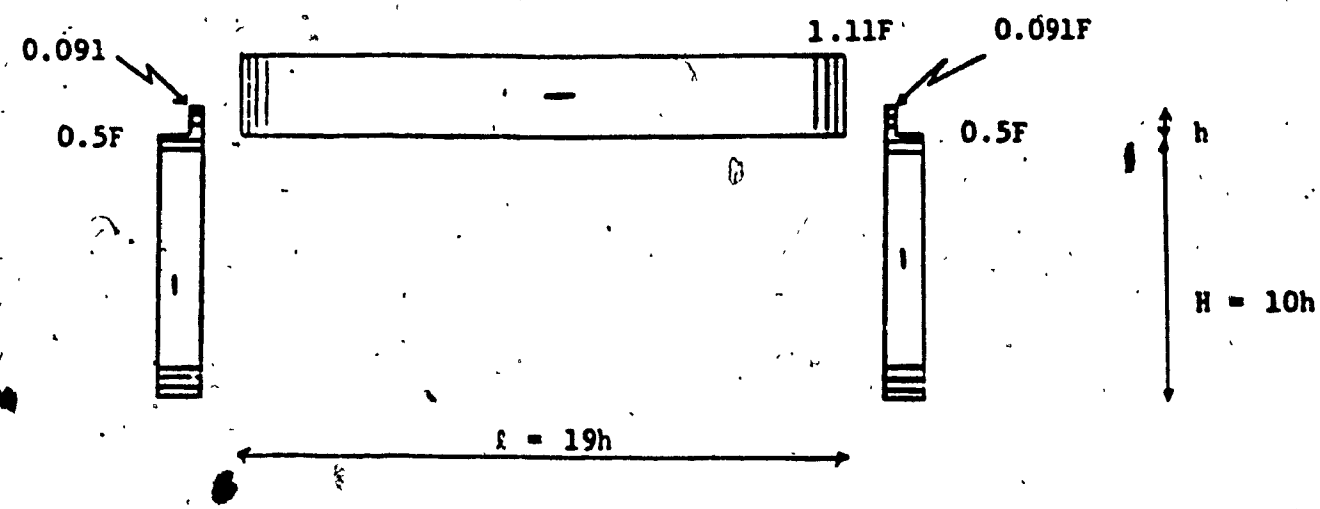

Figure 2.9 The N.F.D. (When Q = F)

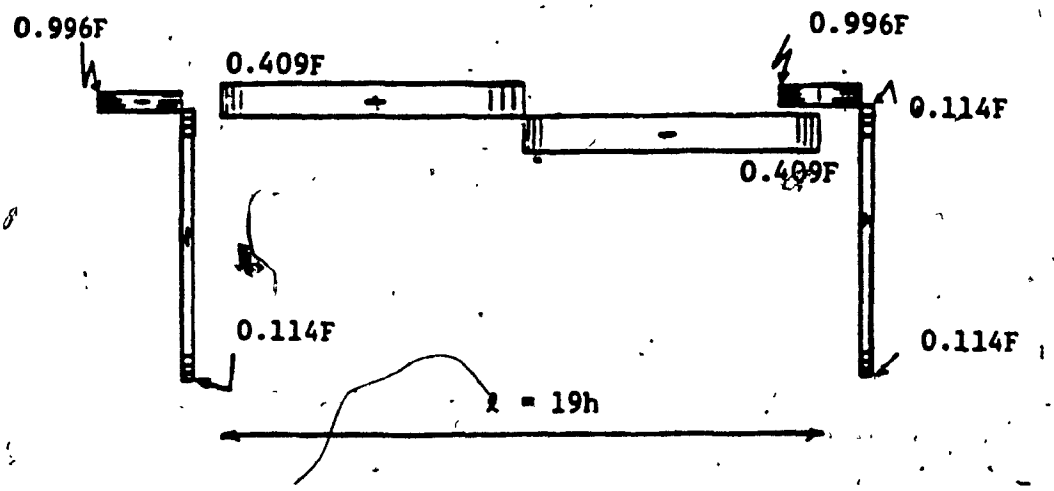

Figure 2.10 The S.F.D. (When Q = F)

When Q = F, the corresponding normal force diagram and the shearing force diagram are as shown in Figure 2-9 and Figure 2-10, respectively.

Case #2 - Prestressing

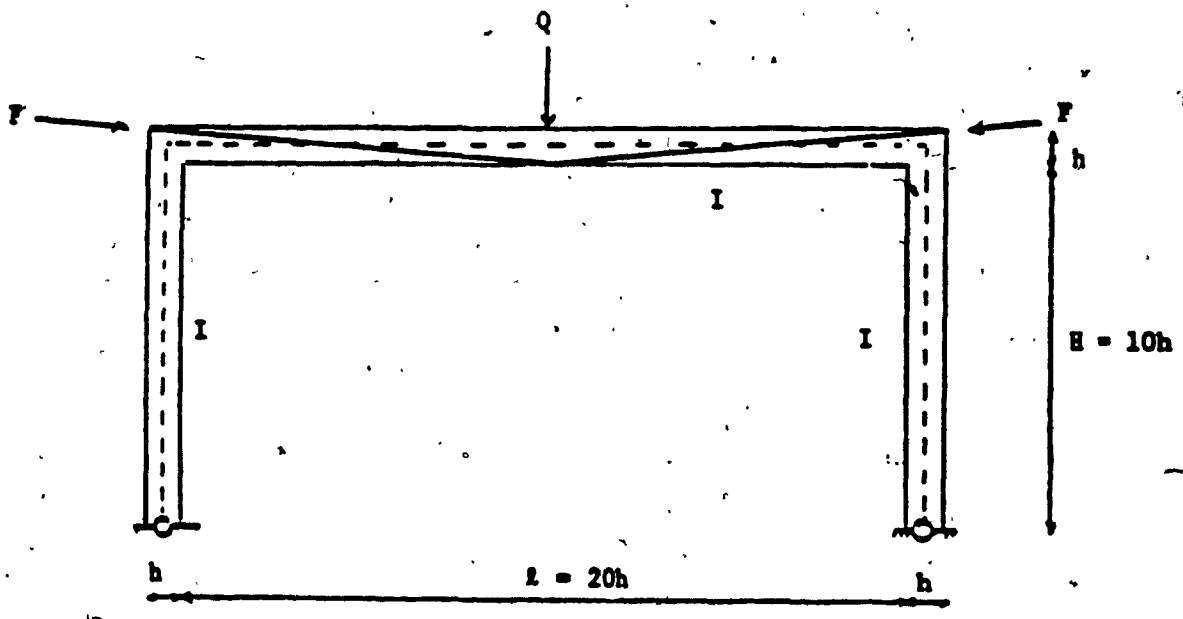

Figure 2-11 Prestressed frame

For the prestressed frame shown in Figure 2-11, the bending moment diagram due to the pretensioning force F in the tendon is given in Figure 2-12.

The moment distribution method has been employed to drive that bending moment (the complete analysis of the bending moment diagram shown in Figure 2-12 is given in Appendix A).

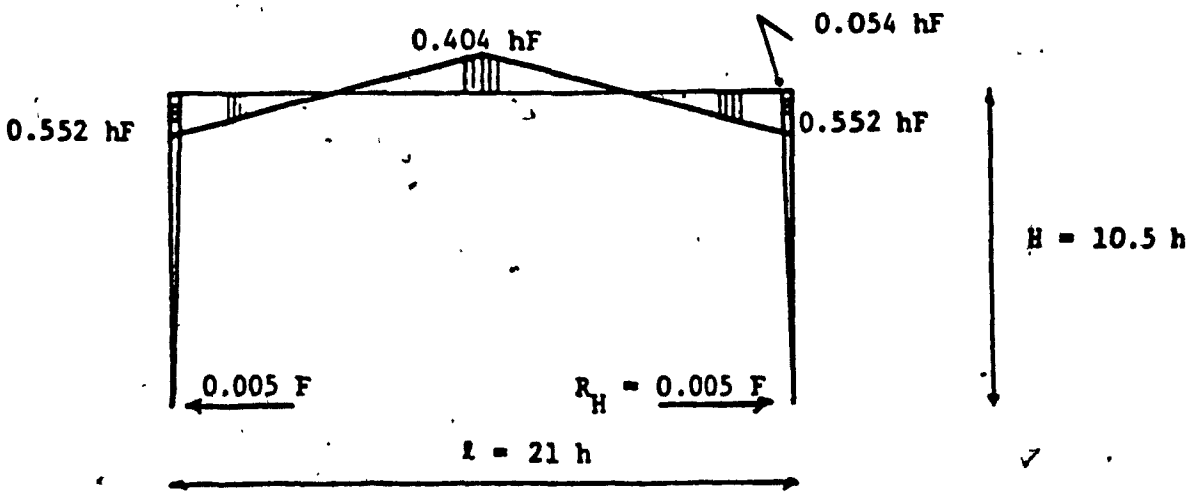

Figure 2-12 The B.M.D. due to prestressing only

(see appendix A)

The value of the pretensioning force F is independent of the concentrated load Q (when Q changes from zero to F, the value of the pretensioning force F remains constant). Consequently, due to the application of the external force Q to the midspan of the frame, two sets of moments will appear on that frame. The first is due to the pretensioning force F (Fig. 2-12) and the second is due to the external load Q

(Fig. 2-13). The final bending moment on the frame will result from superpositioning the two sets of moments as shown in Figure 2-14.

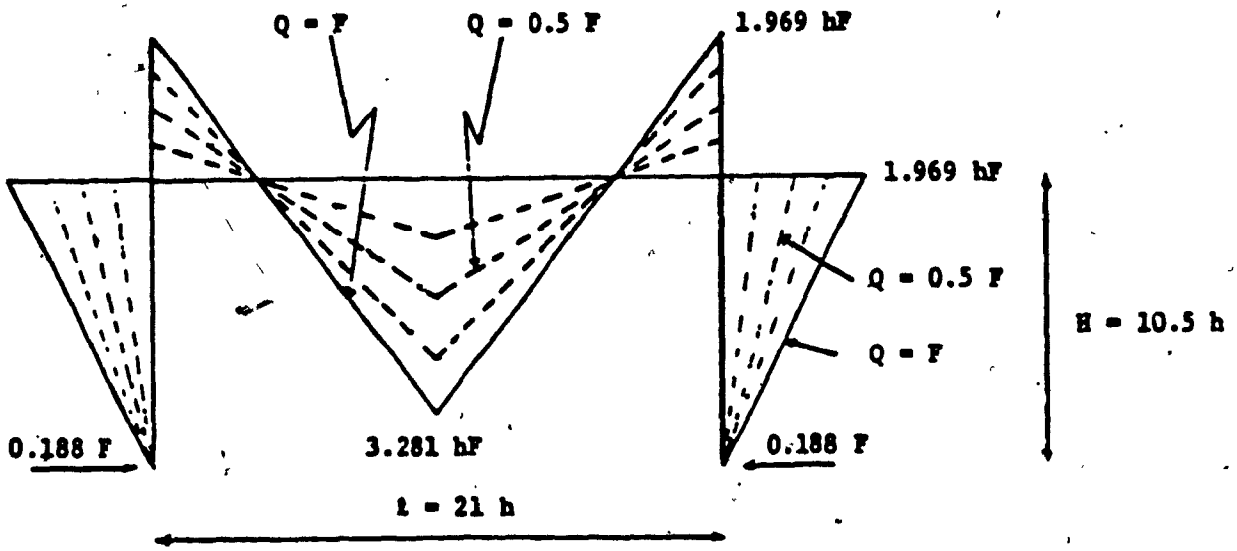

Figure 2-13 The B.M.D. due to Q only

Note: Q changes from zero to F

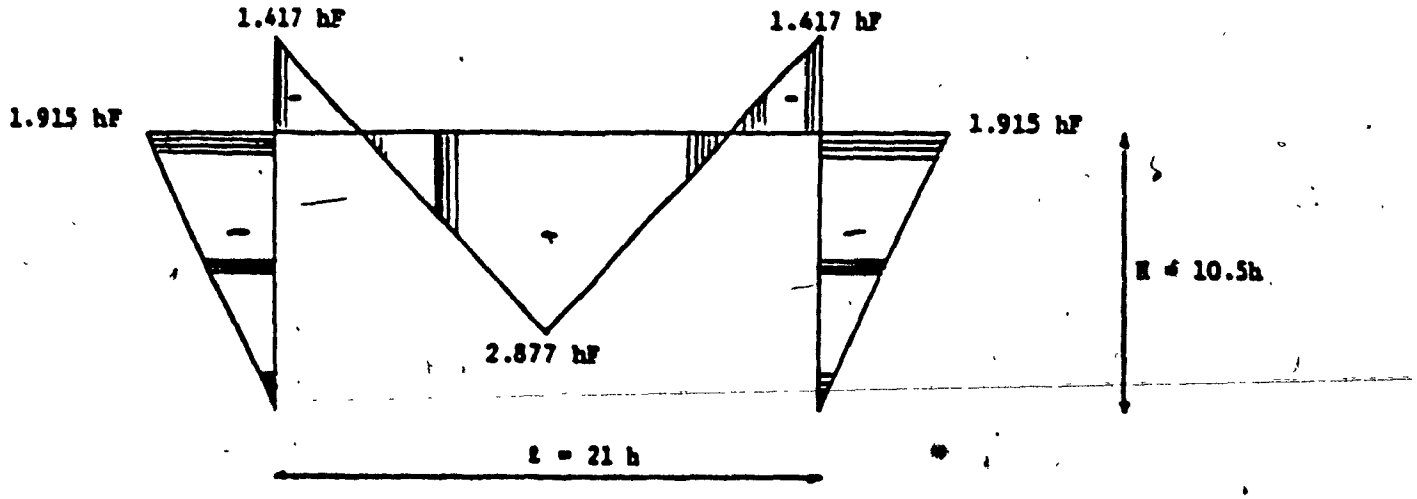

Figure 2-14 The final B.M.D. (when Q = F)

The normal force diagram and the shearing force diagram are shown in Figure 2-15 and Figure 2-16, respectively.

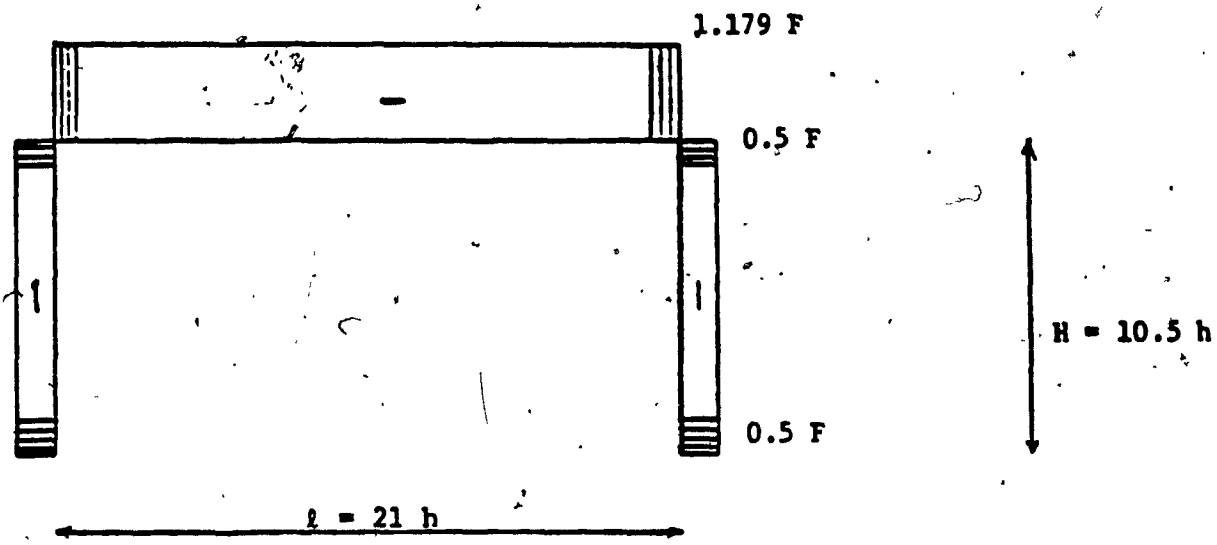

Figure 2-15 The final N.F.D. (when Q = F)

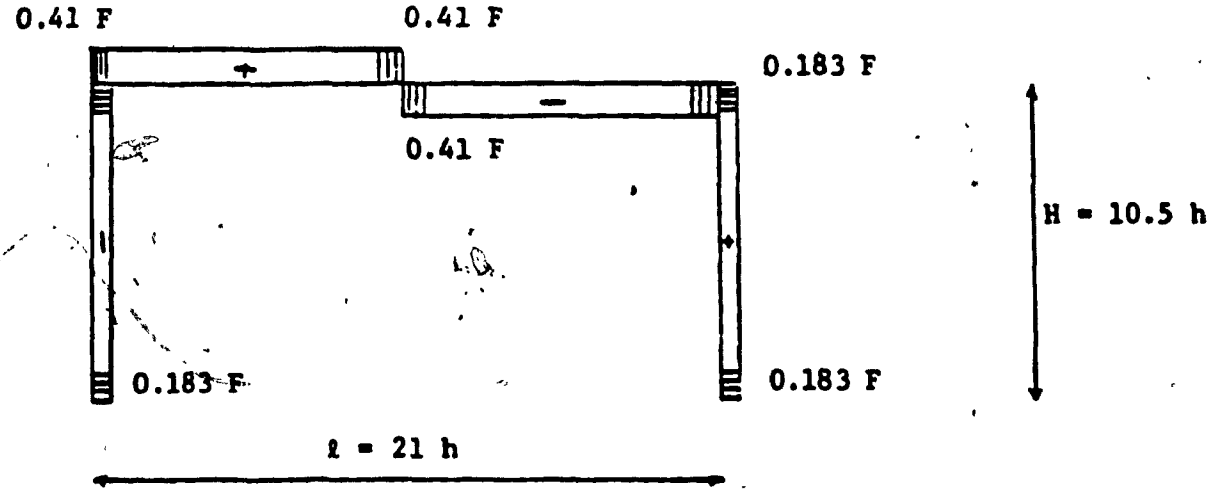

Figure 2-16 The final S.F.D. (when Q = F)

By comparing the bending moment diagram for the preloaded frame and the prestressed frame in Figures 2-8 and 2-14 respectively, we can conclude that in the preloaded

frame, the horizontal member acts as partially fixed to the columns, thus the value of the bending moment at midspan is greater than the value of bending moment at the midspan of the prestressed frame. However, at the ends of the horizontal member and the columns of the preloaded frame, the bending moment is much less than the bending moment located at the same sections in the prestressed frame.

The overall bending moment area on the prestressed frame (Fig. 2-14) is greater than the overall bending moment area on the preloaded frame (Fig. 2-8).

The normal force diagrams, in Figures 2-9 and 2-15, for preloading and prestressing are almost the same. In the shearing force diagrams in Figures 2-10 and 2-16, the shearing force of the horizontal member of the preloaded frame is almost the same as that of the horizontal member of the prestressed frame. However, on the columns of the preloaded frame, the shearing force is almost half that of the vertical members of the prestressed frame.

The overall shearing force area on the preloaded frame is less than the overall shearing force area on the prestressed frame.

CHAPTER 3

CHAPTER 3

DESIGN OF SECTIONS

3.1 Behavior of the Structure Under Initial and Final Stresses

The behavior of the structure due to the sequence of changing stresses is shown in Figures 3-1, 3-2 and 3-3.

Obviously, before the application of the pretensioning force F and the service load Q, the stresses in all the sections of the structure are zero (assuming the structure is weightless). Therefore, there are no deformations at any section shown in Figure 3-1.

After the application of the initial pretensioning F_i, the horizontal member will deflect upward with the maximum value at midspan and the deformation of the structure will be as shown in Figure 3-2.

In the final, stage the structure will be subjected to an external concentrated load Q at midspan acting simultaneously with the final value of the tensioning force F in the cable. The horizontal member will deflect downward at midspan and upward near the ends, as shown in Figure 3-3.

3.2 Analysis of the Horizontal Member

The initial bending moment which is due to initial pretensioning force F_i, consists of two parts: Mi due to the

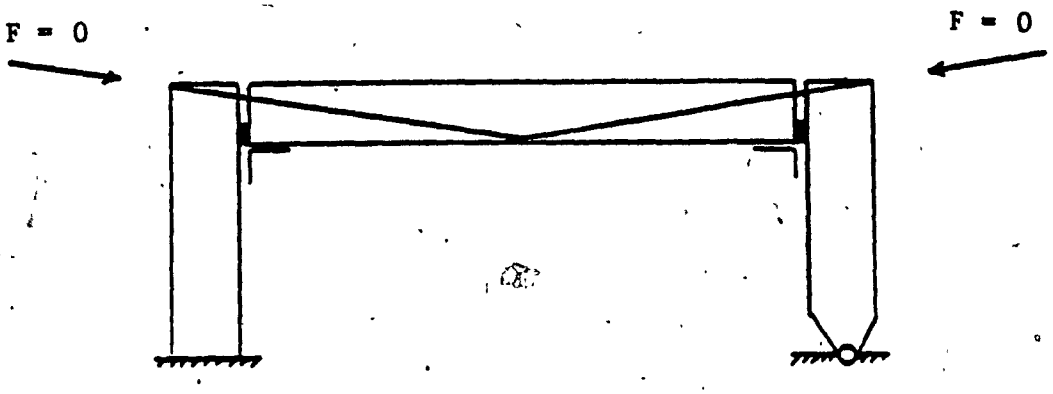

Figure 3-1 The pretensioning force is zero (assume the beam is weightless)

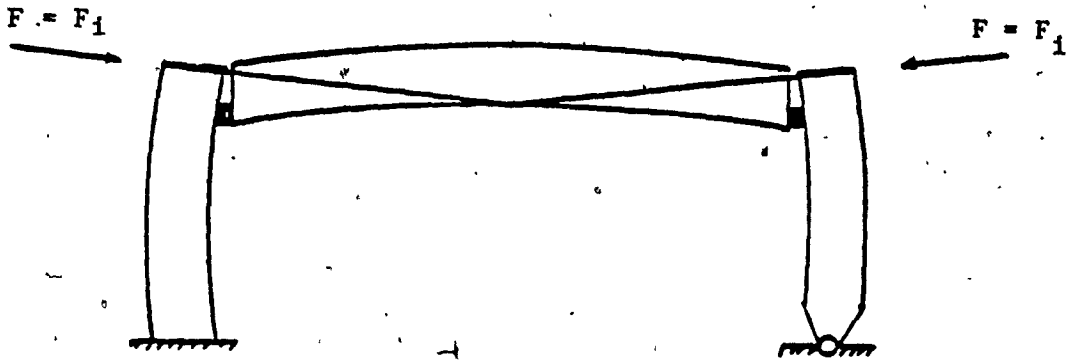

Figure 3-2 The initial force in the cable is the pretensioning force F_i

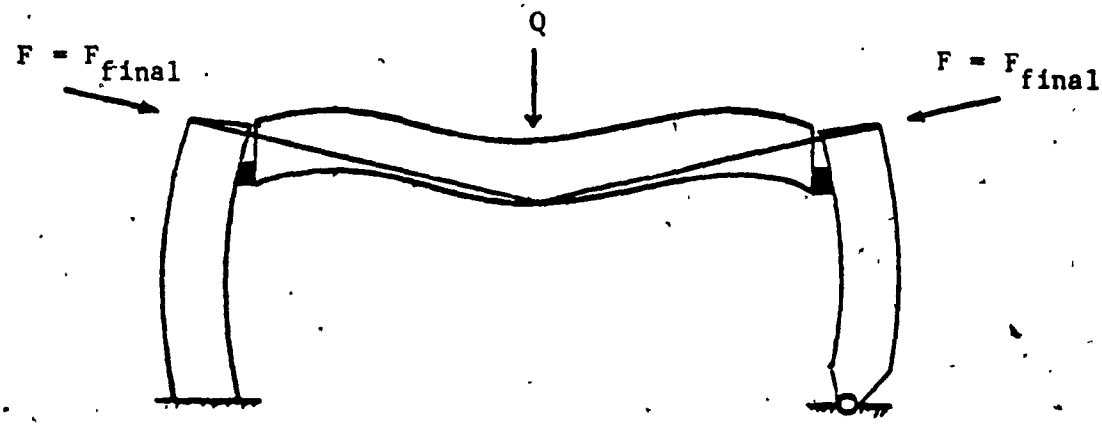

Figure 3-3 After the application of the service load, the final force F_{final} will act on the cable

eccentricity of the initial horizontal compression force P_i and M2 due to the initial vertical force V_i, see Figure 3-4.

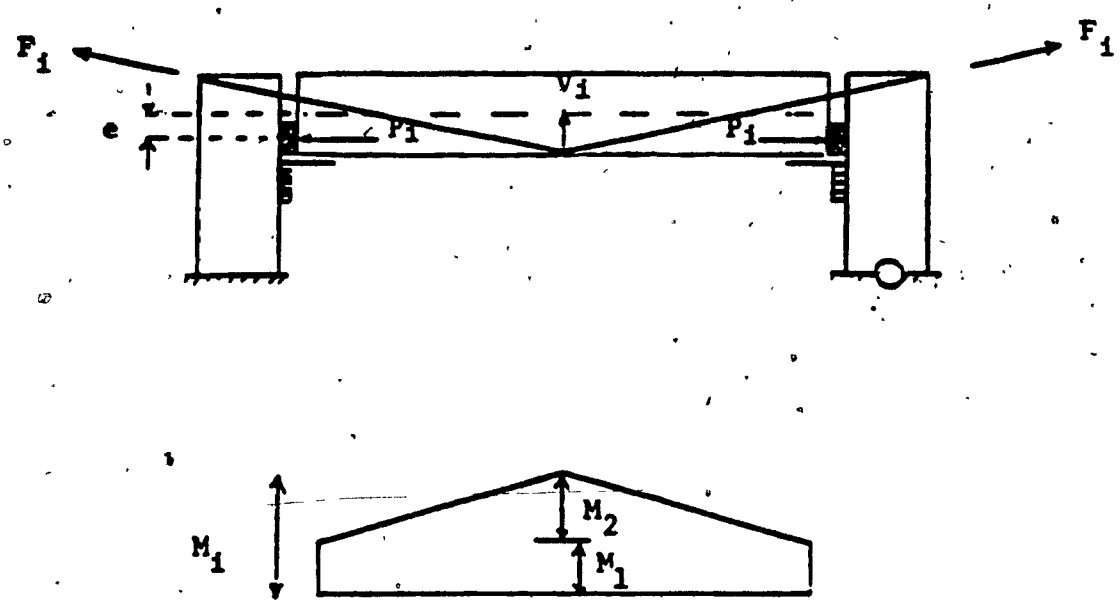

Figure 3-4 Initial B.M.D. on the horizontal member

the two columns and not in any way attached to the columns by means of cables, it will behave as a simply supported beam. Thus, due to the application of the concentrated load Q on this simply supported member, the bending moment M_q will be as shown in Figure 3-5 (assuming the beam is weightless, however in practice M_q should include the bending moment due to the dead load of the beam as in example no. 1)

However, in reality the addition of the external load Q will increase the initial pretensioning force F_i which in turn will become the final tensioning force F that is acting in the cable. Consequently, the initial values of P_i and V_i will increase to reach the final values P and V

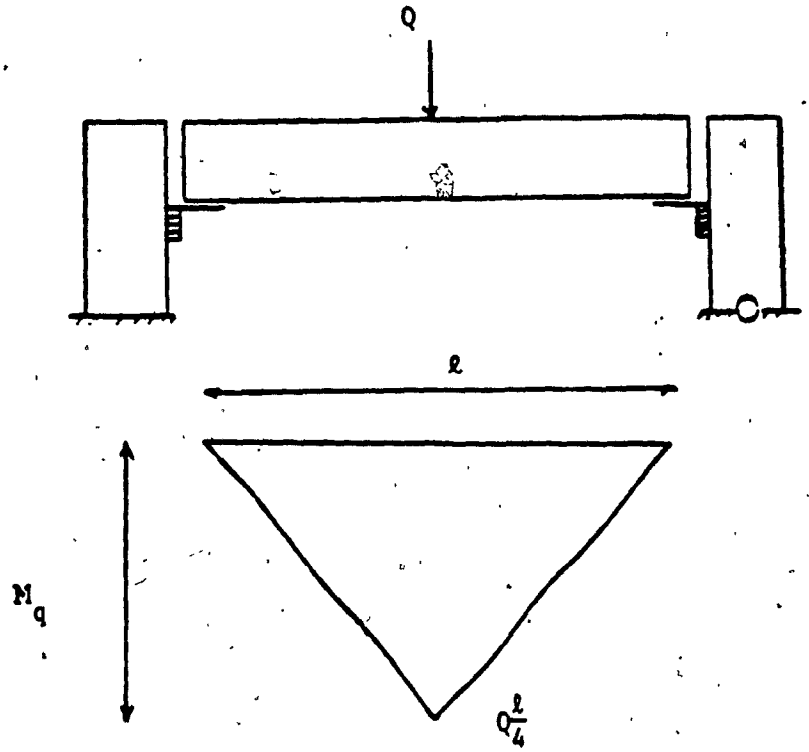

Figure 3-5 The B.M.D. due to Q on simply supported beam

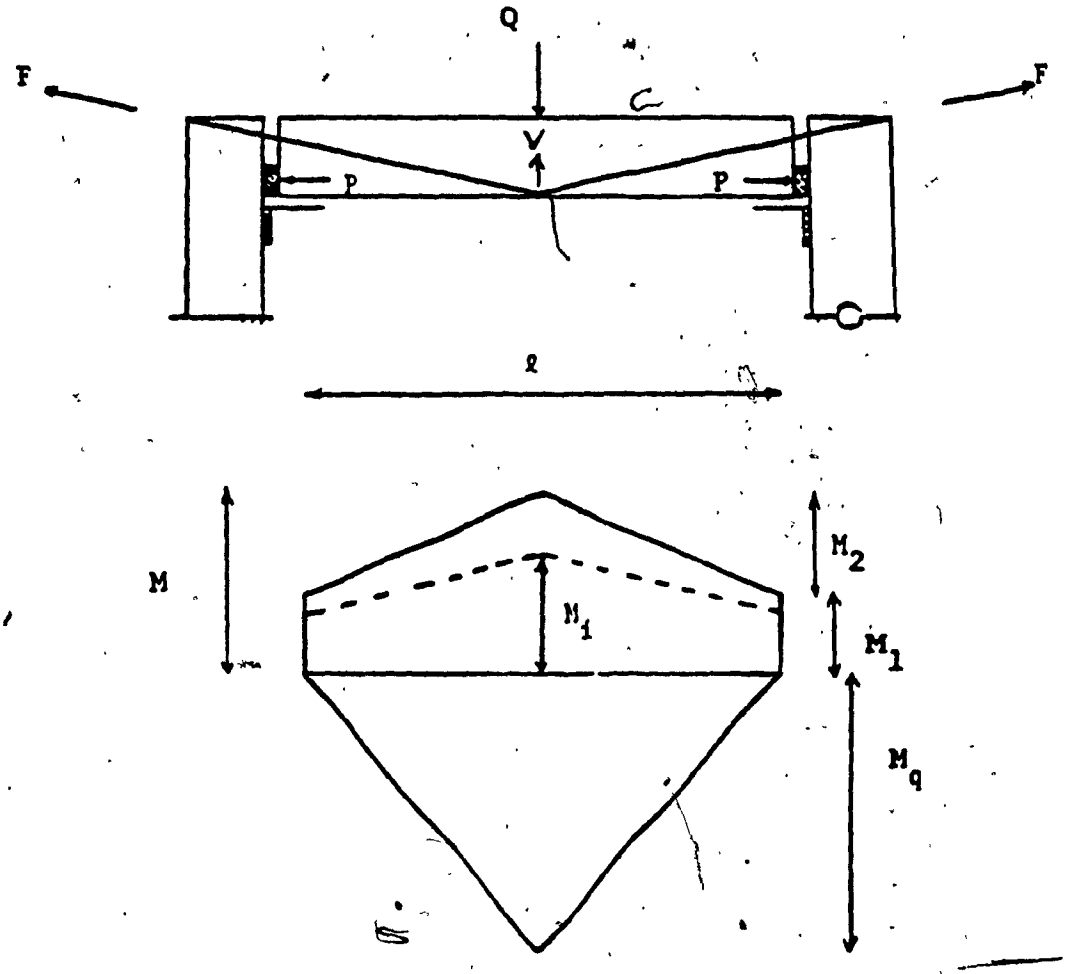

Figure 3-6 The B.M.D. due to F, Q and V

respectively.

Due to the increasing of P_i and V_i, the initial bending moment M_i will increase also to become M, see Figure 3-6. The bending moment M, due to the final values of P and V will act simultaneously with the bending moment M_q. The bending moment produced by Q and the final values of P and V are represented in Figure 3-6.

By using the principle of superposition, the final bending moment M_f at midspan of the horizontal member will be as follows, see Figure 3-7 below.

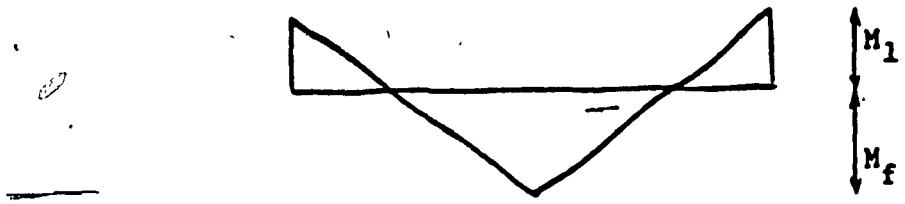

Figure 3-7 The final bending moment on the horizontal member

By comparing Figure 3-7 and Figure 3-4, we can conclude that it will be desirable for economic purposes if:

$$M_i = M_f \qquad (3.1)$$

If $M_i > M_f$ and the service load Q is absent, the horizontal member will be heavily reinforced at the top fibers at midspan to resist the initial bending moment M_i.

Also if $M_f > M_i$, the beam is not fully preloaded, which will require heavily reinforcing in the bottom fibers

of the cross section at midspan.

But if $M_i = M_f$, the member at midspan will require equal reinforcement at the top and bottom fibers, which is very desirable since the member is subjected to a compression force acting eccentrically at both ends, also subjected to a bending moments at midspan and near the ends. Therefore, this member behaves as eccentricity loaded column.

As has been mentioned above, due to the application of Q, the value of the bending moment M_i will increase to become M, see Figure 3-6. For small angle θ, this increment varies between 30% to 40% of M_i, as will be seen later in Example No. 1. Supposing this increment is 35% of M_i, the following will be obtained,

$$M \approx 1.35\ M_i \qquad (3.2)$$

Using Figures 3-6 and 3-7, the final bending moment M_f at midspan will be as follows:

$$M_f \approx M_q - M \qquad (3.3)$$

Using Equations (3.1), (3.2) and (3.3):

$$M_i \approx M_q - 1.35\ M_i$$

Therefore,

$$M_q \approx 2.35\ M_i$$

i.e.
$$M_i \approx 0.43\ M_q \qquad (3.4)$$

Where M_q is known because Q is given, M_i can be estimated from equation (3.4). From the value of the initial bending moment M_i, the value of the effective pretensioning force F_i can be established. Therefore, the values of the

initial vertical component V_i and the horizontal compression P_i will be known, hence all the initial forces acting on the structure are established.

For design purposes, the cross-section of the horizontal member at midspan will be initially subjected to the bending moment M_i and the compression force P_i. However, after applying the concentrated load Q, this cross-section will be subjected to the final bending moment M_f and the final compression force P. As mentioned in equation (3.1), M_i and M_f are equal in value but opposite in direction. It is also recognized that $P > P_i$.

The use of the interaction diagram to design the cross section will be most useful. The values of M_i, P_i, M_f and P are located in the diagram shown in Figure 3-8.

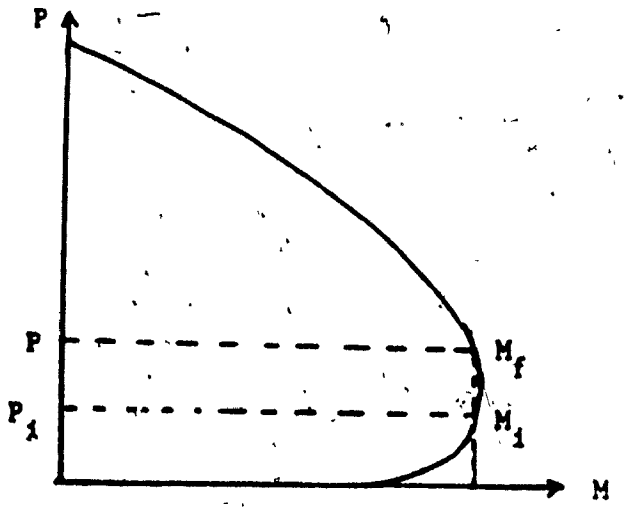

Figure 3-8 The interaction diagram

Using figure 3-8, the cross section of the horizontal

member at midspan can be designed as a beam-column in tension controls region using the value of P_i and M_i. When the exact values of P and M_f are known, this cross-section can be checked for the last two values in compression controls region.

3.3 <u>The Increment in the Pretensioning Force Fi</u>

The deflection of the horizontal member will be considered to define the increment in the pretensioning force F_i, when applying the service load.

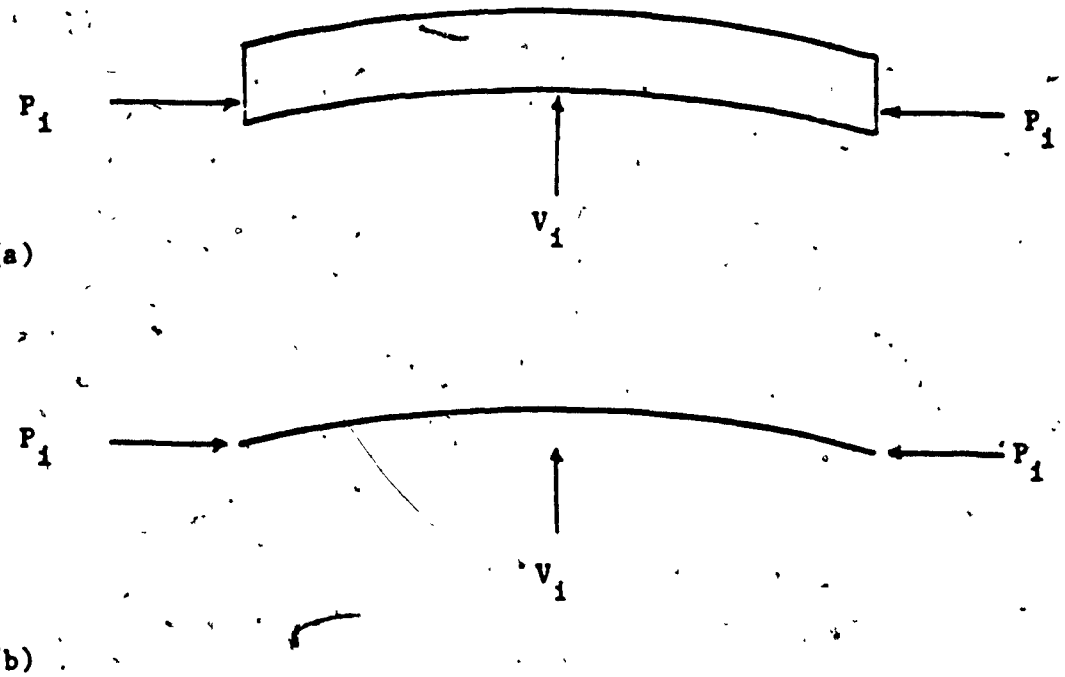

Figure 3-9 (a) The behaviour of the horizontal member due to the action of F_i

(b) The corresponding elastic line

The deflection of the horizontal member due to F_i will be as shown in Figure 3-9, however after applying the

external load Q, the values of P_i and V_i will increase by the values of ΔP and ΔV respectively, as shown in Figure 3-10.

In comparing Figure 3-10 and Figure 3-9, we can conclude that: the deflection of the member at midspan will equal the deflection of the cable at midspan. The value of the changing in the deflection between the initial and final cases is δ, see Figure 3-10. The change in deflection of the member will be due to ΔP, ΔV and Q which can be represented by the following equation.

$$\delta_q . Q - \delta_v . \Delta V - \delta_p . \Delta P = \delta . 1 \qquad (3.5)$$

where:

δ_q = the deflection at midspan due to unit value of Q.

δ_v = the deflection at midspan due to unit value of ΔV.

δ_p = the deflection at midspan due to unit value of ΔP.

δ = the total deflection at midspan.

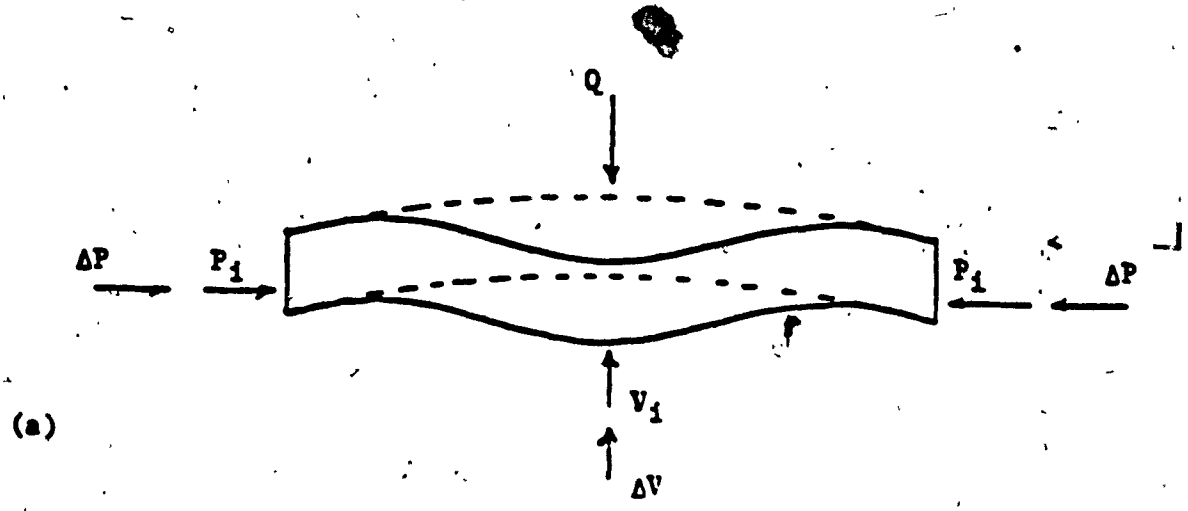

Figure 3-10 (a) The behaviour of the horizontal member due to the action of the final forces

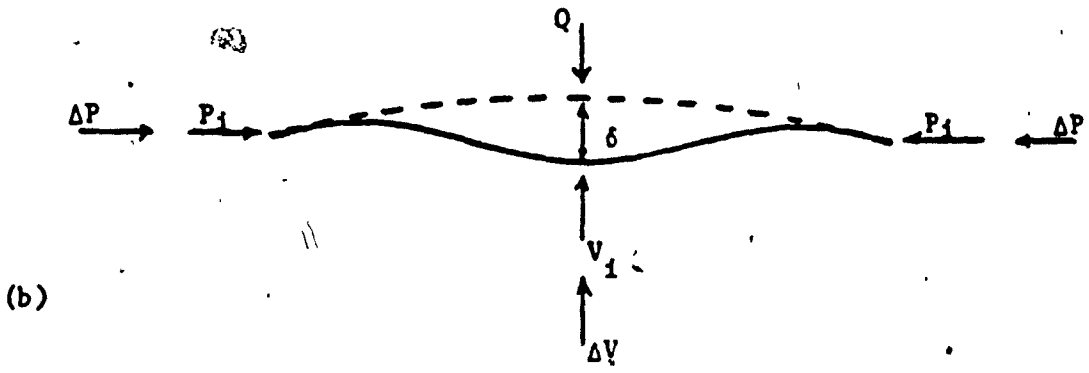

(b)

(b) The corresponding elastic line

At midspan, the deflection of the cable will be also δ and this deflection is due to ΔV only. From equation (1.3) the deflection δ of the cable will be as follows:

$$\Delta V \cdot C_d = \delta \qquad (3.6)$$

By considering equations (3.5) and (3.6), the deflection's equation can be written as follows:

$$\delta_q \cdot Q - \delta_V \cdot \Delta V - \delta_p \cdot \delta P = \Delta V \cdot C_d \qquad (3.7)$$

Since

$$\left.\begin{aligned} \Delta V &= f(\Delta F) \\ \Delta P &= f(\Delta F, Q) \end{aligned}\right] \qquad (3.8)$$

ΔV and ΔP can be substituted by ΔF and Q in equation (3.7), where ΔF is the increment of the force acting in the cable. As it can be seen, the value of ΔF will be the only unknown in that equation. By solving equation (3.7), the value of ΔF will be known. Substituting in equation (3.8), the values of ΔV and ΔP will also be known.

The loss in the force acting in the cable, due to the increment ΔF, will be discussed in the next section. Upon knowing the loss in the increment ΔF, the net values of ΔV and ΔP can be calculated, and all the final forces acting on the member are known. The values of P, V and F are as follows:

$$\left.\begin{aligned} F &= \Delta F + F_i \\ P &= \Delta P + P_i \\ V &= \Delta V + V_i \end{aligned}\right] \quad \ldots\ldots\ldots\ldots\ldots\ldots\ldots\ldots (3.9)$$

where:

ΔF, ΔP and ΔV are the increments after the application of the service load Q.

By knowing the final values P and V, the exact value of the final bending moment M_f can be estimated. Therefore, the cross section of the member at midspan can be checked for the values M_f and P, as shown in the interaction diagram (Figure 3-8).

3-4. Loss Of Preload

The loss in this system will be calculated in two

stages:

1. The initial loss due to F_1
2. The increment of the loss due to the increment of the tensioning force by ΔF

For a concrete member and steel cables, it is difficult to generalize the amount of losses, because they depend upon various factors such as : the properties of concrete and steel, curing and moisture conditions, magnitude and time of application the initial pretensioning force to magnitude and time of application the external loads and the process of tensioning the cables.

If we consider the horizontal member, these losses will be due to elastic shortening(26), creep and shrinkage of concrete. For the cables, the loss will be due to relaxation (2)(9). When considering the columns, their deflection must be taken into account. Since the losses due to creep, shrinkage and relaxation are time dependent. They should be calculated once, based on the final value of the tension force F that act on the cable.

After applying the initial pretensioning force F_1, losses due to shortening of the beam and deflection of the columns will take place. However, after the application of the external load there will be increments in the shortening and in the deflection. These increments will produce increases in the losses which must be taken into account.

If we have more than one tendon and the tendons are

stressed in succession, then the initial stretching is gradually applied. The shortening of the beam and the deflection of the columns will increase as each cable is tightened and the loss of the stretching force due to the shortening and the deflection differ in the tendons. The tendon that is first tensioned would suffer the maximum amount of loss due to the shortening and the deflection by the subsequent application of tensioning from all the other tendons. The tendon that is tensioned last will not suffer any loss, since all shortening and deflection will have already taken place when the stretching force has been measured.

The loss due to the deflection of the columns will be as shown in Figure 3-11.

The deflection of the columns shown in Figure 3-11 will occur due to Fi and this deflection will increase due to ΔF.

If there is only a single tendon in each side of the horizontal concrete member and these tendons are stretched simultaneously, the horizontal concrete member will shorten and the columns will deflect during the time of jacking. Since the force in the cable is measured after the elastic shortening of the horizontal member and after the deflection of the columns have taken place, no loss in the tensioning force due to these shortening and deflection need be accounted for.

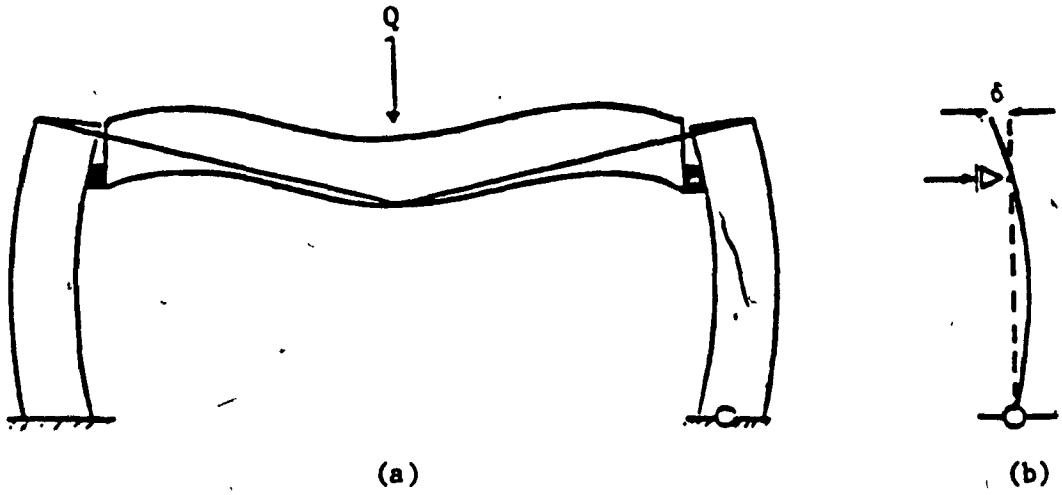

Figure 3-11 (a) The deflection of the columns

(b) The elastic line of the right side column showing the deflection δ at the top of the column

If the cables are pretensioned in succession, it is difficult to calculate the exact value of any losses which may occur. However, for all practical purposes, the loss for the cable which is first to be prestressed can be determined. The average loss of all the cables can be obtained by using half of the value of the loss for the first cable.

After applying the external load, the loss will increase due to the increase of the shortening and the deflection. The value of the loss will differ for each cable, depending upon the value of the initial stretching force. The total initial stretching force can be divided by the number of cables to get the average initial force in each cable.

The loss will increase due to ΔF, this increment in the loss has to be added to the loss due to the initial stretching to get the final loss due to the total shortening

and the total deflection.

The rest of the losses due to creep and shrinkage of concrete and the relaxation of the steel can be calculated as for the post-tensioning method.

EXAMPLE NO. 1

Determine the pretensioning force F_i, the initial horizontal compression force P_i and the initial vertical reaction V_i at the saddle for the structure shown in Fig.3-12, before the application of the service load Q. Check, if the cross-section A-A (Fig.3-12) can carry M_i and P_i or not. Then, determine the final values of F, P and V after the application of the service load Q = 100 kips. Check again, if the cross-section A-A at midspan can carry the final values of the bending moment M and the compression force P.

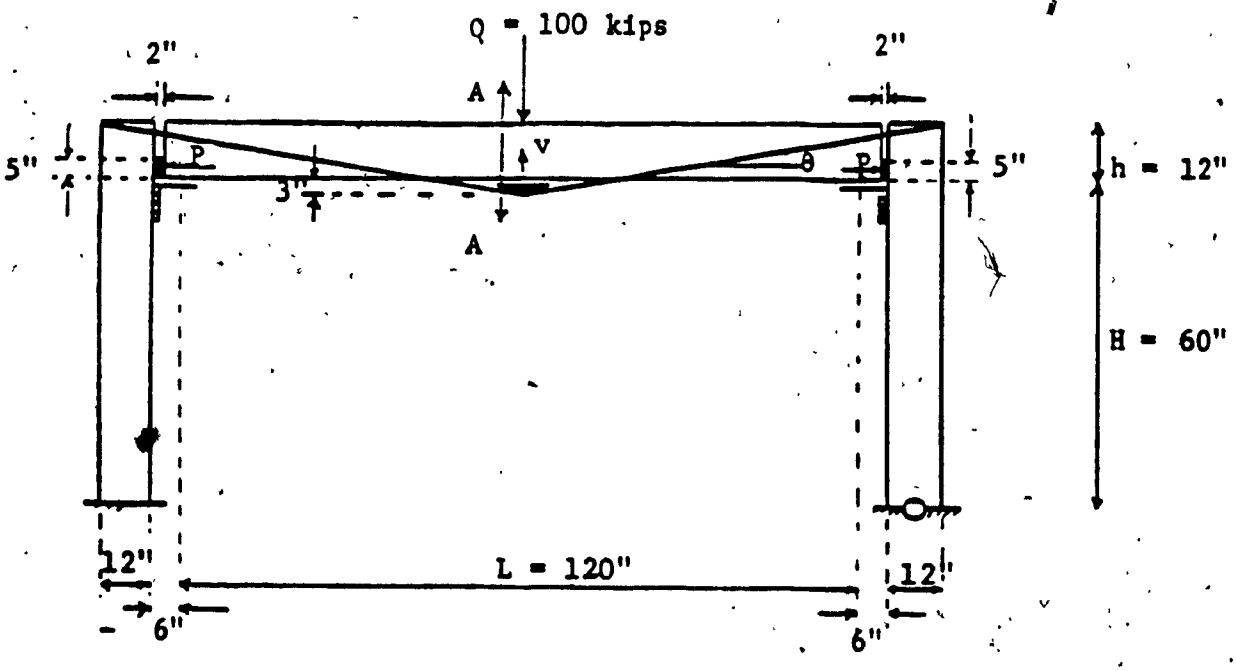

Figure 3-12(a) Preloaded frame

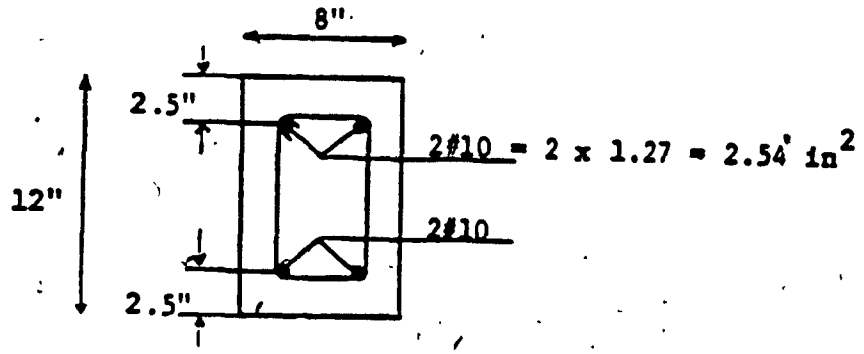

Figure 3-12(b) Cross-section A-A

GIVEN DATA

1 - f'_c = 5000 lb , f_y = 50,000 lb

2 - Using 4 tendons(19), Uncoated Seven Wire Stress Relieved Strand ASTM A-416 grad 250 with diameter of 0.5 in. each, total cross- section area = 4 X 0.144 = 0.576 in² .
and total strength of 4 X 30.6 = 122.4 kips at extension 1%

3 - Design using ACI code(23)(24), the example is free from any overload factors or any capacity reduction factors specified by the code.

4 - The pretensioning force F_i and the final tensioning force F that acting in the cable are the effective values after deducting all the losses.

Solution

The own weight of the beam = $\frac{12 \times 8 \times 145}{12 \times 12 \times 1000}$ = 0.097 kip/ft.

The bending moment due to the own weight of the beam is

$$= 0.097 \times \frac{10^2}{8} = 1.208 \text{ kip-ft.}$$

The bending moment due to Q = $100 \times \frac{10}{4}$ = 250 kip-ft.

The moment at midspan M_q = 250 + 1.288 = 251.208 kip-ft.

From equation (3.4)

$M_i = 0.43\ M_q$

$M_i = 0.43 \times 251.208 = 108.02$ kip-ft.

From Fig. (3-4) and Fig. (3-12)

$$M_i = (P_i \times e) + \left(\frac{V_i \times L}{4}\right)$$

$$= 3.5\ P_i + 30\ V_i \qquad (3.10)$$

From Fig. (3-12)

$\tan\theta = \frac{15}{78} = 0.192$

$\theta = 10.886^\circ$

$\sin\theta = 0.189$

$\cos\theta = 0.982$

Determining F_i, P_i and V_i

Taking the moment about the hinge of all the forces that are acting on the column shown in Fig.(3-13).

$\Sigma M = 0.0$

$M = P_i (2.5 + 60) + F_i \sin\theta (6) + F_i \sin\theta (12)$

$- F_i \cos\theta (12 + 60) = 0.0$

i.e $P_i = 1.077\ F_i$ (3.11)

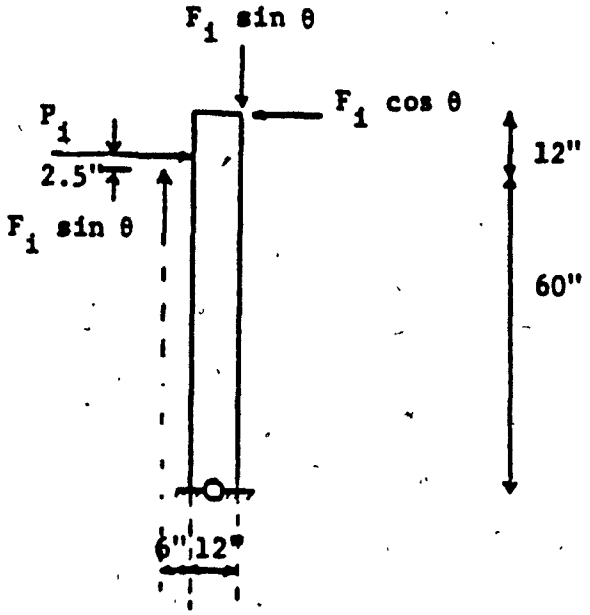

Figure 3-13 The forces acting on the right side column

From Fig. (3-12)

$V_i = 2\ F_i \sin\theta = 0.378\ F_i$

$$\frac{P_i}{V_i} = \frac{1.077\ F_i}{0.378\ F_i} = 2.849$$

$$P_i = 2.849\ V_i \qquad (3.12)$$

Substituting from equation (3.12) into equation (3.10)

$M_i = 9.972\ V_i + 30\ V_i = 108.02 \times 12$ kip-in.

$= 39.972\ V_i = 1296.24$ kip-in.

$$V_i = 32.429 \text{ kips} \qquad (3.13)$$

Substituting from equation (3.13) into equation (3.12)

$$P_i = 2.847 \times 32.429 = 92.389 \text{ kips} \qquad (3.14)$$

Substituting from equation (3.14) into equation (3.11)

$$F_i = 92\ 389/1.077 = 85.784 \text{ kips} \qquad (3.15)$$

Checking the Cross Section at Midspan

The cross section A-A Fig.(3-12) is subjected to initial bending moment M_i=108.02 kip-ft. and initial compression force P_i = 92.389 kip-ft.

$T = A_s f_y = 2.54 \times 50 = 127$ kips

$C_s = A'_s (f_y - 0.85 f'_c) =$

$= 2.54 [50 - (0.85 \times 5)] = 116.205$ kips

$C_c = 0.85 f'_c \beta x b = (0.85)(5)(0.8)(x)(8)$

$= 27.2(x)$

From Fig.(3-14)

$P_i = C_c + C_s - T$

$92.389 = (27.2 x) + 116.205 - 127$

i.e. $x = 3.794$ in.

$a = \beta x = 0.8 \times 3.794 = 3.035$ in.

$C_c = 27.2 x = 27.2 \times 3.794 = 103.184$ kips

Taking the moment about the center line of the cross

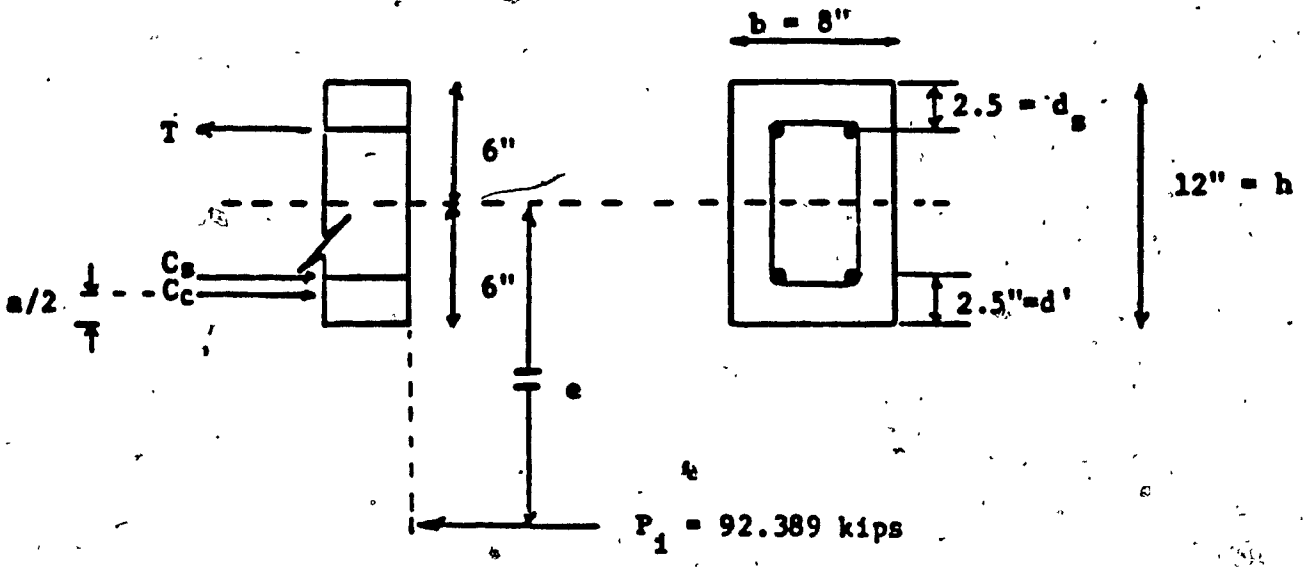

Figure 3-14 Analysis for the section

section area shown in Fig.(3-14), to determine the bending moment that can be carried by that cross section,

$P.e = C_c (h/2 - a/2) + C_s (h/2 - d') + T (h/2 - d_s)$

$= 103.184 (6 - 3.035/2) + 116.205 (6 - 2.5)$

$+ 127 (6 - 2.5) = 1313.74$ kip-in

$P.e = 109.479$ kip-ft. $> M_i = 108.02$ kip-ft.

O.K.

Determining the Final Values of F, P and V

Taking the moment at the hinge (Fig. 3-15) for all the final forces that are acting on the column,

$\Sigma M = 0.0$

$(P_i + \Delta P)(2.5 + 60) + 18(F_i + \Delta F)\sin\theta$

$- (12 + 60)(F_i + \Delta F)\cos\theta - (Q/2)12 = 0.0$

Substituting by the values of F_i and P_i from Equation (3.15) and equation (3.14) into the above equation,

$\Delta P = 1.077\ \Delta F + 9.578$ (3.16)

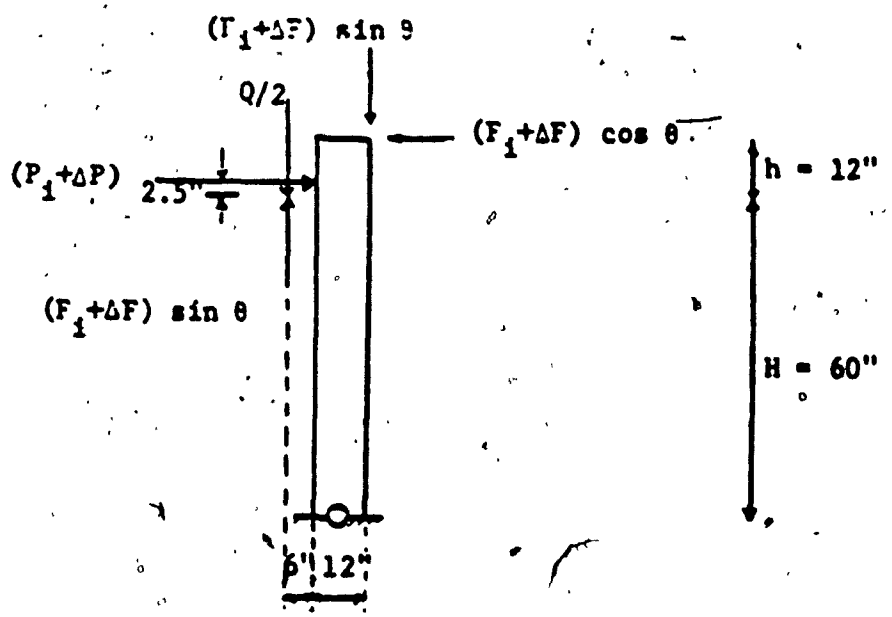

Figure 3-15 The forces acting on the column

From Equation (3.9),

$V = V_1 + \Delta V = 2 (F_1 + \Delta F) \sin\theta$

Substituting by the values of F_1 and V_1 from Equations (3.15) and (3.13) into the above equation,

$\Delta V = 0.378\ \Delta F$ (3.17)

From equation (3.6)

$\delta_q \cdot Q - \delta_v \cdot \Delta V - \delta_p \cdot \Delta P = C_d$

The values of the terms contributing in the above equation are as follow :

$$C_d = \frac{0.5\ S}{2\ A_{ca}\ E_e \sin^2\theta}$$

Where

$$E_e = \frac{E}{1 + \frac{(\gamma\ S_p)^2}{12\ \sigma^2} E}$$

E_e : Equivalent modulus of elasticity for cable having sag

E : modulus of elasticity for the steel of the cable

E : 27,500,000 psi

γ : specific weight of the cable = 0.49 lb/ft for each tendon

S_p : the horizontal projection of the cable = 13.5 ft.

σ : Tensile stress in the cable = 100% form its total strength = 30.6 X 1.00 = 30.6 kips

$$E_e = \frac{27500000}{1 + \left[\frac{(0.49 \times 13.5)^2}{12 \times (30600)^2}\right] 27500000} = 27499903.76 \text{ psi}$$

$0.5\ S = 78.429$ in.

$$C_d = \frac{78.429}{2 \times 0.576 \times 27499903.76 \times (0.189)^2} = 0.000070189 \text{ in.}$$

The modulus of elasticity for the concrete is defined as: $E_c = 57000 (f'_c)^{1/2}$

$= 57000 (5000)^{1/2} = 4030508.653$ psi

The moment of inertia of the cross section of the beam is :

$$I = \frac{b h^3}{12} = \frac{8 \times (12)^3}{12} = 1152 \text{ in}^4$$

i.e. $E_c I = 4643145968 = 0.464 \times 10^{10}$

The downward deflection of the beam, due to Q, is :

$$\delta_q Q = \frac{L^3}{48 E_c I} 100,000 = \frac{(120)^3 \times 100,000}{48 \times 0.464 \times 10^{10}}$$

$= 0.7759$ in.

The upward deflection of the beam, due to ΔV, is

$$\delta_v \Delta V = \frac{L^3}{48 E_c I} 0.378 \Delta F = \frac{(120)^3 \times 0.378 \Delta F}{48 \times 0.464 \times 10^{10}}$$

$= 0.000002932 \Delta F$ in.

The upward deflection of the beam, due to ΔP, is :

$$\delta_p \Delta P = \frac{3.5 L^2}{8 E_c I} \Delta P$$

$$\delta p \Delta P = \frac{3.5 \times (120)^2}{8 \times 0.464 \times 10^{10}} (1.077 \Delta F + 9587)$$

$= 0.000001462 \Delta F + 0.013017$

The downward deflection of the cable, due to ΔV, is :

$C_d \Delta V = 0.00002653 \Delta F$

Substituting by the values of the above equations into equation (3.7).

$0.7759 - 0.000002932 \Delta F - 0.000001462 \Delta F$

$- 0.013017 - 0.000026531 \Delta F = 0.0$

i.e $\Delta F = 24668.812$ lb

ΔF = 24.669 kips

Substituting from the above equation into equation (3.16)

ΔP = 36155.31 lb

= 36.155 kips

Substituting from the above equation into equation (3.17)

ΔV = 9324.811 lb

= 9.325 kips

The final values of F, P and V are :

$F = F_i + \Delta F = 85.784 + 24.669 = 110.453$ kips

$P = P_i + \Delta P = 92.389 + 36.115 = 128.504$ kips

$V = V_i + \Delta V = 32.429 + 9.325 = 41.754$ kips

The final bending moment M_f on the midspan of the beam is :

$M_f = M_q - M_p - M_v$

Where

M_p = The bending moment due to P

M_v = The bending moment due to V

$M_f = 251.208 - (128.504 \times \frac{3.5}{12}) - (41.754 \times \frac{10}{4}) =$

= 109.343 kip-ft.

Checking the cross section at midspan

The cross section at midspan is subjected to a final bending moment M_f and final compression force P have the following values :

M_f = 109.343 kip-ft.

P = 128.504 kips

$T = A_s f_y$ = 2.54 X 50 = 127 kips

$C_s = A'_s (f_y - 0.85 f'_c)$

= 2.54 [50 - (0.85 X 5)] = 116.205 kips

$C_c = 0.85 f'_c \beta x b$ = (0.85) (5) (0.8) (x) (8)

= 27.2 x

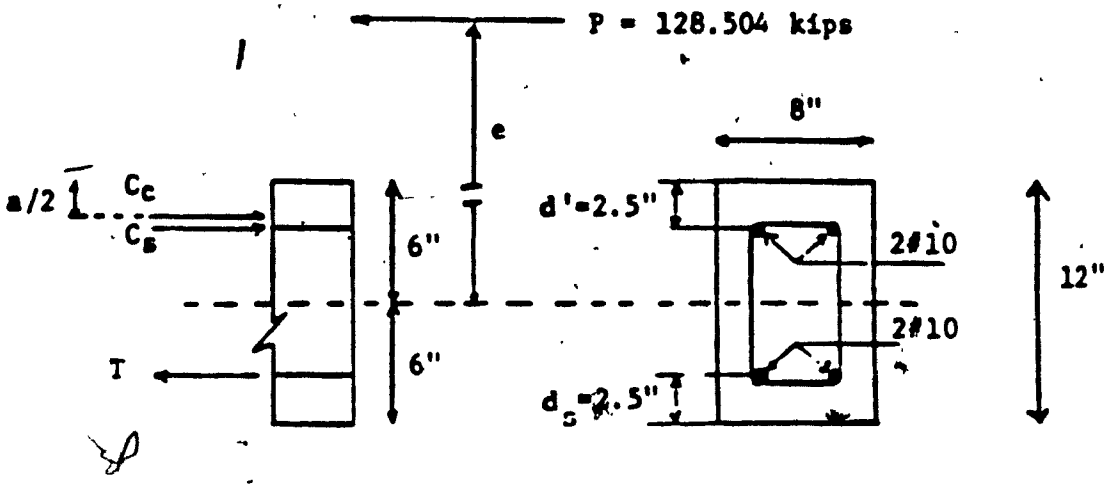

Figure 3-16 Analysis for the section

From Fig. 3-16

$P = C_c + C_s - T$

128.504 = (27.2 x) + 116.205 - 127

i.e. x = 5.121 in.

$a = \beta x$ = 0.8 X 5.121 = 4.097 in.

C_c = 27.2 x = (27.2) (5.121) = 139.299 kips

Taking the bending moment about the center line of the

cross section (Fig. 3-16), to determine the bending moment that can be carried by this cross section.

$$P.e = C_c\,(h/2 - a/2) + C_s\,(h/2 - d_s) + T\,(h/2 - d_s)$$

$$= 139.299\,\left(6 - \frac{4.097}{2}\right) + 116.205\,(6 - 2.5)$$

$$+ 127\,(6 - 2.5) = 1401.656 \text{ kip-in.}$$

$$= 116.805 \text{ kip-ft.} > M_f = 109.343 \text{ kip-ft.}$$

O.K.

CHAPTER 4

CHAPTER 4

UNIFORMLY DISTRIBUTED LOADS

4.1 Cable Response to a Point Load

Several papers have dealt with suspension cable problems and the response of cables to various types of applied loading(1)(3)(6)(7)(10)(11)(22)(25). Since the nineteenth century, it is realized that the response of a cable to applied load is nonlinear: successive equal increments of load were seen to cause successive increments in the corresponding deflection, each smaller than the last. This nonlinear stiffening has been discussed by many authors.

Irvine(11), in his treatment of the response of the cable to the applied load, provided a nonlinear solution and was then able to simplify it to a linearized solution.

The nonlinear solution will be considered for a cable's response to uniformly distributed loads (see Section 4.3). The linearized solution is adopted here as follows. Consider a point load R acting at distance X_1 from the left hand support (Fig. 4-2). The vertical deflection W at any point X is:

$$W = \frac{R}{T} \left[\left(1 - \frac{X_1}{l}\right) X - \frac{t\ l\ mg}{2\ T\ R} X \left(1 - \frac{X}{l}\right) \right] \qquad (4.1)$$

For $0 \leq X \leq X_1$

$$W = \frac{R}{T} \left[X_1 \left(1 - \frac{X}{l}\right) - \frac{t\ l\ mg}{2\ T\ R} X \left(1 - \frac{X}{l}\right) \right] \qquad (4.2)$$

For $X_1 \leq X \leq l$

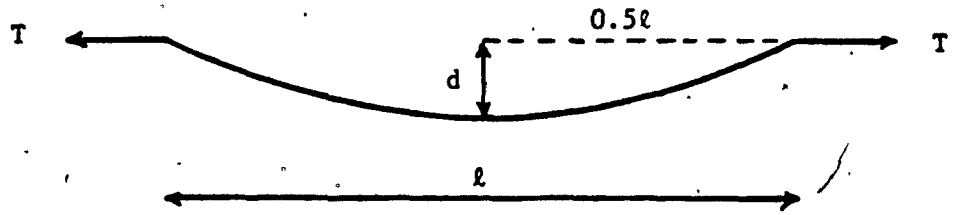

Figure 4-1 Freely hanging cable under its own weight

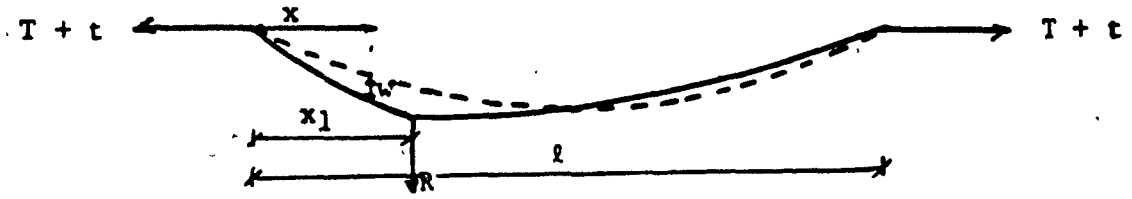

Figure 4-2 Cable response to a point load

Where

$$t = \frac{6\,R\,T}{mg\,l\,(1 + \frac{12}{\lambda^2})} \cdot \frac{X_1}{l}\left(1 - \frac{X_1}{l}\right) \qquad (4.3)$$

And

$$\lambda^2 = \frac{l\left(\frac{mg\,l}{T}\right)^2}{\left(\frac{T\,L_e}{E\,A}\right)}$$

$$L_e = l\left[1 + 8\left(d/l\right)^2\right]$$

Where:

mg = The weight of the cable per unit length.

T = The horizontal component of the cable tension under its own weight.

t = The increment in the horizontal component T owing to the point load R.

R = Point load

l = The distance between the two points, where the cable is suspended

W = The vertical deflection

Equation (4.3) can be simplified as follows:

$$t = \alpha \frac{R\ T}{mg\ l} \qquad (4.4)$$

Where

$$\alpha = \frac{6}{(1 + \frac{12}{\lambda^2})} \cdot \frac{X_1}{l} (1 - \frac{X_1}{l})$$

Substituting from Equation (4.4) into Equations (4.1) and (4.2).

$$W = \frac{R}{T} [(1 - \frac{X_1}{l}) X - \frac{\alpha}{2} X (1 - \frac{X}{l})] \qquad (4.5)$$

For $0 \leq X \leq X_1$

$$W = \frac{R}{T} [X_1 (1 - \frac{X}{l}) - \frac{\alpha}{2} X (1 - \frac{X}{l})] \qquad (4.6)$$

For $X_1 \leq X \leq l$

Equations (4.5) and (4.6) can be reduced to:

$$W = R \beta \qquad (4.7)$$

Where β is the deflection due to a unit point load

$$\beta = \frac{1}{T} [(1 - \frac{X_1}{l}) X_o - \frac{\alpha}{2} X_o (1 - \frac{X_o}{l})]$$

For $0 \leq X_o \leq X_1$

$$\beta = \frac{1}{T} [X_1 (1 - \frac{X_o}{l}) - \frac{\alpha}{2} X_o (1 - \frac{X_o}{l})]$$

For $X_1 \leq X_o \leq l$

4.2 Cable Response to Several Point Loads

If more than one point load is acting on the cable,

the total vertical deflection W_O at distance X_O can be derived using the previous principles for a single point load. Consider two point loads R_1 and R_2 (Fig. 4-2) located at distances X_1 and X_2, respectively. The vertical deflection W_O at distance X_O will be as follows:

$$W_O = W_{O1} + W_{O2}$$

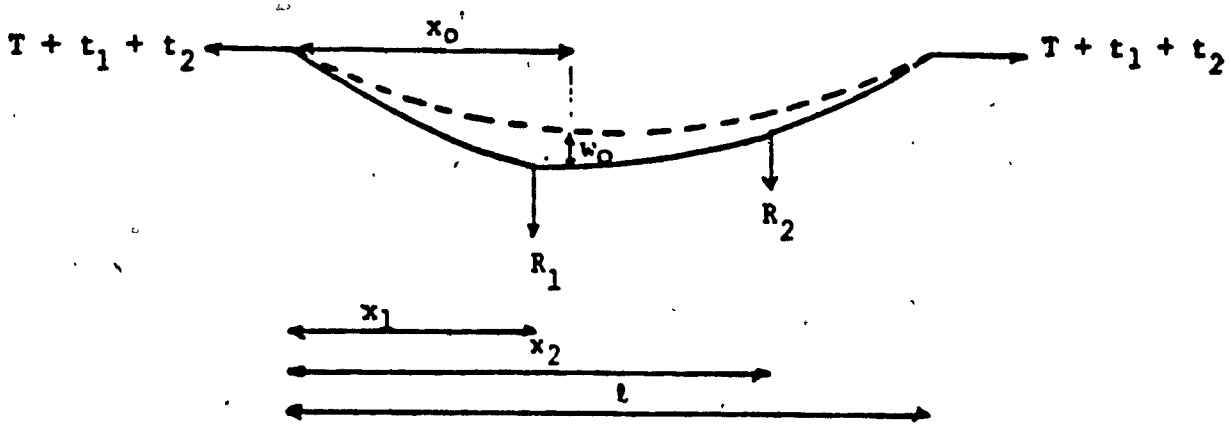

Figure 4-3 Cable response to several point loads

Where:

W_{O1}, W_{O2} = the corresponding deflection due to R_1 and R_2 respectively (the values of W_{O1} and W_{O2} could be positive or negative depending on the value and the location of each load and the location of the measured deflection).

The first subscript refers to the location of the deflection; the second subscript designates the location of the load.

Using Equation (4.7)

$$W_{O1} = R_1 \beta_{O1}$$

Where: β_{O1} is the deflection at location X_O due to a unit load acting at location X_1.

$$\beta_{O1} = \frac{1}{T} \left[X_1 \left(1 - \frac{X_O}{l}\right) - \frac{\alpha_1}{2} X_O \left(1 - \frac{X_O}{l}\right) \right]$$

For $X_1 \leq X_O \leq l$

also:

$$\alpha_1 = \frac{6}{\left(1 + \frac{12}{\lambda^2}\right)} \cdot \frac{X_1}{l} \left(1 - \frac{X_1}{l}\right)$$

$$W_{O2} = R_2 \beta_{O2}$$

Where: β_{O2} is the deflection at location X_O due to a unit load acting at location X_2.

$$\beta_{O2} = \frac{1}{T} \left[\left(1 - \frac{X_2}{l}\right) X_O - \frac{\alpha_2}{2} X_O \left(1 - \frac{X_O}{l}\right) \right]$$

For $0 \leq X_O \leq X_2$

also:

$$\alpha_2 = \frac{6}{\left(1 + \frac{12}{\lambda^2}\right)} \cdot \frac{X_2}{l} \left(1 - \frac{X_2}{l}\right)$$

If there are n point loads $R_1, R_2, \ldots R_n$ the vertical deflection W_O at any distance X_O is:

$$W_O = \sum_{i=1}^{n} W_{Oi} \qquad (4.8)$$

4.3 Cable Response to a Uniformly Distributed Load

The nonlinear solution will be considered for this case. Consider a uniformly distributed load of intensity r

per unit length applied from $X = X_2$ to $X = X_3$ (Fig. 4-4).

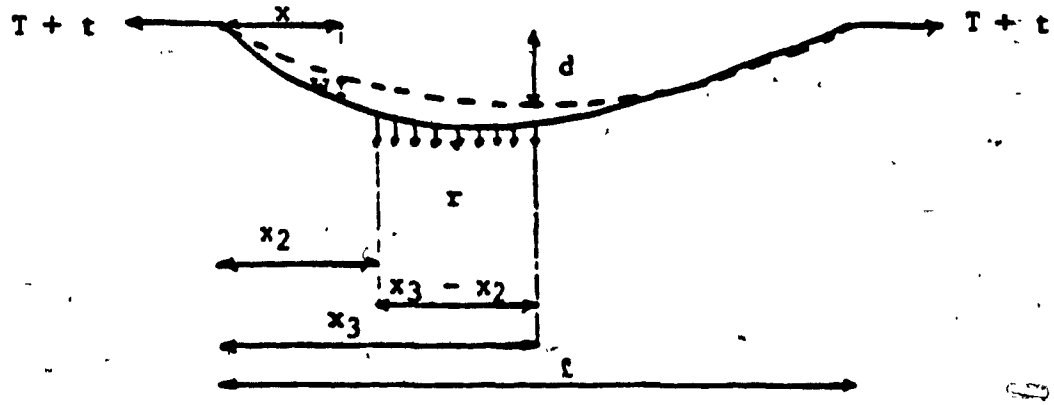

Figure 4-4 Cable response to a distributed load

The vertical deflection W of the cable at distance X is:

$$W = \frac{r}{(T + t)} \left[X (X_3 - X_2) - \frac{X}{2\,l} (X_3^2 - X_2^2) - \frac{t\ l\ mg}{2\ T\ r} X \left(1 - \frac{X}{l}\right) \right] \qquad (4.9)$$

For $0 \leq X \leq X_2$

$$W = \frac{r}{(T + t)} \left[X_3 X - \frac{1}{2} (X_2^2 + X^2) - \frac{X}{2\,l} (X_3^2 - X_2^2) - \frac{t\ l\ mg}{2\ T\ r} X \left(1 - \frac{X}{l}\right) \right] \qquad (4.10)$$

For $X_2 \leq X \leq X_3$

$$W = \frac{r}{(T + t)} \left[\frac{1}{2} (X_3^2 - X_2^2) \left(1 - \frac{X}{l}\right) - \frac{t\ l\ mg}{2\ T\ r} X \left(1 - \frac{X}{l}\right) \right] \qquad (4.11)$$

For $X_3 \leq X \leq 1$

The values of t can be obtained from Tables 2 to 6 taken from Irvine's book *Cable Structures*, included in

Appendix B of this thesis. The values of t in the above-mentioned table are confined to loads spread evenly about the midspan. Table 1 gives the values of t for a point load R.

4.4 Cable Supporting Several Stops (Saddles)

In order to carry a uniformly distributed load using the preloading technique, the parabolic cable profile is recommended. When the cables are placed outside the beam, there are two practicable methods to connect them to the span of the beam. The first is to rest the cable on several saddles in view of obtaining, as much as possible, the required parabolic shape (Fig.4-5). The second is to place the cable inside a groove cut in the beam which has the exact required parabolic profile (Fig.4-6)

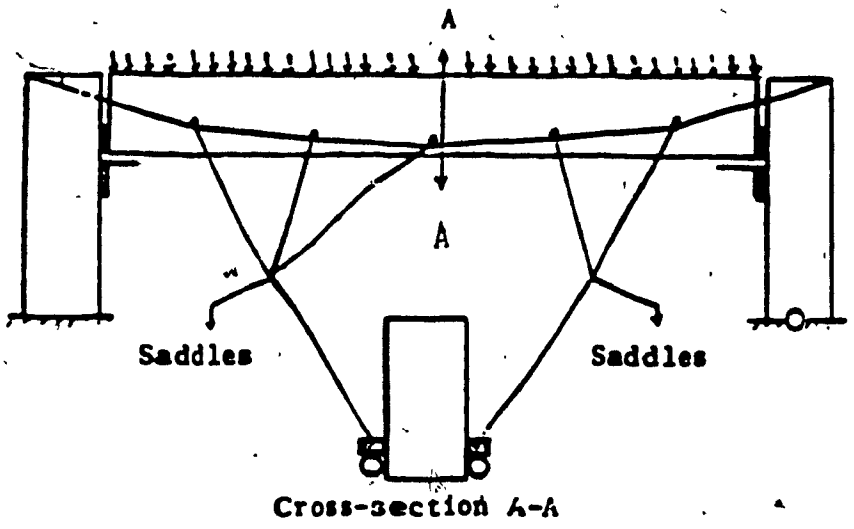

Figure 4-5 Cables resting on several saddles

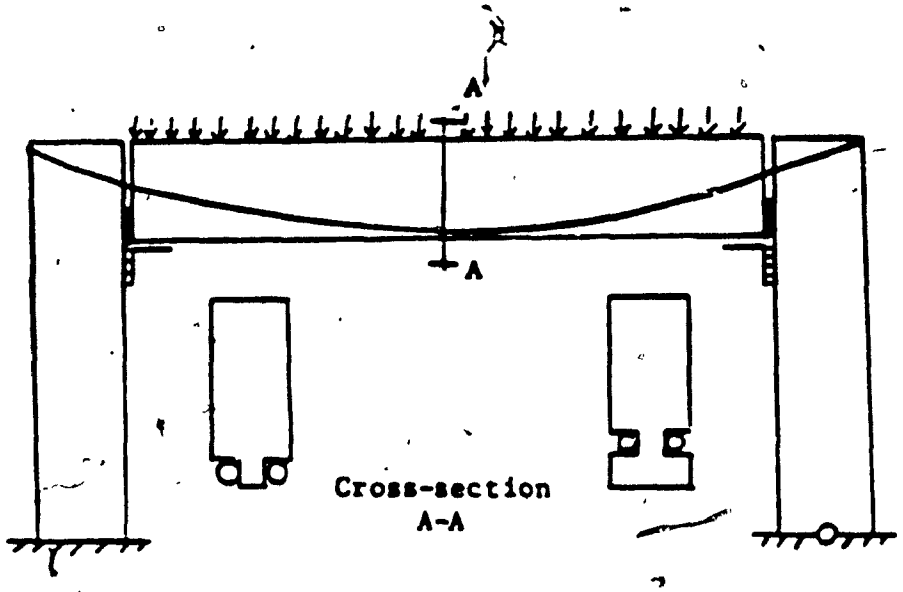

Figure 4-6 Cable placed in groove inside the beam

In this section, the case of using several saddles will be discussed. In Figure 4-7, three saddles are used to support the cable. Assuming the cable has been jacked initially by the force F, the total initial tensioning force in the cable is $(T/\cos\theta) + F$, where $(T/\cos\theta)$ is the force in the cable due to its own weight. Thus, the vertical component of the cable force is $(F \sin\theta) + (1/2\ s\ mg)$, where mg is the self weight of the cable per unit length, and s is the length of the cable. The term $\frac{1}{2}$ s mg represents half the total weight of the cable. The value of T represents the horizontal component due to the weight of the cable and can be determined as follows:

$$(F + T/\cos\theta) \sin\theta = F \sin\theta + 1/2\ s\ mg$$

$$T = \frac{s\ mg}{2\ \tan\theta} \qquad (4.12)$$

It should be recognized that the horizontal member of

this system consists of the cable and the beam. For this stage, the forces that are acting on the cable are analyzed and not the forces that are acting on the beam.

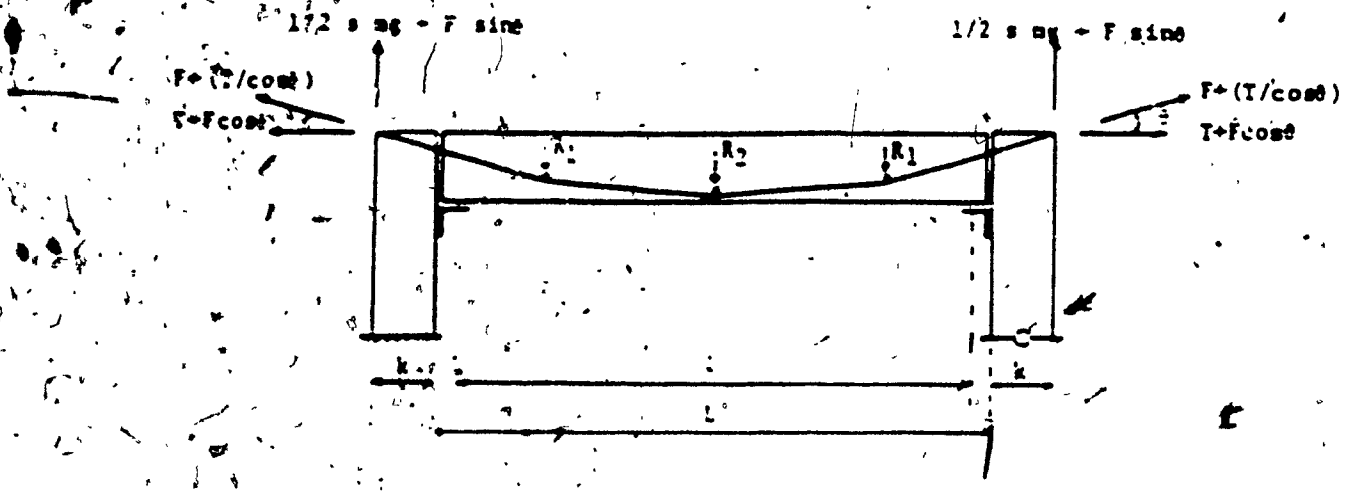

Figure 4-7 The forces acting on the cable due to the initial pretensioning F

To determine the vertical reaction at each saddle, the reaction R_2 at the saddle located at midspan must be analyzed first. The value of this reaction, as shown in Figure 4-8, is $2 (F + T/\cos\theta) \sin\phi$, where ϕ is the inclination angle of the cable with the horizontal plane at midspan.

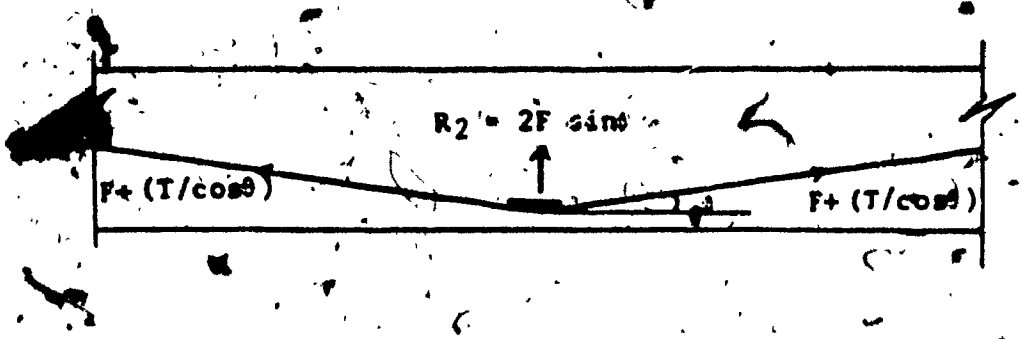

Figure 4-8 The value of the reaction R_2 located at mid-span

Since we are concerned, in this case, with the force acting on the cable and considering the fact that the system is of course in static equilibrium condition. Thus, the saddle at midspan must be acting on the cable by the force R_2. This force is as follows:

$$R_2 = 2 F \sin\phi \qquad (4.13)$$

As shown in Fig.(4-9)

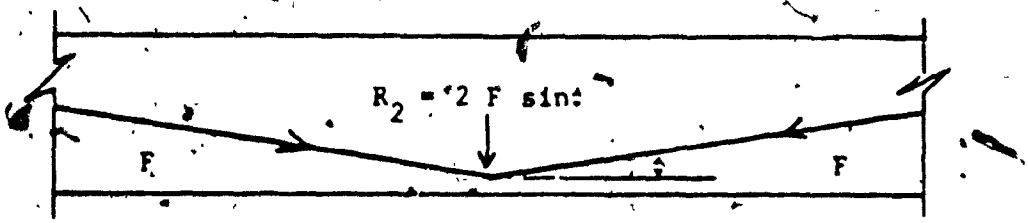

Figure 4-9 The reaction force acting on the cable at mid-span

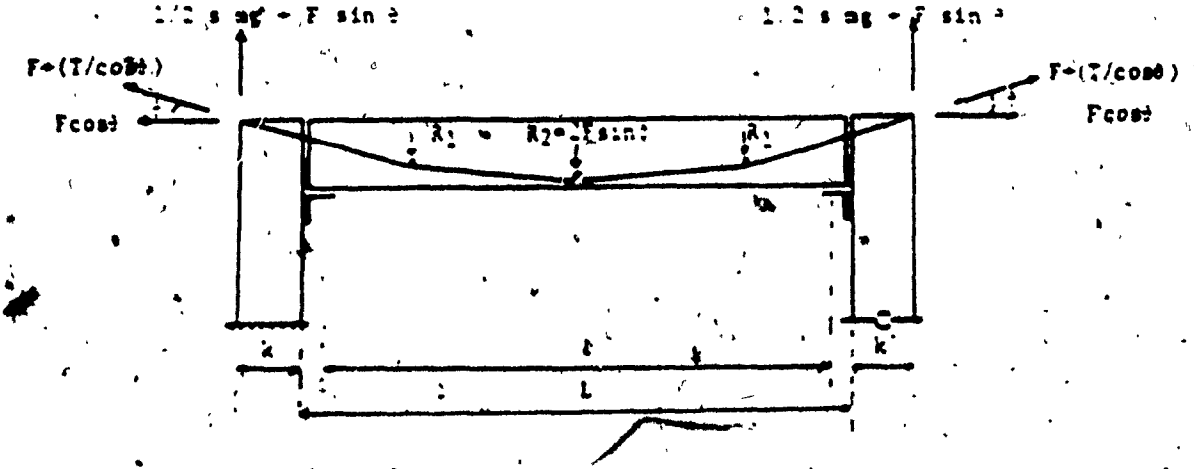

Figure 4-10 The forces acting on the cable due to the initial pretensioning "F"

The saddle on the right and the saddle on the left side (Fig.4-10) are symmetrical and the two forces R_1 and R_1 acting on these saddles are equal as shown in Fig.(4-10).

From equilibrium:

$\Sigma F_y = 0.0$

i.e. $2(1/2\ s\ mg + F \sin\theta) = s\ mg + 2\ F \sin\phi + 2\ R_1$

$2\ F \sin\theta = 2\ F \sin\phi + 2\ R1$

Thus,

$$R_1 = F \sin\theta - F \sin\phi$$

$$R1 = F\ (\sin\theta - \sin\phi) \qquad (4.14)$$

The angles θ and ϕ are known as well as F, thus the value of R_1 can be obtained from Equation (4.14).

If many saddles are used and placed on equal intervals, all the reactions of the saddles can be considered equal. The summation of these reactions nR will be equal to 2 F sinθ, where n is the number of the saddles.

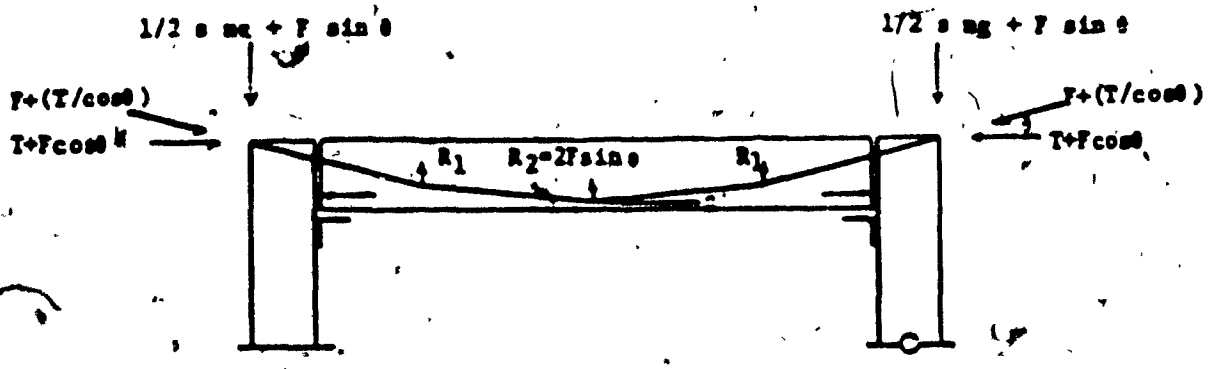

Figure 4-11 The forces acting on the beam and the columns due to the initial pretensioning force F and the weight of the cable

The vertical forces that are acting on the beam and the columns, due to the action of the cable, will be the same forces as those acting on the cable but in the opposite direction, as shown in Fig.(4-11), (compare with Fig.4-10).

To get the initial horizontal force P, the right columns at Figure 4-11 will be analyzed ; as shown in Figure 4-12. Assuming the two vertical forces (1/2 own) and (1/2 R2 + R1) are in intimate contact with the side surface of the columns where P is acting. Which means, there is integral joint, as will be determined in chapter 5.

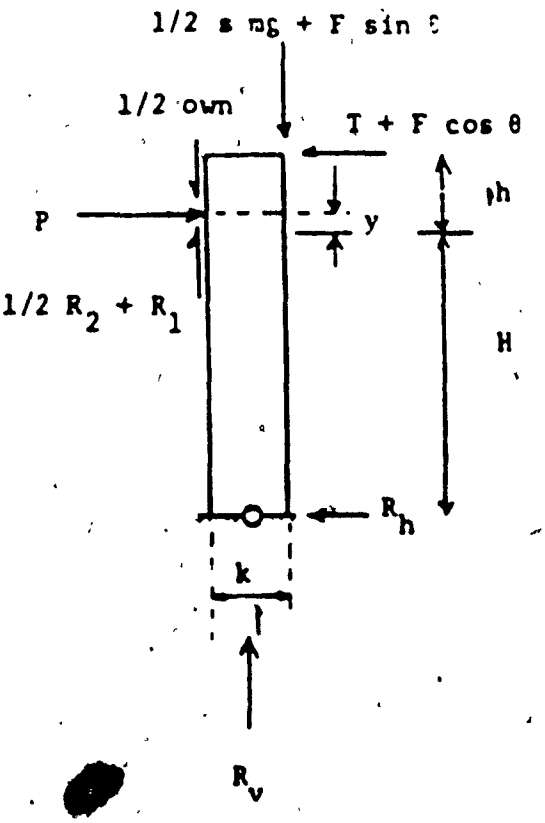

Figure 4-12 The forces acting on the column

By taking the moments at the location of the hinge, where the vertical center line of the column intersects with horizontal line at the bottom of the column (Fig.4-12).

$$\Sigma M = 0.0$$

$$P(y + H) + (\frac{1}{2}R_2 + R_1)\frac{K}{2} + (\frac{1}{2} s\, mg + F \sin\theta)\frac{K}{2}$$

$$= (T + F\cos\theta)(h + H) + (\frac{1}{2}own)\frac{K}{2}$$

Where

own = the own weight of the beam.

$$P = (T + F\cos\theta)(\frac{h + H}{y + H}) + \frac{1}{2}(\frac{K}{y + H})(\frac{1}{2}own - \frac{R_2}{2} - R_1 - \frac{s\, mg}{2} - F\sin\theta) \qquad (4.15)$$

Assuming there is a uniformly distributed load acting on the beam, as shown in Figure 4-13:

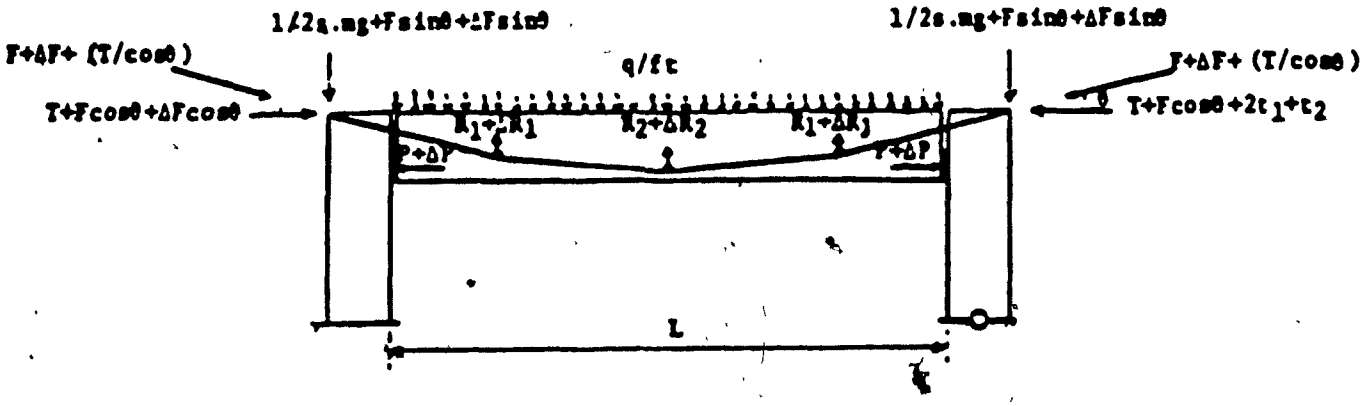

Figure 4-13 Preloaded frame carrying a uniformly distributed load.

Because of the application of the distributed load, the tensioning force F in the cable will increase by the amount

ΔF, also the vertical reactions on the saddles R_1, R_2 and R_1 will increase by the amount ΔR_1, ΔR_2 and $\Delta R1$ respectively. Due to these increments in the reactions ΔR_1, ΔR_2 and ΔR_1 that act on the saddles, there will be increments in the horizontal components of the cable's force at the ends of the cable t_1, t_2 and t_1 respectively (as mentioned in Sections 4.1 and 4.2).

The following equation refers to Figure 4-13.

$$\Delta F \cos\theta = t_2 + 2\, t_1 \qquad (4.16)$$

Also

$$2\, \Delta F \sin\theta = 2\, \Delta R_1 + \Delta R_2 \qquad (4.17)$$

To get the final horizontal compression force (P + ΔP), we will take the moment at the hinge for the column located on the right side (Fig.4-14) as has been done before.

$$\Sigma M = 0.0$$

$$(P + \Delta P)\,(y + H) + [\,0.5(R_2 + \Delta R_2) + R_1 + \Delta R_1]\, K/2 + (1/2\ s\ mg + F \sin\theta + \Delta F \sin\theta)\, K/2 = (T + F\cos\theta + \Delta F \cos\theta)\,(h + H) + (1/2\ q\ L + 1/2\ own)\, K/2$$

Thus,

$$P + \Delta P = \left[(T + F\cos\theta + \Delta F\cos\theta)\left(\frac{h + H}{y + H}\right)\right] + \left(\frac{1}{2}\left(\frac{K}{y + H}\right)\left[\frac{1}{2}own + \frac{1}{2}qL - \frac{1}{2}R_2 - \frac{1}{2}\Delta R_2 - R_1 - \Delta R_1 - \left(\frac{1}{2}s\ mg\right) - F\sin\theta - \Delta F \sin\theta\right]\right) \qquad (4.18)$$

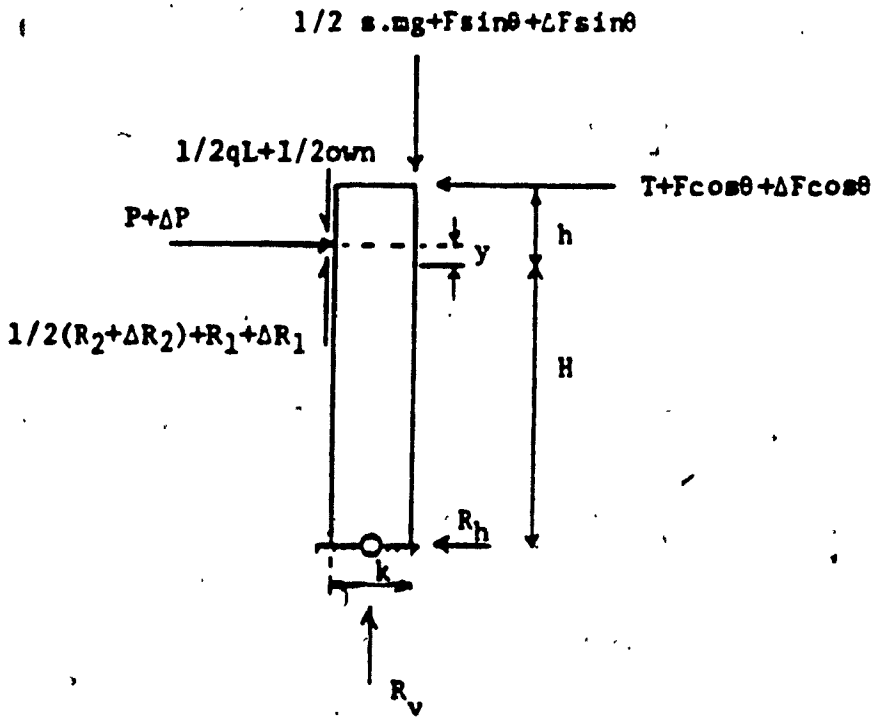

Figure 4-14 The forces acting on the column after the application of the service load

Subtracting Equation (4.15) from Equation (4-18).

$$P = [(\Delta F \cos\Theta)\ (\frac{h + H}{y + H})] + [\frac{1}{2}\ (\frac{K}{y + H})\ (\frac{1}{2}qL - \frac{1}{2}\Delta R_2 - \Delta R_1 - \Delta F \sin\Theta)] \qquad (4.19)$$

Following the same way of Equation (4-13)

$$R_2 + \Delta R_2 = 2\ (F + \Delta F)\ \sin\phi$$

$$\Delta R_2 = 2\ \Delta F \sin\phi \qquad (4.20)$$

From Equation (4.14)

$$\Delta R_1 = \Delta F\ (\ \sin\Theta - \sin\phi\ ) \qquad (4.21)$$

Substituting into equation (4.19) from equations (4.20) and (4.21).

$$\Delta P = (\Delta F \cos\theta)\left(\frac{h + H}{y + H}\right) + \left[\frac{1}{2}\left(\frac{K}{y + H}\right)\left(\frac{1}{2}qL - 2\,\Delta F \sin\theta\right)\right] \qquad (4.22)$$

Equation (4.22) can be rewritten as follows:

$$\Delta P = \Delta F\,(\psi - \zeta) + \eta \qquad (4.23)$$

Where

$$\left.\begin{aligned} \psi &= \left(\frac{h + H}{y + H}\right)\cos\theta \\ \eta &= \frac{1}{4}\,q\,L\left(\frac{k}{y + H}\right) \\ \zeta &= \left(\frac{K}{y + H}\right)\sin\theta \end{aligned}\right] \qquad (4.24)$$

In Equation 4.23 and 4.24 the coefficients ψ, η and ζ are known; the only unknown in this equation is ΔF.

As has been maintained in Chapter 3 Section 3.3, the change in the deflection, at midspan, from the initial condition, before applying the service load, to the final condition, after applying the service load, are due to q, ΔF, ΔP, ΔR_1 and ΔR_2.

The changes of the deflection of the beam at the sections where the saddles are located must be equal to the changes of the deflection of the cable at the corresponding locations (the locations of the saddles).

In Figure 4-15, the changes of the deflection of the beam at Sections 1-1, 2-2 and 3-3 will equal the changes of the deflections of the cable at Sections 1-1, 2-2 and 3-3

respectively.

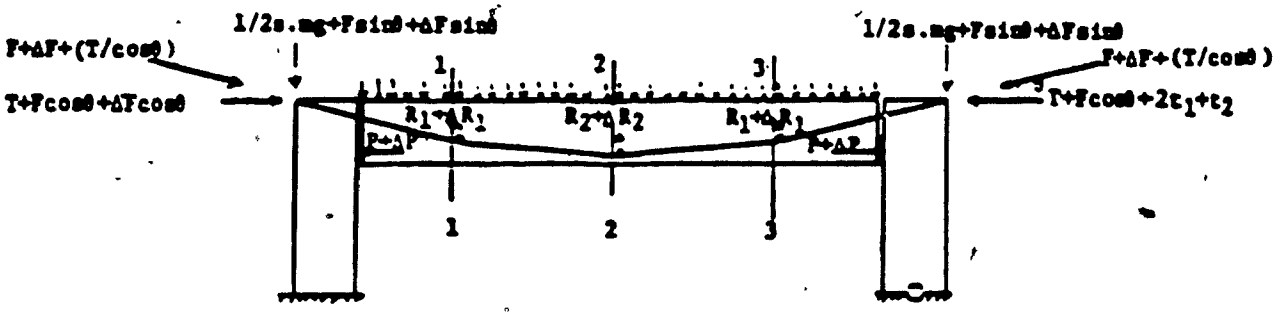

Figure 4-15 Preloaded frame under the final forces

The change of the deflection of the beam at section 1-1 will be as follows:

$$= \delta_{q1} \cdot q - \delta_{p1} \cdot \Delta P - \delta_{r11} \cdot \Delta R_1 - \delta_{r12} \cdot \Delta R_2 - \delta_{r13} \cdot \Delta R_1 \qquad (4.25)$$

where

δ_{q1} : The deflection of the beam at section 1-1 due to a unit distributed load.

δ_{p1} : The deflection of the beam at section 1-1 due to a unit horizontal eccentric axial load acting at the ends of the beams.

δ_{r11} : The deflection of the beam at section 1-1 due to a unit reaction from the saddle located at section 1-1.

δ_{r12} : The deflection of the beam at section 1-1 due to a unit reaction from the saddle located at section 2-2.

δ_{r13} = The deflection of the beam at section 1-1 due to a unit reaction from the saddle located at section 3-3.

The changes of the deflection of the cable at section 1-1, Figure 1-15 will be as follows:

$$= \Delta R_1 \cdot \beta_{11} \pm \Delta R_2 \cdot \beta_{12} \pm \Delta R_1 \cdot \beta_{13} \qquad (4.26)$$

where

β_{11}, β_{12} and β_{13} are the deflections of the cable at sections 1-1 due to a unit point loads acting in sections 1-1, 2-2 and 3-3 respectively (see section 4.2 chapter 4).

Since the change of the deflection of the beam at section 1-1 is equal to the change of the deflection of the cable at the same section and since the linearized solution for the deflection of the cable is adopted, thus equation (4.25) must equal equation (4.26).

$$\delta_{q1} \cdot q - \delta_{p1} \cdot \Delta P - \delta_{r11} \cdot \Delta R_1 - \delta_{r12} \cdot \Delta R_2 - \delta_{r13} \cdot \Delta R_1 = \Delta R_1 \cdot \beta_{11} \pm \Delta R_2 \cdot \beta_{12} \pm \Delta R_1 \cdot \beta_{13} \qquad (4.27)$$

An equation for the change of the deflection at section 2-2 can be also obtained:

$$\delta_{q2} \cdot q - \delta_{p2} \cdot \Delta P - \delta_{r21} \cdot \Delta R_1 - \delta_{r22} \cdot \Delta R_2 - \delta_{r23} \cdot \Delta R_1 = \Delta R_2 \cdot \beta_{22} \pm \Delta R_1 \cdot \beta_{21} \pm \Delta R_1 \cdot \beta_{23} \qquad (4.28)$$

In the above two equations there are three unknown ΔR_1, ΔR_2 and ΔP, thus equations (4.17) and (4.23) will be used.

$$2\,\Delta F \sin\Theta = 2\,\Delta R_1 + \Delta R_2 \qquad (4.17)$$

$$\Delta P = \Delta F.(\psi - \xi) + \eta \qquad (4.23)$$

Rearrange equations (4.17), (4.23), (4.27) and (4.28).

$$\Delta R_1(\delta_{r11}+\delta_{r13}+\beta_{11}\pm\beta_{13}) + \Delta R_2(\delta_{r12}\pm\beta_{12}) + \Delta P.\delta_{p1} + 0.0 = q.\delta_{q1} \quad (4.27)$$

$$\Delta R_1(\delta_{r12}+\delta_{r23}\pm\beta_{21}\pm\beta_{23}) + \Delta R_2(\delta_{r22}\pm\beta_{22}) + \Delta P.\delta_{p2} + 0.0 = q.\delta_{q2} \quad (4.28)$$

$$0.0 + 0.0 + \Delta P - \Delta F(\psi - \zeta) = \eta \quad (4.23)$$

$$\Delta R_1.2 + \Delta R_2 + 0.0 - \Delta F(2\sin\theta) = 0.0 \quad (4.17)$$

The above equations can be transformed to a matrix system as follows:

$$\begin{bmatrix} \delta_{r11}+\delta_{r13}+\beta_{11}\pm\beta_{13} & \delta_{r12}\pm\beta_{12} & \delta_{p1} & 0.0 \\ \delta_{r21}+\delta_{r23}+\beta_{21}\pm\beta_{23} & \delta_{r22}+\beta_{22} & \delta_{p2} & 0.0 \\ 0.0 & 0.0 & 1 & -\psi+\zeta \\ 2 & 1 & 0.0 & -2\sin\theta \end{bmatrix} \begin{bmatrix} \Delta R_1 \\ \Delta R_2 \\ \Delta P \\ \Delta F \end{bmatrix} = \begin{bmatrix} q.\delta_{q1} \\ q.\delta_{q2} \\ \eta \\ 0.0 \end{bmatrix}$$

The above matrix will be considered as equation number(4.29)

By solving the above matrix, the four unknown coefficients ΔR_1, ΔR_2, ΔP and ΔF can be obtained.

Since the system shown in Figure 4-15 is a determinate system and since 3 saddles only are used to simplify the solution, another solution can be used as follows:

Substituting from equations (4.20), (4.21) and (4.23) into equation (4.27).

$\delta_{q1}.q - \delta_{p1}.\Delta F(\psi-\zeta) - \delta_{p1}.\eta - \delta_{r11}.\Delta F(\sin\theta-\sin\phi) -$
$\delta_{r12}.2.\Delta F.\sin\phi - \delta_{r13}.\Delta F(\sin\theta-\sin\phi) = \beta_{11}.\Delta F(\sin\theta-\sin\phi)$
$\pm \beta_{12}.2.\Delta F.\sin\phi \pm \beta_{13}.\Delta F(\sin\theta-\sin\phi)$

The above equation can be rearranged as follows:

$\Delta F[(\sin\theta-\sin\phi)(\beta_{11}\pm\beta_{13}+\delta_{r11}+\delta_{r13}) + \delta_{p1}(\psi-\zeta) +$
$2.\delta_{r12}.\sin\phi \pm \beta_{12}.2.\sin\phi] + \delta_{p1}.\eta - \delta_{q1}.q = 0.0$ (4.30)

In equation (4.30) there is only one unknown ΔF, by solving the above equation ΔF can be obtained. Substituting by the value of ΔF in equations (4.20), (4.21) and (4.23), the values of ΔR_2, ΔR_1 and ΔP are obtained. The same results can be obtained by using equation (4.28) instead of equation (4.27) in the above solution.

Whether the matrix system solution or the solution mentioned above is used, both solutions will depend mainly on the number of saddles and also the availability of the computer.

4.5 Cable Placed with Exact Parabolic Profile

In this section, the analyses of the case in which the cables are placed inside a groove made in the beam will be considered (Fig.4-16). The cable will take the exact required parabolic profile. If the cable is under pretension force F, it will create an upward uniformly distributed reaction on the beam.

where: $r = \frac{8 F d}{L^2}$ (4.31)

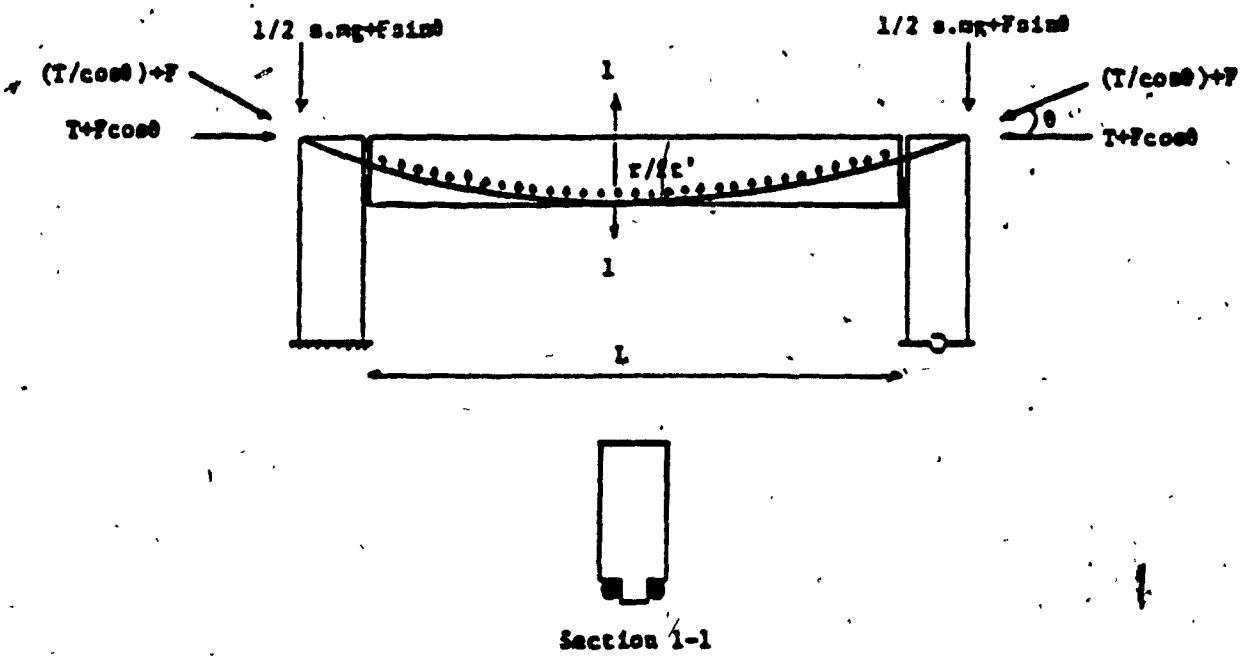

Figure 4-16 The cable placed in groove to have the exact required parabolic profile

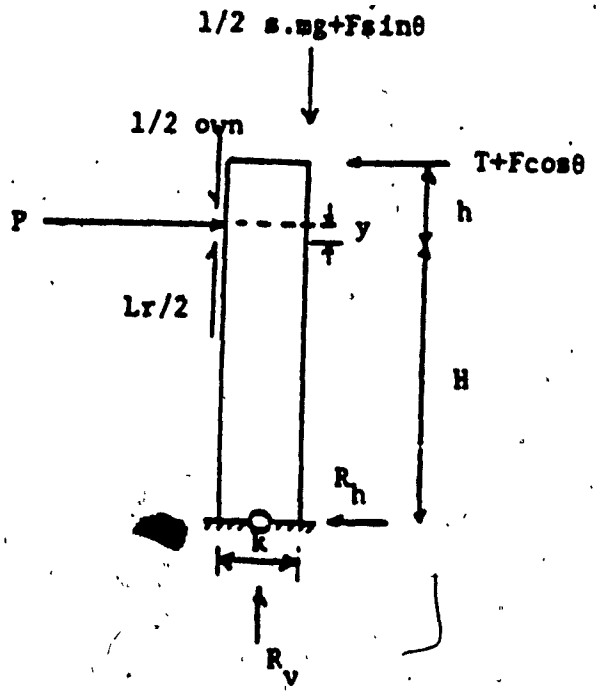

Figure 4-17 The forces acting on the column before the application of the service load

By analyzing the column located at the right side in Figure 4-16 as shown in Figure 4-17, we can obtain the value of P (by taking the moment about the hinge).

$$P = (T + F.\cos\Theta)\left(\frac{h + H}{y + H}\right) + \left(\frac{k}{y + H}\right)\left(\frac{1}{4}\text{own} - \frac{L.r}{4} - \frac{1}{4}.s.mg - \frac{1}{2}.F.\sin\Theta\right) \qquad (4.32)$$

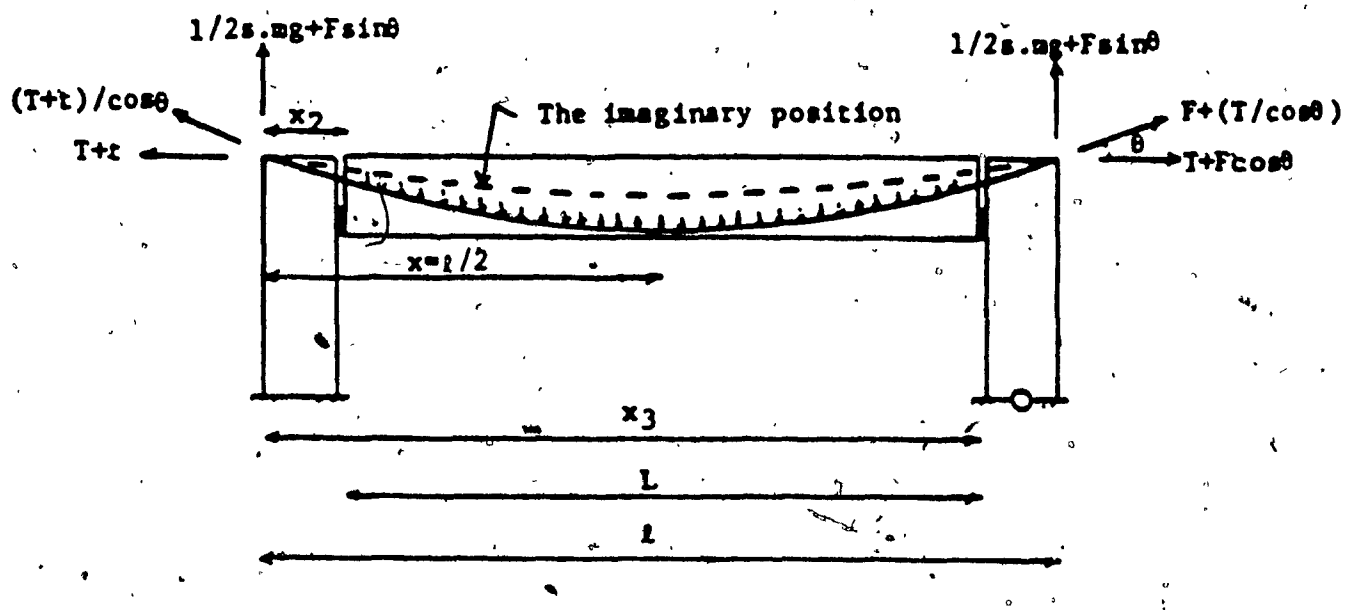

Figure 4-16 The dashed line shows the imaginary position of the cable, if it is freely hanging at the tops of the columns and not loaded

Since the cable is acting on the beam by uniformly distributing reaction r and the system is in equilibrium, thus, the beam on the other hand must be acting on the cable by uniformly distributing load r. If the cable is already

loaded by a uniformly distributed load r, then the cable is already under a certain value of deflection W, which means the original position of the cable, if it is hanging freely at the top of the column, will be located above the present position. (see Figure 4-18).

The deflection of the cable at midspan from its original position (the imaginary position in Figure 4-18) to the real position is given by equation (4.10).

$$W = \frac{r}{(T + t)} \left[X_3 . X - \frac{1}{2}(X_2^2 + X^2) - \frac{X}{2\,l}(X_3^2 - X_2^2) - \frac{t . l . mg}{2 . t . r} X \left(1 - \frac{X}{l}\right) \right] \qquad (4.10)$$

Where

$$T = \frac{s\ mg}{2\ \tan\theta} \qquad (4.12)$$

From Figure 4-18

$$t = F \cos\theta$$

After applying the service load which is the uniformly distributed load q per unit length, the force F in the cable will increase by ΔF, and the uniformly distributed reaction r will increase by Δr. The change in the deflection of the beam at midspan is due to q, Δr and ΔP (see chapter 3 section 3.3 and chapter 4 section 4.4) and the increase of the deflection W of the cable at midspan by the value ΔW is due to Δr. This increase in the cable's deflection will be calculated as follows:

$$(W + \Delta W) - W = \Delta W \qquad (4.33)$$

Since the nonlinear solution is adopted in this section,

therefore the successive equal increments of the distributed load r on the cable will cause successive increments in the corresponding deflection of the cable, each smaller than the last. Hence, the term (W + ΔW) should be calculated as one value and the term W as another value. The difference between the last two values will give the value of the change in the deflection ΔW due to the increment Δr (as in equation 4.33). This change in the cable's deflection should equal the change in the deflection of the beam.

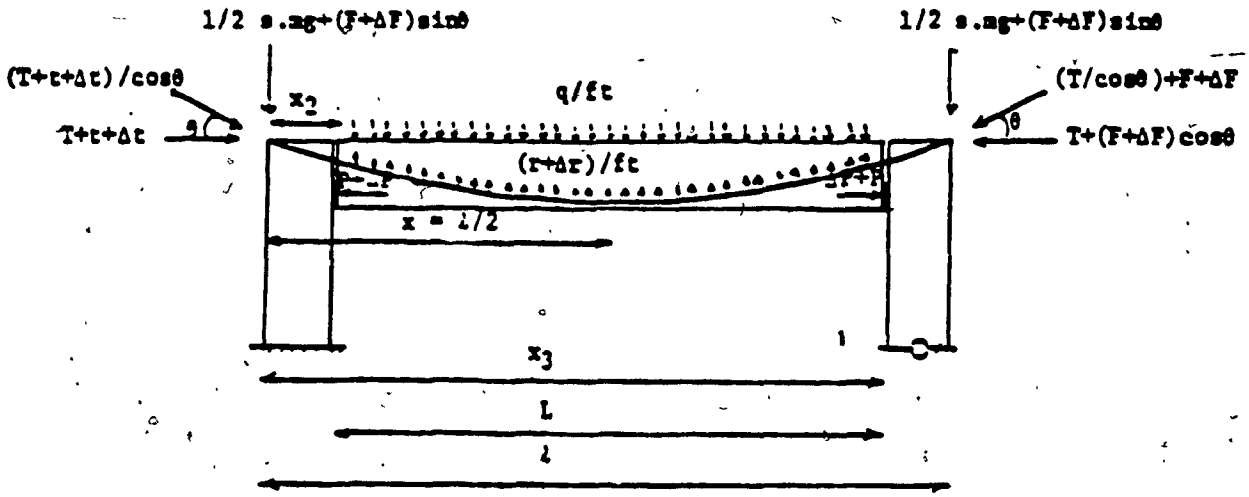

Figure 4-19 Uniformly distributed load acting on a preloaded frame

Figure 4-19 shows all the forces that are acting on the beam and the columns. The problem is how to determine the unknowns ΔF, Δr and ΔP. Let us start by discussing the forces that are acting on the cable. Since the cable is in

equilibrium, the summation of all the vertical forces equals zero:

$$s\,mg + (r + \Delta r)L = 2\left[\frac{1}{2}\,s\,mg + (F + \Delta F)\sin\theta\right]$$

$$(r + \Delta r) = \frac{2\sin\theta}{L}(F + \Delta F) \qquad (4.34)$$

$$\Delta r = \frac{2\sin\theta}{L}(F + \Delta F) - r \qquad (4.35)$$

The summation of the horizontal forces equals zero too:

$$T + (t + \Delta t) = T + (F + \Delta F)\cos\theta$$

$$t + \Delta t = (F + \Delta F)\cos\theta \qquad (4.36)$$

Where

t = The horizontal tension force that acting at the ends of the cable due to the action of the vertical distributed load r.

Δt = The increment in the force t due to the increment Δr in the distributed force r.

By analyzing the column located at the right side in Figure 4-19, as has been done in section 4.4, the value of $P + \Delta P$ can be obtained. Figure 4-20 shows all the forces acting on that column.

If we take the moment at the hinge in Figure 4-20, the value of $P + \Delta P$ is obtained.

$$P + \Delta P = (T + F.\cos\theta + \Delta F.\cos\theta)\left(\frac{h + H}{y + H}\right) +$$

$$\left(\frac{k}{y + H}\right)\left(\frac{1}{4}q.L + \frac{1}{4}own - \frac{L.r}{4} - \frac{L.\Delta r}{4} - \right.$$

$$\left.\frac{1}{4}s.mg - \frac{1}{2}.F.\sin\theta - \frac{1}{2}.\Delta F.\sin\theta\right) \qquad (4.37)$$

Subtracting equation (4.32) from equation (4.37).

$$\Delta P = (\Delta F \cos\theta)\left(\frac{h + H}{y + H}\right) + \left(\frac{1}{4} q.L - \frac{L.\Delta r}{4} - \frac{1}{2}.\Delta F.\sin\theta\right)\left(\frac{K}{y + H}\right) \quad (4.38)$$

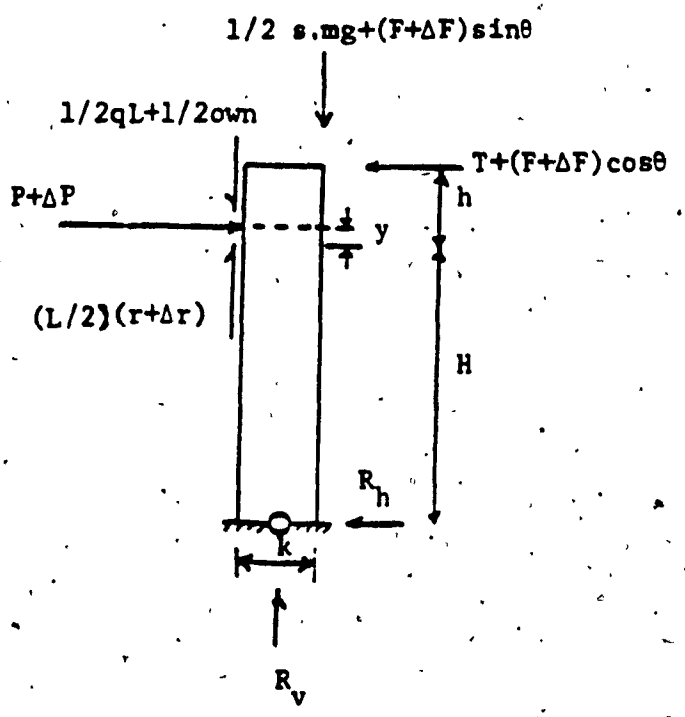

Figure 4-20 The forces acting on the column after the application of the service load

Substituting from equation (4.35) into equation (4.38).

$$\Delta P = \Delta F.\cos\theta\left(\frac{h + H}{y + H}\right) + \left(\frac{K}{y + H}\right)\left(\frac{1}{4} q.L + \frac{L.r}{4} - \frac{1}{2}.F.\overline{\sin\theta} - \Delta F.\sin\theta\right) \quad (4.39)$$

Equation (4.39) can be rewritten as follows:

$$\Delta P = \Delta F(\psi - \zeta) + \eta + \gamma - (1/2)F.\zeta \quad (4.40)$$

Where

$$\left.\begin{aligned} \psi &= \left(\frac{h + H}{y + H}\right)\cos\theta \\ \eta &= \frac{1}{4} q L \left(\frac{K}{y + H}\right) \\ \zeta &= \left(\frac{K}{y + H}\right)\sin\theta \\ y &= \frac{L.r}{4}\left(\frac{K}{y + H}\right) \end{aligned}\right\} \qquad (4.41)$$

Equations (4.41) are the same as equation (4.24) except the coefficient y which is not included in equation (4.24).

The change in the deflection of the beam at midspan will be as follows:

$$\delta_m . q - \delta_m . \Delta r - \delta_p . \Delta P = \delta \qquad (4.42)$$

Where

δ = the change of the deflection of the beam at midspan

δ_m = the deflection of the beam at midspan due to the action of a unit distributed load.

δ_p = the deflection of the beam at midspan due to the action of a unit eccentric axial force.

The change in the deflection of the cable at midspan ΔW will be as mentioned in equation (4.33).

$$(W + \Delta W) - W = \Delta W \qquad (4.33)$$

Since the cable is connected to the beam, the change in the deflection of the beam δ must equal the change in the deflection of the cable.

$$\delta = \Delta W \qquad (4.43)$$

Substituting from equations (4.33) and (4.42) into equation (4.43).

$$\delta_m \cdot q - \delta_m \cdot \Delta r - \delta_p \cdot \Delta P = (W + \Delta W) - W \qquad (4.44)$$

Where the value of $(W + \Delta W)$ can be obtained from equation (4.10) as follows:

$$(W + \Delta W) = \frac{r + \Delta r}{T + (t + \Delta t)} \left[X_3 \cdot X - \frac{1}{2}(X_2'^2 + X'^2) - \frac{X}{2.1}(X_3'^2 - X_2'^2) - \frac{(t + \Delta t) 1 . mg}{2T(r + \Delta r)} \cdot X \cdot (1 - \frac{X}{1}) \right]$$

The above equation will be number ..... (4.45)

Where X, X_2 and X_3 are shown in Figure 4-19.

Substituting from equations (4.34) and (4.36) into equation (4.45).

$$(W + \Delta W) = \frac{2 (F + \Delta F) \sin\Theta}{L [T + (F + \Delta F)\cos\Theta]} \left[X_3 \cdot X - \frac{1}{2}(X_2'^2 + X'^2) - \frac{X}{2.1}(X_3'^2 - X_2'^2) - \frac{L\ 1\ mg\ \tan\Theta}{4\ T} \cdot X \cdot (1 - \frac{X}{1}) \right] \qquad (4.46)$$

Substituting from equation (4.10), (4.35), (4.40) and (4.46) into equation (4.44) will lead to an equation having only one unknown, which is ΔF. By solving this equation, the value of ΔF can be obtained.

It must be recognized that, due to the deflection of the beam, there will be certain change in the value of the angle Θ (see Figure 4-19) which is the angle between the tangent to the cable at its end and the horizontal plane. For a shallow beam, this angle is small, thus the change in this angle will also be very small. Therefore, the

resulting changes on the values of $\sin\theta$, $\cos\theta$ and $\tan\theta$ will be very small and can be omitted, which has been done in the previous analysis.

If ΔF is determined, it can be substituted in equation (4.35) by its value, and the value of Δr can then be obtained. Consequently, if the value of Δr is known, it can be substituted in equation (4.40) by its value, and the value of ΔP can be also obtained.

If ΔF, Δr and ΔP are known, all forces acting on the preloaded frame are known, therefore, all the sections of the preloaded frame can be designed.

CHAPTER 5

CHAPTER 5

BUCKLING, BEARING AND DIFFERENTIAL SETTLEMENT

5.1 Buckling Due To Preloading

Structural engineers are aware of the possibility of buckling of a long compression member of a small cross section area. It is entirely reasonable to question the possibility of buckling of a preloaded member as a result of the compression force action. Obviously, when the compression force is applied by an external load, such as a structure member compressed by abutments, as in the case of preloading, and the tendons are placed externally and are not in contact with the member, the possibility exists that the member may buckle. If buckling does occur, it is essential that this problem be investigated in the conventional manner.

Libby(12) explained in his book about prestressed concrete the relation between the buckling of a prestressed member and the points of contact between the tendons and the member, throughout the length of the member.

Although his explanation referred to a prestressed member, it may also be used as a general explanation for any member compressed directly (prestressed) or indirectly (preloaded) by tendons.

When the tendons are in contact with the member at

points between the ends of the member, the tendency to buckle is reduced significantly. When the tendons are in intimate contact with the member throughout the length of the member, as in certain cases of preloading (section 4.5, Chapter 4), the possibility of buckling will not occur. According to Libby, this fact has been demonstrated both experimentally and mathematically.

For a preloaded member, the possibility of buckling depends mainly on whether or not the tendons are in contact with the member. If the tendons are not in contact with the member, a possibility of buckling exists. If the tendons are in contact with the member at various points between the ends (see section 4.4, Chapter 4), the possibility of buckling is reduced. If the tendons are in intimate contact with the member throughout the length of the member (see section 4.5, Chapter 4), the possibility of buckling is non-existent.

5.2 The Bearing System

Bearings are mechanical devices capable of transmitting loads from the superstructure to the substructure. Bearings have been designed as simple as two steel plates and as complex as precisely machined devices containing numerous parts. Failure of bearings to adequately tie the superstructure to the substructure when subjected to an earthquake force resulted in the collapse of several structures in

southern California in 1971 (13).

A frequent consequence of conventional design practice is the necessity for continual maintenance of bearings in order to prevent deterioration of the superstructure.

Many engineers have concluded that it is better to avoid the problem, when possible, rather than try to solve it. In the case of a preloaded system, it is possible to avoid the use of bearings by utilizing a flexible integral connection between the horizontal member and the columns, as shown in Figure 5-1.

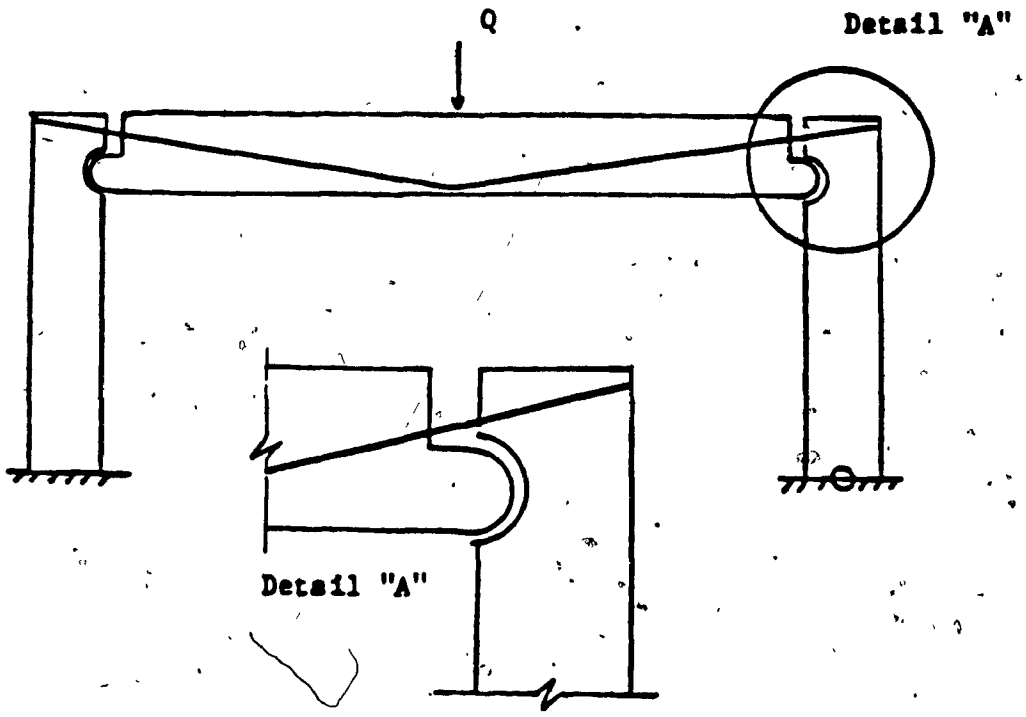

Figure 5-1 Flexible integral connection

This connection can actually perform three functions. The first is to allow rotation (in the following section,

the advantages of rotation are explained). The second function is to transfer a compression force from the columns to act as an axial force on the horizontal member. Thirdly, it transmits the vertical load from the horizontal member to the columns. Following is an analysis of each one of these three functions performed by this type of joint.

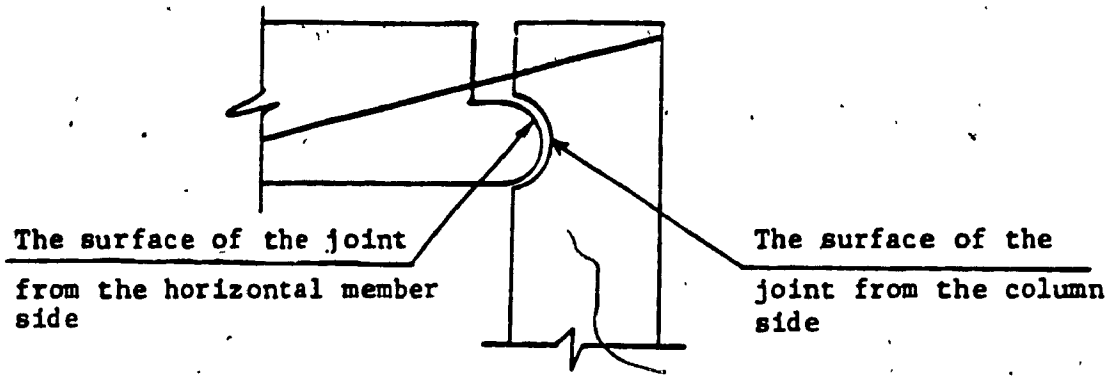

Figure 5-2 The joint between the horizontal member and the column

If the surface of the joint from the side of the column and the side of the horizontal member (Fig. 5-2) are concrete, the rotation between the horizontal member and the columns will not be permitted because of the friction between these two surfaces (the friction coefficient for concrete has a high value). Thus, to allow smooth rotation, these two surfaces should be covered by material for which the coefficient of friction has a low value. The material recommended is Teflon or Neoprene. Teflon (13) has a low coefficient of friction = 0.06. Therefore, it can be used to cover both contact surfaces of this joint (Figure 5-3).

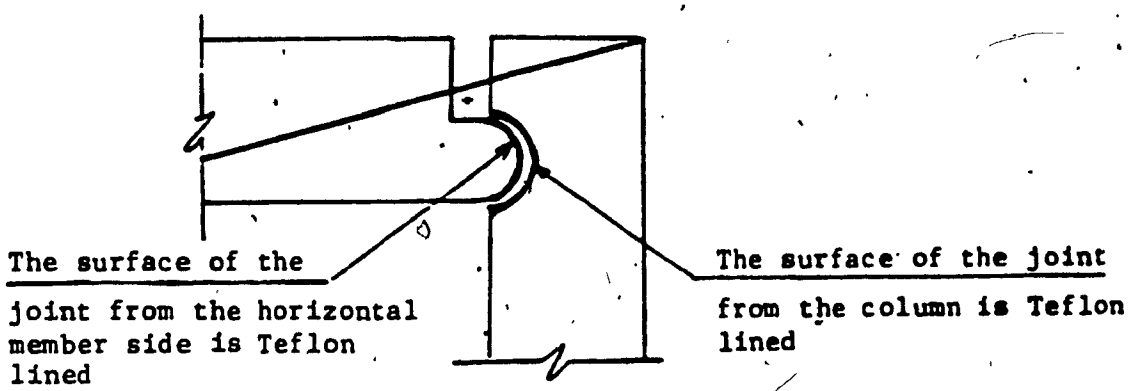

Figure 5-3 Using Teflon in the joint

The use of Teflon ensures smooth rotation between the horizontal member and the columns. The usual thickness of Teflon coating is 3/32 in. for each surface. Teflon is also capable of transmitting the axial compression force from the columns to the horizontal member. The design value of maximum compression on the Teflon varies from 1 to 2 Ksi.

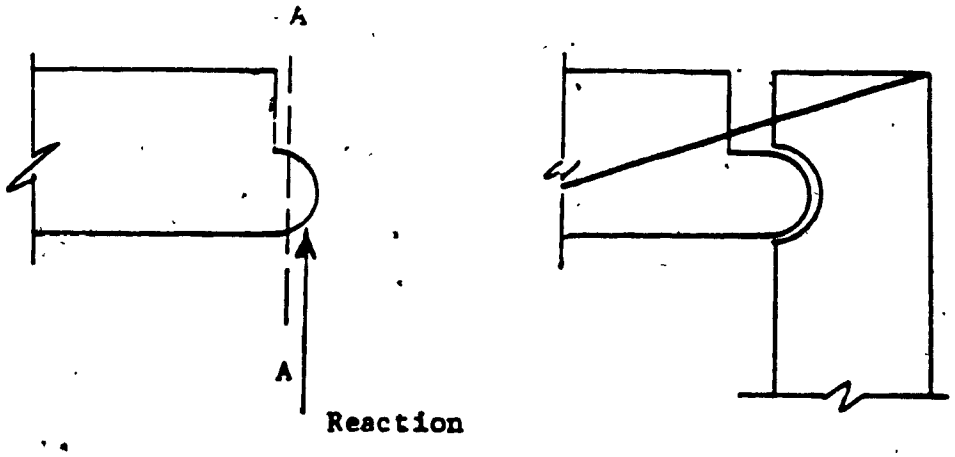

Figure 5-4 Shearing force acting at Section A-A

The vertical reactions at the ends of the horizontal member can be transmitted through the Teflon to the columns, since Teflon carries a compression force.

In Figure 5-4, the shearing force at section A-A, due to the reactions at the ends of the horizontal member, should be verified to see if the shearing force can be carried by the concrete only or reinforcement is required. If reinforcement is required, it will be placed as shown in Figure 5-5.

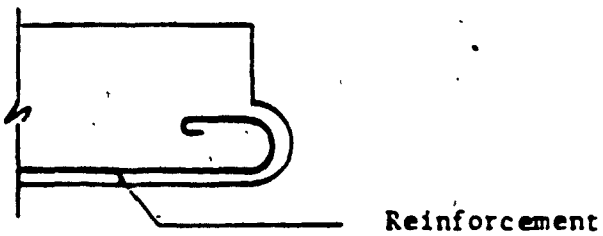

Figure 5-5 Reinforcement of the joint

5.3 Differential Settlements

Foundation settlements(14) must be assessed as accurately as possible for most structures. Since soil is not exactly a homogeneous substance, different values of settlements may occur under one structure. This kind of settlement is known as a differential settlement and is the main reason why many structures collapse.

In general, differential settlements do not affect statically determinate structures. However, it creates different types of stresses on the statically indeterminate

structures. Therefore, the statically indeterminate structures should be designed to withstand this kind of stress which is due to the differential settlements.

For a single bay frame, it can be designed as a statically determinate structure; resting on a roller support from one side and on a hinged support from the other side, see Figure 5-6.

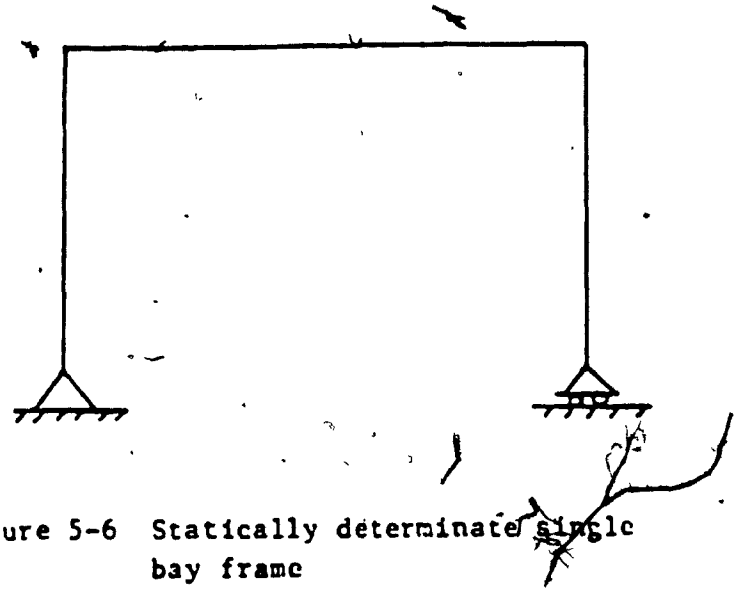

Figure 5-6 Statically determinate single bay frame

The frame shown in Figure 5-6 will not be affected by the differential settlement, however for prestressed frame structures, the leges usually would not be found on a roller foundations. If a hinged support or fixed support are used, the prestressed frame will be statically indeterminate. Therefore, the structure will be affected by the differential settlement. Following is an analysis of the effects of differential settlements on statically indeterminate prestressed frames and preloaded frames.

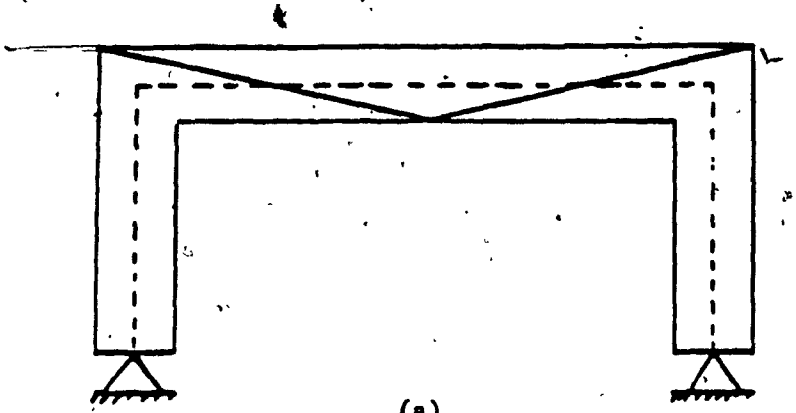

Prestressed frame
(no service load)

(a)

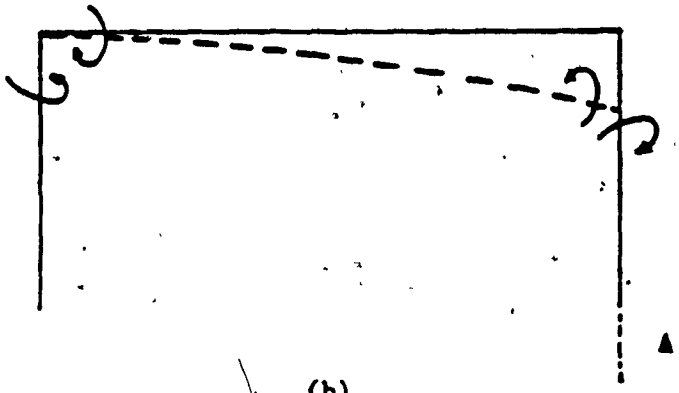

Distortion of the right angles at the corners of the frame due to differential settlement Δ

(b)

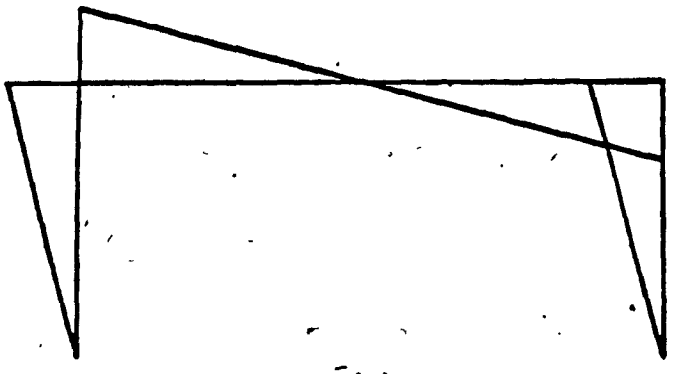

Bending moment on the frame due to the differential settlement only

(c)

Figure 5-7 Differential settlement acting on prestressed frame

Case 1: Prestressed Frame

For the frame shown in Figure 5-7-a, the horizontal member is only prestressed and there is no service load on the frame. Since the frame is statically indeterminate, it will be affected by the differential settlement. Assuming there is settlement Δ under the right side support of the frame as shown in Figure 5-7-b. Distortion of the angles will occur between the horizontal member and the legs of the frame. The material of the frame will resist the distortion of these angles, therefore a bending moment will act on the frame, as shown in Figure 5-7-c. This bending moment is only due to the action of the differential settlement.

Case 2: Preloaded Frame

The preloaded frame shown in Figures 5-8-a and 5-8-b also will be subjected to a settlement Δ acting under the right side columns, as shown in Figure 5-8-b. This settlement will distort the angles between the horizontal member and the columns. Since there are flexible integral joints between the horizontal member and the columns, these joints will not resist the distortion of the angles if the two columns remain parallel after the occurrence of the differential settlement, thus the bending moment on the preloaded frame will be zero, as shown in Figure 5-8-c. However, if the two columns become nonparallel after the occurrence of the differential settlement, the length of the cable may

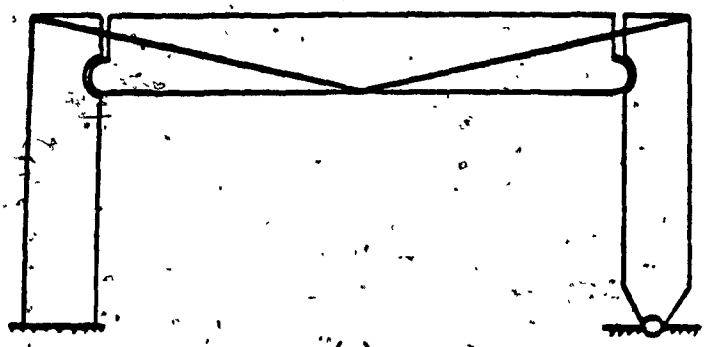

(a)

Preloading frame
(no service load)

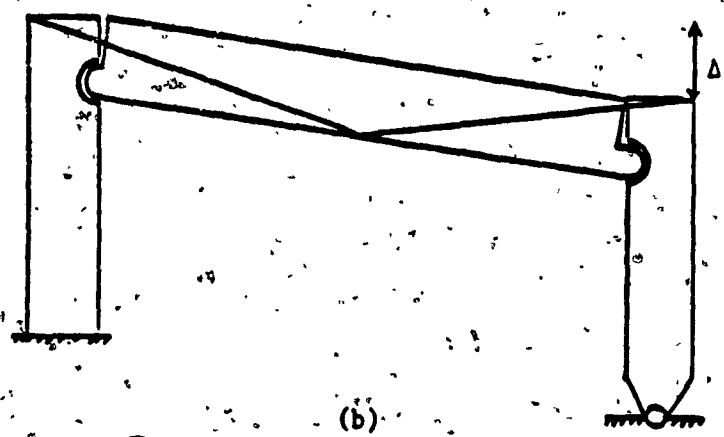

(b)

Differential settlement Δ
acting on the system

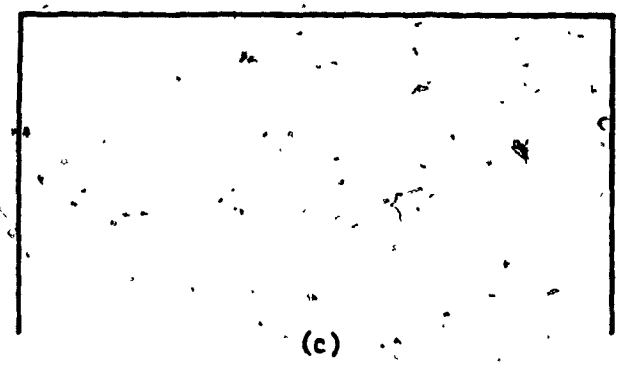

(c)

The bending moment on
a preloading frame is
zero

Figure 5-8 Differential settlement acting on preloaded frame

change, which in turn may affect the preloaded frame.

From the comparison between the prestressed frame and the preloaded frame, it can be concluded that the preloaded frame has better performance, under the action of the differential settlement, than the prestressed frame.

5.4 Multi-Bay Preloaded Frame

The preloaded technique can be used in the case of a continuous system, as shown in Figure 5-9. In Figure 5-9, there is two bay preloaded frame, the column at the left side is found on fixed support and the other two columns are rested on hinged supports. The cable for the left side bay is anchored at the top exterior side of the column located on the left side and anchored from the other end to the middle column at the top right side.

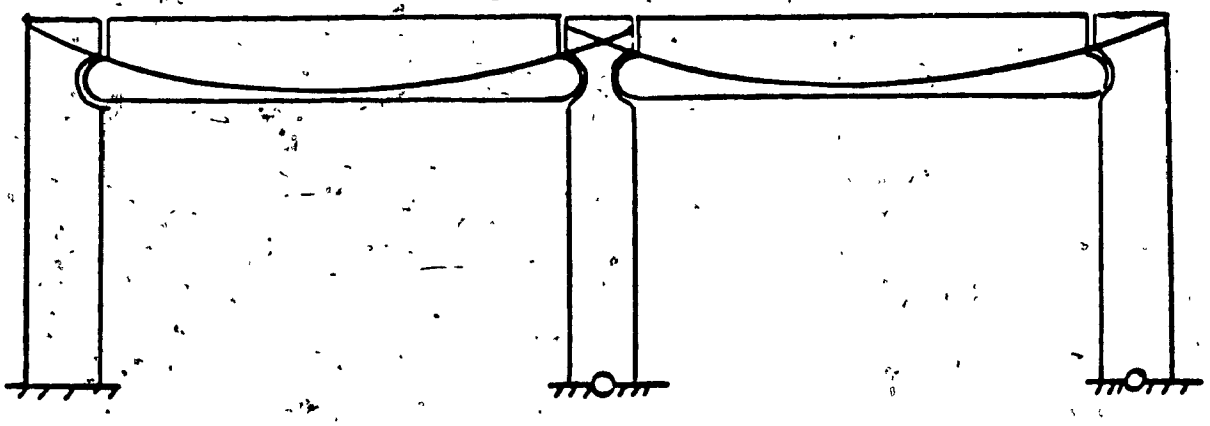

Figure 5-9 Multi-bay preloaded frame

The cable for the right side bay is anchored to the top exterior side of the column located at the right side, and anchored from the other end to the middle column at the top left side of this column.

5.5 The Advantages of the Preloaded Technique

To explain the benefits of the preloaded technique, the advantages and disadvantages should be compared to those of simply supported prestressed beams carried by two columns and a prestressed frame.

1 - Prestressed simply supported beam

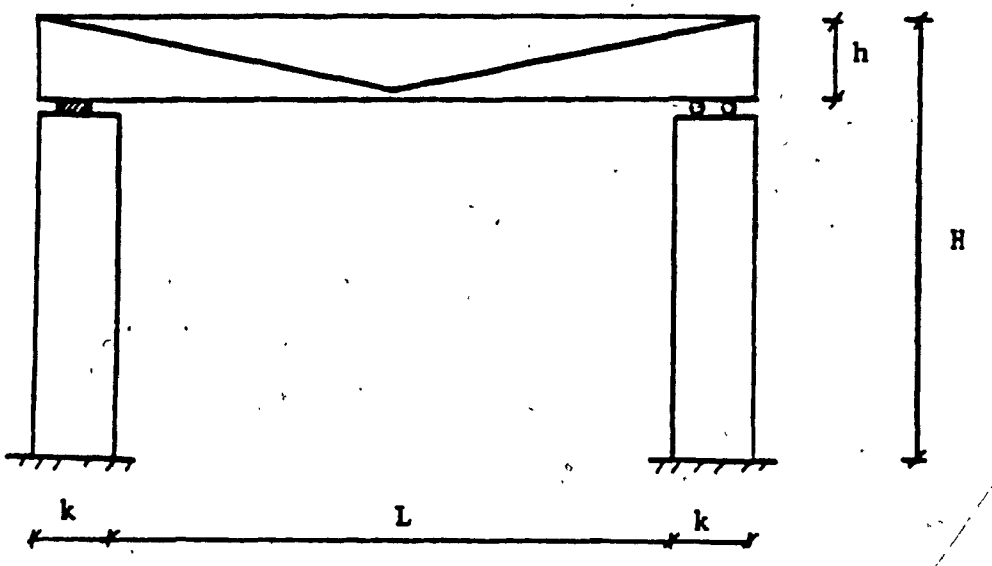

Figure 5-10 Prestressed beam

Advantages

1 - Since the system shown in Figure 5-10 is statically determinate, the beam will not be affected by the differential settlement.

2 - The system does not need complex design calculation, since it is statically determinate.

Disadvantages

1 - The bending moment due to the service load is carried totally by the beam and the columns have zero moment.

2 - There are bearing systems at the ends of the beam to transfer the vertical loads from the superstructure to the columns.

2 - Prestressed Frame

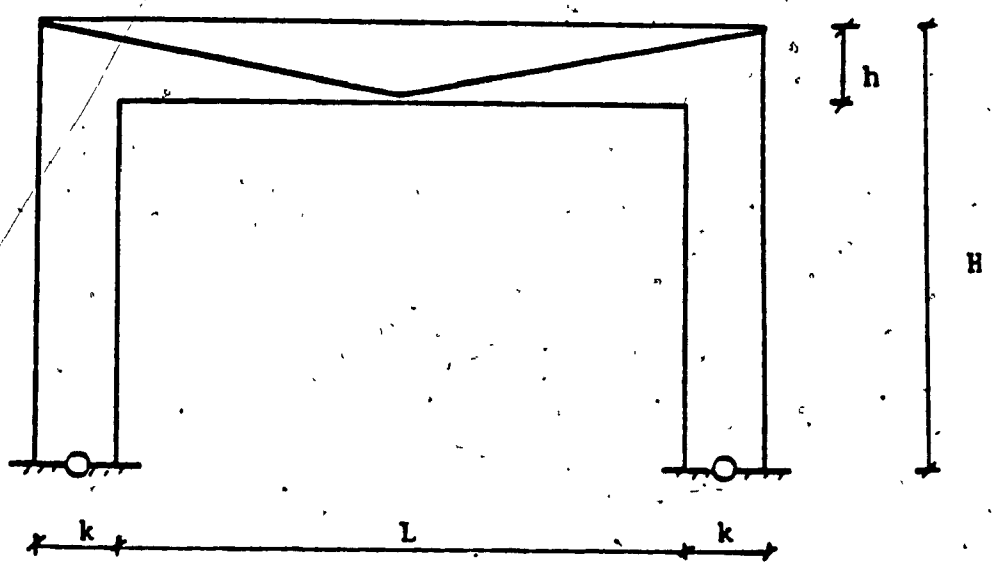

Figure 5-11 Prestressed frame

Advantages

1 - The bending moment due to the vertical loads is distributed over the horizontal member and the legs of the frame.

2 - Since the horizontal member has integral fixation with the legs of the frame, thus the system does not require bearings to transfer the loads from the horizontal member to the legs of the frame.

Disadvantages

1 - The prestressed frame is affected by the differential settlement.

2 - Since the prestressed frame shown in Figure 5-11 is statically indeterminate, it requires complex design calculations.

3 - Preloaded Frame

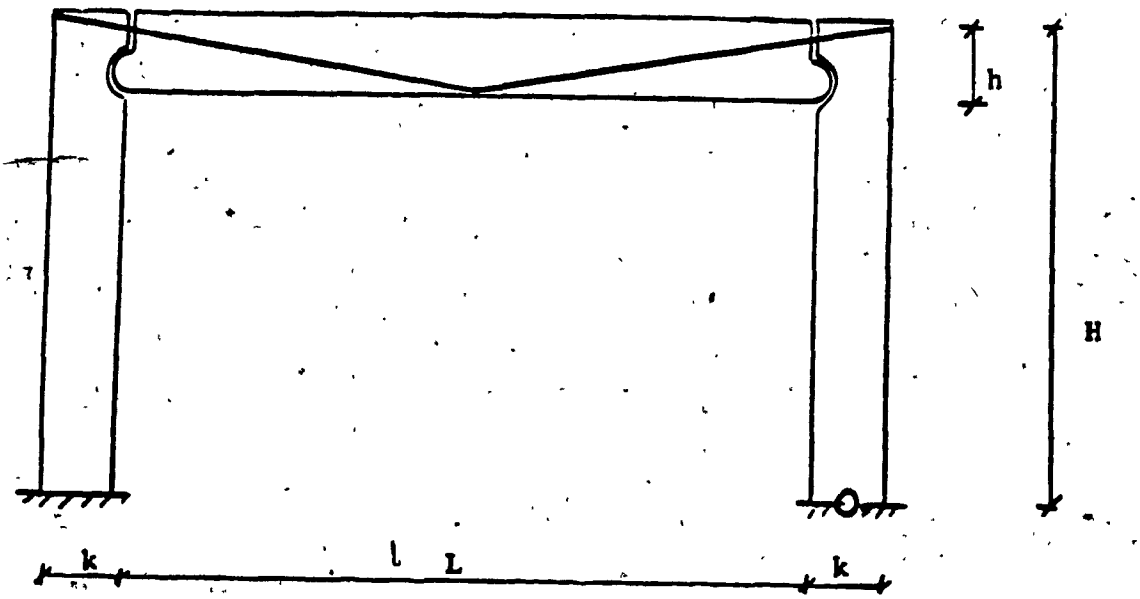

Figure 5-12 Preloaded frame

Advantages

1 - The bending moment due to the vertical loads is

distributed over the horizontal members and the columns.

2 - Does not require bearings to transfer the vertical loads from the horizontal member to the columns.

3 - It requires less pretensioning procedure than that is required for the prestressed frame.

4 - The system has better performance, than the prestressed frame, under the action of the differential settlement.

5 - The design calculation of this system is not very complex, since it is not statically indeterminate.

CONCLUSION

CONCLUSION

1- Single and multi-bay preloaded frames can be used instead of prestressed frames as an alternative economical solution.

2- Preloaded frames require pretensioning force less than prestressed frames

3- Preloaded frame structures can be recommended when the effect of differential settlement is significant.

4- Experimental tests on preloaded frames are required to veryfy the results that obtained from the analytical study.

APPENDIX A

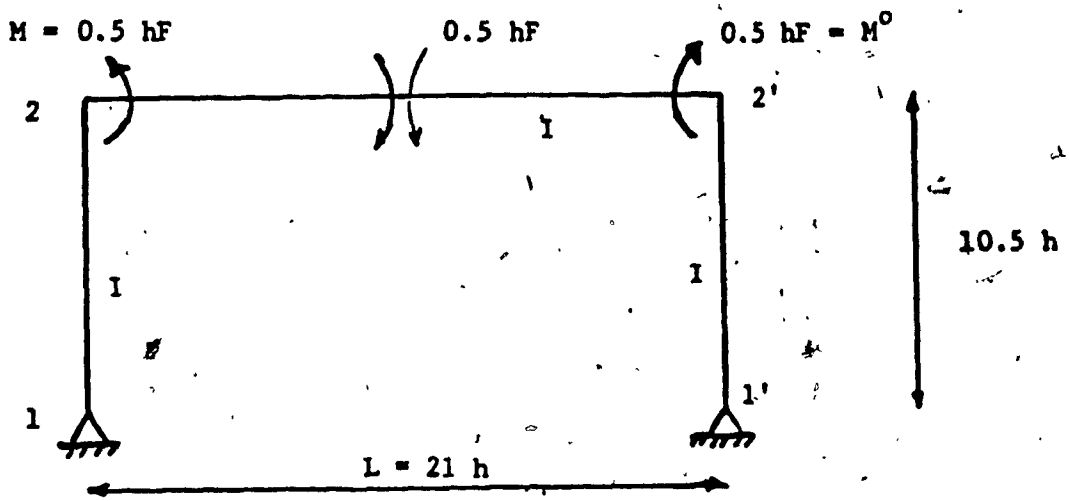

Joint	1	2		2'		1'
Member	1, 2	2, 1	2, 2'	2', 2	2', 1'	1', 2'
DF	1	0.6	0.4	0.4	0.6	1
Moments						
Fixed-end	0	0	-0.475	+0.475	0	0
External		-0.299	-0.199	+0.199	+0299	
Balancing		+0.285	+0.19	-0.19	-0.285	
CO			-0.095	+0.095		
Balacing		+0.057	+0.038	-0.038	-0.057	
CO			-0.019	+0.019		
Balancing		+0.011	+0.008	-0.008	-0.011	
Totals		+0.054	-0.552	+0.552	-0.054	

APPENDIX B

Table 1 Values of $(\frac{t}{T})/\frac{R}{mgl}$ with load at midspan

↓ λ^2 \ (R/mgl) →	0.1	0.2	0.4	0.6	0.8	1.0	2.0	4.0
0.1	0.014	0.015	0.017	0.019	0.022	0.024	0.033	0.045
0.2	0.027	0.029	0.034	0.038	0.041	0.045	0.059	0.074
0.4	0.053	0.057	0.064	0.071	0.077	0.083	0.101	0.115
0.6	0.077	0.083	0.093	0.102	0.109	0.116	0.135	0.146
0.8	0.101	0.108	0.120	0.130	0.138	0.145	0.163	0.171
1.0	0.124	0.132	0.145	0.156	0.164	0.171	0.188	0.192
2.0	0.226	0.237	0.252	0.263	0.270	0.275	0.282	0.271
4.0	0.388	0.397	0.408	0.414	0.416	0.416	0.403	0.371
6.0	0.510	0.516	0.522	0.521	0.518	0.514	0.486	0.439
8.0	0.607	0.610	0.610	0.605	0.598	0.590	0.551	0.493
10.0	0.686	0.687	0.682	0.673	0.663	0.652	0.604	0.537
20.0	0.935	0.929	0.913	0.894	0.875	0.857	0.784	0.690
40.0	1.153	1.148	1.130	1.109	1.087	1.066	0.978	0.864
60.0	1.254	1.252	1.239	1.221	1.201	1.181	1.092	0.972
80.0	1.312	1.313	1.305	1.291	1.273	1.255	1.170	1.049
100.0	1.350	1.354	1.351	1.339	1.324	1.308	1.229	1.109
200.0	1.435	1.446	1.457	1.457	1.451	1.443	1.388	1.285
400.0	1.482	1.499	1.520	1.529	1.533	1.532	1.506	1.434
600.0	1.498	1.518	1.543	1.557	1.564	1.567	1.555	1.503
800.0	1.507	1.528	1.555	1.571	1.580	1.585	1.583	1.544
1,000.0	1.512	1.533	1.562	1.580	1.590	1.596	1.600	1.570

↓ λ^2 \ (R/mgl) →	6.0	8.0	10.0	20.0	40.0	60.0	80.0	100.0
0.1	0.051	0.054	0.056	0.057	0.053	0.049	0.046	0.044
0.2	0.079	0.082	0.082	0.079	0.070	0.064	0.060	0.057
0.4	0.118	0.118	0.116	0.106	0.092	0.084	0.078	0.073
0.6	0.146	0.144	0.141	0.126	0.108	0.097	0.090	0.085
0.8	0.169	0.164	0.160	0.142	0.120	0.108	0.100	0.094
1.0	0.188	0.182	0.176	0.155	0.131	0.117	0.108	0.101
2.0	0.258	0.246	0.236	0.202	0.169	0.150	0.138	0.129
4.0	0.346	0.326	0.311	0.262	0.216	0.192	0.176	0.164
6.0	0.406	0.382	0.362	0.303	0.249	0.221	0.202	0.189
8.0	0.454	0.425	0.403	0.336	0.275	0.244	0.223	0.208
10.0	0.493	0.461	0.437	0.363	0.298	0.263	0.241	0.225
20.0	0.631	0.589	0.557	0.461	0.337	0.333	0.304	0.284
40.0	0.791	0.739	0.699	0.580	0.474	0.419	0.383	0.357
60.0	0.893	0.836	0.791	0.659	0.540	0.478	0.438	0.408
80.0	0.968	0.908	0.861	0.720	0.591	0.524	0.480	0.448
100.0	1.026	0.965	0.917	0.770	0.634	0.562	0.515	0.481
200.0	1.207	1.146	1.096	0.936	0.780	0.696	0.640	0.599
400.0	1.370	1.316	1.270	1.112	0.945	0.850	0.785	0.737
600.0	1.451	1.404	1.364	1.214	1.047	0.948	0.880	0.828
800.0	1.500	1.460	1.23	1.284	1.120	1.020	0.950	0.896
1,000.0	1.533	1.498	1.465	1.336	1.177	1.077	1.006	0.951

Table 2 Values of $(\frac{t}{T})/\frac{r}{mg}$ with load uniformly distributed over the central one-tenth of the span

↓ λ^2	(r/mg) 0.1 →	0.2	0.4	0.6	0.8	1.0	2.0	4.0
0.1	0.001	0.001	0.001	0.001	0.001	0.001	0.001	0.002
0.2	0.002	0.002	0.003	0.003	0.003	0.003	0.003	0.003
0.4	0.005	0.005	0.005	0.005	0.005	0.005	0.006	0.006
0.6	0.007	0.007	0.007	0.007	0.008	0.008	0.008	0.009
0.8	0.009	0.009	0.010	0.010	0.010	0.010	0.011	0.012
1.0	0.012	0.012	0.012	0.012	0.012	0.012	0.013	0.014
2.0	0.021	0.022	0.022	0.022	0.022	0.022	0.023	0.025
4.0	0.037	0.038	0.038	0.038	0.038	0.038	0.039	0.040
6.0	0.050	0.050	0.050	0.050	0.050	0.051	0.051	0.051
8.0	0.060	0.060	0.060	0.060	0.060	0.060	0.060	0.060
10.0	0.068	0.068	0.068	0.068	0.068	0.068	0.068	0.067
20.0	0.093	0.093	0.093	0.093	0.093	0.093	0.092	0.090
40.0	0.115	0.115	0.115	0.115	0.115	0.114	0.113	0.111
60.0	0.125	0.125	0.125	0.124	0.124	0.124	0.124	0.122
80.0	0.130	0.130	0.130	0.130	0.130	0.130	0.130	0.128
100.0	0.134	0.134	0.134	0.134	0.134	0.134	0.134	0.133
200.0	0.141	0.141	0.142	0.142	0.142	0.142	0.143	0.143
400.0	0.145	0.146	0.146	0.146	0.147	0.147	0.148	0.149
600.0	0.147	0.147	0.147	0.148	0.148	0.149	0.150	0.152
800.0	0.148	0.148	0.148	0.149	0.149	0.149	0.151	0.153
1000.0	0.148	0.148	0.149	0.149	0.150	0.150	0.151	0.154

↓ λ^2	(r/mg) 6.0 →	8.0	10.0	20.0	40.0	60.0	80.0	100.0
0.1	0.002	0.002	0.002	0.003	0.004	0.005	0.005	0.005
0.2	0.004	0.004	0.004	0.006	0.007	0.008	0.008	0.008
0.4	0.007	0.008	0.008	0.010	0.011	0.011	0.011	0.011
0.6	0.010	0.011	0.011	0.013	0.014	0.014	0.014	0.014
0.8	0.013	0.013	0.014	0.016	0.017	0.016	0.016	0.016
1.0	0.015	0.016	0.017	0.018	0.019	0.018	0.018	0.017
2.0	0.026	0.026	0.027	0.027	0.026	0.025	0.024	0.023
4.0	0.041	0.041	0.041	0.039	0.036	0.034	0.032	0.030
6.0	0.051	0.051	0.050	0.047	0.043	0.040	0.037	0.035
8.0	0.059	0.059	0.058	0.054	0.048	0.044	0.041	0.039
10.0	0.066	0.065	0.064	0.059	0.052	0.048	0.045	0.043
20.0	0.088	0.086	0.084	0.077	0.067	0.062	0.057	0.054
40.0	0.109	0.107	0.104	0.096	0.084	0.077	0.072	0.068
60.0	0.120	0.118	0.116	0.107	0.095	0.087	0.082	0.077
80.0	0.127	0.125	0.123	0.114	0.102	0.094	0.089	0.084
100.0	0.131	0.130	0.128	0.120	0.108	0.100	0.094	0.089
200.0	0.143	0.142	0.141	0.135	0.125	0.118	0.112	0.107
400.0	0.150	0.150	0.150	0.147	0.139	0.133	0.128	0.124
600.0	0.153	0.153	0.153	0.151	0.146	0.141	0.136	0.133
800.0	0.154	0.154	0.155	0.154	0.150	0.146	0.142	0.138
1,000.0	0.155	0.155	0.156	0.156	0.152	0.149	0.145	0.142

Table 3 Values of $(\frac{t}{T})/\frac{r}{mg}$ with load uniformly distributed over the central two-tenths of the span

↓ λ^2 | (r/mg) →	0.1	0.2	0.4	0.6	0.8	1.0	2.0	4.0
0.1	0.002	0.003	0.003	0.003	0.003	0.003	0.003	0.004
0.2	0.005	0.005	0.005	0.005	0.005	0.006	0.006	0.008
0.4	0.010	0.010	0.010	0.010	0.011	0.011	0.012	0.015
0.6	0.014	0.015	0.015	0.015	0.016	0.016	0.018	0.021
0.8	0.019	0.019	0.020	0.020	0.020	0.021	0.023	0.026
1.0	0.023	0.023	0.024	0.024	0.025	0.026	0.028	0.031
2.0	0.043	0.043	0.044	0.045	0.045	0.046	0.048	0.051
4.0	0.074	0.075	0.075	0.076	0.077	0.077	0.079	0.079
6.0	0.099	0.099	0.100	0.100	0.100	0.100	0.100	0.099
8.0	0.119	0.119	0.119	0.119	0.119	0.119	0.117	0.114
10.0	0.135	0.134	0.134	0.134	0.134	0.133	0.131	0.127
20.0	0.185	0.184	0.183	0.182	0.182	0.181	0.176	0.168
40.0	0.227	0.227	0.226	0.225	0.224	0.223	0.218	0.208
60.0	0.246	0.246	0.246	0.245	0.244	0.243	0.239	0.230
80.0	0.257	0.257	0.257	0.256	0.256	0.255	0.252	0.243
100.0	0.264	0.264	0.264	0.264	0.263	0.263	0.260	0.253
200.0	0.280	0.280	0.280	0.281	0.281	0.281	0.280	0.277
400.0	0.288	0.288	0.289	0.290	0.291	0.291	0.292	0.292
600.0	0.291	0.291	0.292	0.293	0.294	0.295	0.297	0.298
800.0	0.292	0.293	0.294	0.295	0.296	0.297	0.299	0.301
1,000.0	0.293	0.294	0.295	0.296	0.297	0.298	0.300	0.303

↓ λ^2 | (r/mg) →	6.0	8.0	10.0	20.0	40.0	60.0	80.0	100.0
0.1	0.005	0.005	0.006	0.008	0.010	0.011	0.011	0.011
0.2	0.009	0.010	0.011	0.014	0.015	0.015	0.015	0.015
0.4	0.016	0.018	0.019	0.021	0.022	0.021	0.021	0.020
0.6	0.023	0.024	0.025	0.027	0.027	0.026	0.025	0.024
0.8	0.028	0.030	0.031	0.032	0.031	0.029	0.028	0.027
1.0	0.033	0.034	0.035	0.036	0.034	0.032	0.031	0.029
2.0	0.053	0.053	0.053	0.051	0.047	0.043	0.040	0.038
4.0	0.079	0.078	0.076	0.070	0.062	0.056	0.053	0.050
6.0	0.097	0.094	0.092	0.083	0.072	0.066	0.061	0.058
8.0	0.111	0.108	0.105	0.093	0.081	0.073	0.068	0.064
10.0	0.122	0.118	0.115	0.102	0.088	0.079	0.073	0.069
20.0	0.160	0.154	0.149	0.131	0.112	0.101	0.093	0.088
40.0	0.200	0.192	0.186	0.164	0.140	0.127	0.117	0.110
60.0	0.221	0.214	0.208	0.184	0.159	0.144	0.133	0.125
80.0	0.236	0.229	0.222	0.199	0.172	0.156	0.145	0.137
100.0	0.246	0.239	0.233	0.210	0.183	0.167	0.155	0.146
200.0	0.272	0.268	0.263	0.243	0.217	0.200	0.187	0.177
400.0	0.290	0.287	0.285	0.271	0.249	0.233	0.220	0.210
600.0	0.297	0.296	0.294	0.283	0.265	0.250	0.239	0.230
800.0	0.301	0.300	0.299	0.290	0.275	0.262	0.251	0.242
1,000.0	0.303	0.303	0.302	0.295	0.282	0.270	0.260	0.252

Table 4 Values of $(\frac{t}{T})/\frac{r}{mg}$ with load uniformly distributed over the central four-tenths of the span

↓ λ^2 | (r/mg) →	0.1	0.2	0.4	0.6	0.8	1.0	2.0	4.0
0.1	0.005	0.005	0.005	0.006	0.006	0.006	0.007	0.010
0.2	0.010	0.010	0.010	0.011	0.011	0.012	0.014	0.018
0.4	0.019	0.019	0.020	0.021	0.022	0.023	0.027	0.032
0.6	0.028	0.028	0.030	0.031	0.032	0.033	0.038	0.044
0.8	0.036	0.037	0.039	0.040	0.042	0.043	0.048	0.054
1.0	0.045	0.046	0.047	0.049	0.051	0.052	0.058	0.064
2.0	0.082	0.084	0.086	0.088	0.089	0.091	0.096	0.099
4.0	0.143	0.144	0.145	0.147	0.147	0.148	0.149	0.145
6.0	0.190	0.190	0.190	0.190	0.190	0.190	0.186	0.177
8.0	0.227	0.227	0.226	0.225	0.223	0.222	0.215	0.202
10.0	0.257	0.256	0.255	0.253	0.251	0.248	0.239	0.222
20.0	0.353	0.350	0.346	0.341	0.337	0.333	0.316	0.290
40.0	0.434	0.432	0.427	0.422	0.417	0.412	0.392	0.362
60.0	0.471	0.469	0.465	0.460	0.456	0.452	0.432	0.402
80.0	0.492	0.490	0.487	0.483	0.479	0.476	0.458	0.429
100.0	0.506	0.504	0.501	0.498	0.495	0.492	0.476	0.449
200.0	0.536	0.535	0.534	0.533	0.531	0.529	0.520	0.500
400.0	0.552	0.552	0.553	0.553	0.552	0.552	0.548	0.537
600.0	0.558	0.558	0.559	0.560	0.560	0.560	0.558	0.551
800.0	0.561	0.561	0.562	0.563	0.564	0.564	0.564	0.559
1,000.0	0.562	0.563	0.564	0.565	0.546	0.567	0.567	0.564

↓ λ^2 | (r/mg) →	6.0	8.0	10.0	20.0	40.0	60.0	80.0	100.0
0.1	0.012	0.013	0.015	0.018	0.020	0.020	0.019	0.019
0.2	0.021	0.023	0.025	0.028	0.028	0.027	0.026	0.025
0.4	0.036	0.038	0.039	0.041	0.039	0.036	0.034	0.033
0.6	0.048	0.049	0.050	0.050	0.046	0.043	0.040	0.038
0.8	0.057	0.059	0.059	0.058	0.052	0.048	0.045	0.043
1.0	0.066	0.067	0.067	0.064	0.057	0.053	0.049	0.047
2.0	0.099	0.097	0.095	0.087	0.076	0.069	0.064	0.060
4.0	0.140	0.136	0.131	0.116	0.099	0.089	0.082	0.077
6.0	0.169	0.162	0.156	0.136	0.115	0.103	0.095	0.089
8.0	0.191	0.183	0.176	0.152	0.128	0.114	0.105	0.099
10.0	0.210	0.200	0.192	0.165	0.138	0.124	0.114	0.107
20.0	0.272	0.258	0.247	0.211	0.176	0.157	0.144	0.135
40.0	0.339	0.322	0.308	0.264	0.221	0.197	0.182	0.170
60.0	0.379	0.361	0.346	0.298	0.251	0.224	0.207	0.194
80.0	0.407	0.387	0.374	0.324	0.273	0.245	0.226	0.212
100.0	0.427	0.409	0.394	0.344	0.292	0.262	0.242	0.227
200.0	0.483	0.468	0.455	0.406	0.352	0.319	0.296	0.279
400.0	0.525	0.514	0.504	0.464	0.413	0.379	0.355	0.337
600.0	0.543	0.535	0.527	0.493	0.446	0.415	0.391	0.372
800.0	0.553	0.546	0.540	0.511	0.469	0.439	0.416	0.397
1,000.0	0.559	0.554	0.548	0.523	0.485	0.457	0.434	0.416

Table 5 Values of $(\frac{t}{T})/\frac{r}{mg}$ with load uniformly distributed over the central six-tenths of the span.

↓ λ^2 | (r/mg) →	0.1	0.2	0.4	0.6	0.8	1.0	2.0	4.0
0.1	0.007	0.007	0.008	0.008	0.009	0.009	0.011	0.015
0.2	0.013	0.014	0.015	0.016	0.017	0.018	0.022	0.028
0.4	0.026	0.027	0.029	0.031	0.032	0.034	0.040	0.048
0.6	0.039	0.040	0.042	0.045	0.047	0.048	0.056	0.064
0.8	0.051	0.052	0.055	0.058	0.060	0.062	0.070	0.078
1.0	0.063	0.064	0.067	0.070	0.073	0.075	0.083	0.090
2.0	0.115	0.117	0.121	0.124	0.126	0.128	0.134	0.135
4.0	0.200	0.201	0.203	0.204	0.204	0.205	0.202	0.193
6.0	0.264	0.264	0.264	0.262	0.261	0.259	0.250	0.233
8.0	0.316	0.314	0.311	0.308	0.305	0.302	0.288	0.265
10.0	0.358	0.355	0.350	0.346	0.341	0.337	0.318	0.290
20.0	0.489	0.484	0.474	0.465	0.457	0.449	0.418	0.377
40.0	0.603	0.597	0.585	0.575	0.565	0.557	0.520	0.471
60.0	0.654	0.649	0.639	0.629	0.620	0.611	0.576	0.525
80.0	0.684	0.679	0.670	0.662	0.653	0.645	0.612	0.563
100.0	0.703	0.699	0.691	0.683	0.676	0.669	0.638	0.590
200.0	0.745	0.743	0.738	0.734	0.729	0.724	0.703	0.666
400.0	0.768	0.767	0.765	0.763	0.761	0.758	0.745	0.721
600.0	0.776	0.776	0.775	0.774	0.772	0.771	0.762	0.744
800.0	0.780	0.780	0.780	0.779	0.778	0.777	0.771	0.757
1,000.0	0.783	0.783	0.783	0.782	0.782	0.781	0.776	0.765

↓ λ^2 | (r/mg) →	6.0	8.0	10.0	20.0	40.0	60.0	80.0	100.0
0.1	0.018	0.021	0.022	0.026	0.027	0.026	0.025	0.024
0.2	0.032	0.034	0.036	0.038	0.037	0.035	0.033	0.032
0.4	0.052	0.054	0.055	0.055	0.050	0.047	0.044	0.042
0.6	0.067	0.069	0.069	0.066	0.060	0.055	0.051	0.048
0.8	0.080	0.081	0.080	0.076	0.067	0.061	0.057	0.054
1.0	0.091	0.091	0.090	0.083	0.073	0.067	0.062	0.059
2.0	0.132	0.129	0.125	0.112	0.096	0.087	0.080	0.075
4.0	0.184	0.177	0.170	0.148	0.124	0.111	0.103	0.096
6.0	0.220	0.209	0.201	0.172	0.144	0.129	0.119	0.111
8.0	0.248	0.235	0.225	0.192	0.160	0.142	0.131	0.123
10.0	0.271	0.256	0.245	0.208	0.173	0.154	0.141	0.132
20.0	0.350	0.330	0.314	0.254	0.219	0.195	0.179	0.167
40.0	0.437	0.413	0.393	0.332	0.276	0.245	0.225	0.211
60.0	0.490	0.464	0.443	0.376	0.313	0.279	0.257	0.240
80.0	0.528	0.501	0.479	0.409	0.342	0.306	0.281	0.263
100.0	0.556	0.529	0.507	0.436	0.366	0.327	0.301	0.282
200.0	0.636	0.612	0.591	0.520	0.444	0.400	0.370	0.348
400.0	0.700	0.681	0.664	0.601	0.526	0.480	0.448	0.423
600.0	0.728	0.713	0.699	0.644	0.574	0.529	0.496	0.470
800.0	0.744	0.731	0.719	0.671	0.606	0.562	0.530	0.504
1,000.0	0.754	0.743	0.733	0.690	0.630	0.588	0.556	0.530

Table 6 Values of $(\frac{t}{T})/\frac{r}{mg}$ with load uniformly distributed over the central eight-tenths of the span

↓ λ^2 | (r/mg) →	0.1	0.2	0.4	0.6	0.8	1.0	2.0	4.0
0.1	0.008	0.009	0.009	0.010	0.011	0.011	0.014	0.019
0.2	0.016	0.017	0.018	0.019	0.021	0.022	0.027	0.035
0.4	0.032	0.033	0.035	0.037	0.040	0.041	0.049	0.058
0.6	0.047	0.048	0.051	0.054	0.057	0.059	0.069	0.077
0.8	0.061	0.063	0.067	0.070	0.073	0.076	0.085	0.093
1.0	0.075	0.077	0.081	0.085	0.088	0.091	0.100	0.107
2.0	0.138	0.141	0.145	0.149	0.151	0.154	0.159	0.158
4.0	0.238	0.239	0.241	0.242	0.242	0.242	0.237	0.269
6.0	0.315	0.314	0.313	0.310	0.308	0.305	0.292	0.269
8.0	0.375	0.373	0.368	0.364	0.359	0.354	0.334	0.304
10.0	0.425	0.421	0.414	0.407	0.400	0.394	0.369	0.333
20.0	0.581	0.573	0.559	0.546	0.535	0.524	0.484	0.432
40.0	0.716	0.707	0.690	0.676	0.662	0.650	0.602	0.540
60.0	0.778	0.769	0.754	0.740	0.727	0.715	0.667	0.603
80.0	0.813	0.806	0.792	0.779	0.767	0.756	0.711	0.647
100.0	0.836	0.829	0.817	0.805	0.795	0.784	0.742	0.680
200.0	0.886	0.882	0.875	0.867	0.860	0.853	0.821	0.772
400.0	0.914	0.912	0.908	0.903	0.899	0.895	0.875	0.841
600.0	0.924	0.923	0.920	0.917	0.914	0.911	0.896	0.871
800.0	0.929	0.928	0.926	0.923	0.921	0.919	0.908	0.887
1,000.0	0.932	0.931	0.929	0.928	0.926	0.924	0.915	0.898

↓ λ^2 | (r/mg) →	6.0	8.0	10.0	20.0	40.0	60.0	80.0	100.0
0.1	0.023	0.026	0.028	0.031	0.031	0.030	0.028	0.027
0.2	0.039	0.042	0.043	0.045	0.043	0.040	0.038	0.036
0.4	0.063	0.064	0.065	0.063	0.057	0.053	0.050	0.047
0.6	0.080	0.081	0.081	0.076	0.068	0.062	0.058	0.055
0.8	0.095	0.095	0.094	0.087	0.076	0.069	0.064	0.061
1.0	0.107	0.106	0.105	0.096	0.083	0.075	0.070	0.066
2.0	0.154	0.149	0.144	0.127	0.108	0.097	0.090	0.085
4.0	0.212	0.202	0.194	0.167	0.140	0.125	0.115	0.108
6.0	0.252	0.239	0.229	0.195	0.162	0.145	0.133	0.124
8.0	0.284	0.268	0.255	0.216	0.180	0.160	0.147	0.137
10.0	0.310	0.292	0.278	0.235	0.194	0.173	0.159	0.148
20.0	0.399	0.375	0.356	0.299	0.246	0.219	0.201	0.187
40.0	0.499	0.469	0.446	0.375	0.310	0.275	0.252	0.236
60.0	0.560	0.528	0.503	0.425	0.352	0.313	0.288	0.269
80.0	0.604	0.571	0.545	0.463	0.385	0.343	0.315	0.295
100.0	0.637	0.604	0.577	0.493	0.412	0.367	0.338	0.316
200.0	0.734	0.703	0.677	0.591	0.501	0.451	0.416	0.391
400.0	0.812	0.788	0.766	0.688	0.598	0.544	0.506	0.477
600.0	0.848	0.828	0.809	0.740	0.654	0.600	0.561	0.531
800.0	0.868	0.851	0.836	0.774	0.693	0.640	0.601	0.571
1,000.0	0.882	0.867	0.853	0.797	0.722	0.670	0.632	0.602

Table 7 Values of $(\frac{t}{T})/\frac{r}{mg}$ with load uniformly distributed over the central whole span

↓ λ^2 | (r/mg) →	0.1	0.2	0.4	0.6	0.8	1.0	2.0	4.0
0.1	0.009	0.009	0.010	0.011	0.011	0.012	0.016	0.021
0.2	0.017	0.018	0.019	0.021	0.022	0.023	0.029	0.037
0.4	0.034	0.035	0.038	0.040	0.042	0.044	0.053	0.063
0.6	0.050	0.051	0.055	0.058	0.061	0.063	0.073	0.082
0.8	0.065	0.067	0.075	0.075	0.078	0.081	0.091	0.099
1.0	0.080	0.082	0.087	0.090	0.094	0.097	0.107	0.113
2.0	0.146	0.149	0.154	0.158	0.161	0.163	0.168	0.167
4.0	0.252	0.254	0.256	0.256	0.256	0.256	0.250	0.235
6.0	0.333	0.333	0.331	0.328	0.325	0.322	0.307	0.282
8.0	0.398	0.395	0.389	0.384	0.379	0.373	0.351	0.319
10.0	0.450	0.446	0.437	0.429	0.422	0.415	0.387	0.349
20.0	0.615	0.606	0.590	0.576	0.563	0.551	0.507	0.452
40.0	0.758	0.748	0.729	0.712	0.697	0.684	0.631	0.565
60.0	0.823	0.814	0.796	0.781	0.766	0.753	0.701	0.632
80.0	0.861	0.852	0.837	0.822	0.809	0.797	0.747	0.678
100.0	0.885	0.877	0.863	0.850	0.838	0.827	0.780	0.713
200.0	0.939	0.934	0.925	0.916	0.908	0.900	0.865	0.811
400.0	0.968	0.966	0.960	0.955	0.950	0.946	0.923	0.885
600.0	0.979	0.977	0.973	0.970	0.966	0.963	0.946	0.917
800.0	0.984	0.982	0.980	0.977	0.974	0.971	0.959	0.935
1,000.0	0.987	0.986	0.984	0.981	0.979	0.977	0.966	0.947

↓ λ^2 | (r/mg) →	6.0	8.0	10.0	20.0	40.0	60.0	80.0	100.0
0.1	0.025	0.028	0.030	0.033	0.033	0.031	0.030	0.029
0.2	0.042	0.045	0.046	0.048	0.045	0.042	0.039	0.038
0.4	0.067	0.068	0.069	0.067	0.060	0.055	0.052	0.049
0.6	0.085	0.086	0.085	0.080	0.071	0.065	0.060	0.057
0.8	0.100	0.100	0.099	0.091	0.079	0.072	0.067	0.063
1.0	0.113	0.112	0.110	0.100	0.087	0.079	0.073	0.069
2.0	0.162	0.156	0.151	0.133	0.113	0.101	0.094	0.088
4.0	0.222	0.212	0.203	0.174	0.146	0.130	0.120	0.112
6.0	0.264	0.250	0.239	0.203	0.169	0.150	0.138	0.129
8.0	0.297	0.280	0.267	0.225	0.187	0.166	0.153	0.143
10.0	0.324	0.305	0.290	0.244	0.202	0.180	0.165	0.154
20.0	0.417	0.391	0.371	0.311	0.256	0.227	0.208	0.195
40.0	0.521	0.490	0.465	0.390	0.322	0.286	0.262	0.245
60.0	0.586	0.552	0.525	0.443	0.366	0.326	0.299	0.279
80.0	0.631	0.596	0.569	0.482	0.400	0.357	0.328	0.306
100.0	0.667	0.631	0.603	0.514	0.428	0.382	0.351	0.329
200.0	0.769	0.736	0.709	0.617	0.522	0.469	0.433	0.407
400.0	0.854	0.827	0.804	0.719	0.624	0.566	0.527	0.496
600.0	0.892	0.870	0.850	0.775	0.683	0.626	0.585	0.553
800.0	0.914	0.896	0.879	0.811	0.725	0.668	0.627	0.595
1,000.0	0.929	0.913	0.898	0.837	0.755	0.701	0.660	0.628

REFERENCES

1- Buchholdt, H. A. " AN INTRODUCTION TO CABLE ROOF STRUCTURES " Cambridge University Press, Cambridge, Great Britain, 1985.

2- Lin, T. Y. & Burns, Ned H. " DESIGN OF PRESTRESSED CONCRETE STRUCTURES " John Wiley & Sons, New York, 1981.

3- Bonasso, S. G & Moulton, L. K. " TENSION ARCH STRUCTURE " Transportation Research Record, U. S. A., 1982.

4- Zielinski, Z. A. " PREFABRYKWANE BETONOWE DZWIGARY SPREZONE " Warsaw, Poland, 1962.

5- Belenya, E. " PRESTRESSED LOAD BEARING METAL STRUCTURES " Mir Publisher, Moscow, 1977.

6- Podolny, W & Scalzi, J. B. " CONSTRUCTION AND DESIGN OF CABLE-STAYED BRIDGES " John Wiley & Sons, New York, 1976.

7- Troitsky, M. S. " CABLE STAYED BRIDGES, THEORY AND DESIGN " Crosby Lockwood Staples, London, 1977.

8- Ernst, H. J. " MONTAGE EINES SEILVERSPANNTEN BALKENS IM GROSS-BRUCKENBAU " Stahlbau, No. 5,

May, 1956.

9- Abeles, P.W. & Bardhan-Roy, B.K.
" PRESTRESSED CONCRETE DESIGNER'S HANDBOOK " A Viewpoint Publication, 3d Edition, Cement and Concrete Association, Wexham Springs, U.S.A.

10- Sir Alfred Pugsley
" THE THEORY OF SUSPENSION BRIDGES " Edward Arnold (Publishers) LTD. London, 2nd edition 1968.

11- Irvine, H.M. " CABLE STRUCTURES " The MIT Press, Cambridge, Massachusetts, and london, England, 1981.

12- Libby, J.R. " MODERN PRESTRESSED CONCRETE " Van Nostrand Reinhold Company, New York, 1977.

13- Heins, C.P. & Firmage, D.A.
" DESIGN OF MODERN STEEL HIGHWAY BRIDGES " John Wiley & Sons Inc., New York, 1979.

14- Bowles, J.B. " FOUNDATION ANALYSIS AND DESIGN " 3d edition, McGraw Hill Book Company, New York, 1982.

15- Vernigora, E. & Marcil, J.R.M.
" BRIDGE REHABILITATION AND STRENGTH ENING BY CONTINUOUS POST-TENSIONING "

PCI Journal, vol. 14, No. 2, Apr. 1969.

16- Ghali, A. & Neville, A. M.
" STRUCTURE ANALYSIS, A UNIFIED CLASSICAL AND MATRIX APPROACH " John Wiley & Sons, New York, 1978.

17- Leonhardt, F.
" PRESTRESSED CONCRETE, DESIGN AND CONSTRUCTION " 2nd edition, Wilhelm Ernst & Sohn, Berlin, Munich, 1964

18- Willems, N. & Lucas, W. M. JR
" STRUCTURE ANALYSIS FOR ENGINEERS" McGraw-Hill Book Company, New York, 1978.

19- PTI " POST-TENSIONING INSTITUTE "
" POST-TENSIONING MANUAL " Post Tensioning Institute, Illinois, U. S. A., 1972.

20- Guyon, Y.
" PRESTRESSED CONCRETE " Volume II, John Wiley & Sons Inc., New York, 1960.

21- Guyon, Y.
" LIMIT-STATE DESIGN OF PRESTRESSED CONCRETE " Volumes I and II. Halsted Press Division, John Wiley & Sons Inc. New York, 1972.

22- Gimsing, N. J.
" CABLE SUPPORTED BRIDGES, CONCEPT AND DESIGN " John Wiley & Sons, New York, 1983.

23- Hassoun, M. N. " DESIGN OF REINFORCED CONCRETE STRUCTURE " PWS Engineering, Boston, 1985

24- Rice, P. F. & Hoffman, E. S. & Gustafson, D. P. & Gouwers, A. J. " STRUCTURE DESIGN GUIDE TO THE ACI BUILDING CODE " Van Nostrand Reinhold Company, 3d Edition, New York, 1985.

25- Piskunov, N. " DIFFERENTIAL AND INTEGRAL CALCULUS " Mir Publishers, Moscow, 1969.

26- Timoshenko, S. P. & Goodier, J. N. " THEORY OF ELASTICITY " 3d Edition, McGraw Hill Book Company, New York, 1970.